UNIVERSIDADE FEDERAL DE MINAS GERAIS
Instituto de Geociências
Programa de Pós-Graduação e Geologia

Tatiana Gonçalves Dias

A INFLUÊNCIA DE FLUIDOS CAMBRIANOS EM DEPÓSITOS DE OURO OROGÊNICO ARQUEANOS, LESTE DO QUADRILÁTERO FERRÍFERO:

geoquímica, geocronologia e geologia isotópica dos metaturbiditos e rochas associadas do Supergrupo Rio das Velhas

Belo Horizonte
2022

Tatiana Gonçalves Dias

A INFLUÊNCIA DE FLUIDOS CAMBRIANOS EM DEPÓSITOS DE OURO OROGÊNICO ARQUEANOS, LESTE DO QUADRILÁTERO FERRÍFERO:

geoquímica, geocronologia e geologia isotópica dos metaturbiditos e rochas associadas do Supergrupo Rio das Velhas

Tese apresentada ao Programa de Pós-Graduação em Geologia da Universidade Federal de Minas Gerais como requisito parcial para obtenção do título de doutora em Geologia.

Área de concentração: Geologia Econômica e Aplicada

Orientadora: Profa. Dra. Rosaline Cristina Figueiredo e Silva

Coorientadores: Profa. Dra. Lydia Maria Lobato e Prof. Dr. Steffen Hagemann

Belo Horizonte
2022

G635I
2022

Gonçalves-Dias, Tatiana.

A influência de fluidos cambrianos em depósitos de ouro orogênico arqueanos, leste do Quadrilátero Ferrífero [manuscrito] : geoquímica, geocronologia e geologia isotópica dos Metaturbiditos e rochas associadas do supergrupo Rio das Velhas/ Tatiana Gonçalves Dias. – 2022.

109 f., enc. il. (principalmente color.)

Orientadora: Rosaline Cristina Figueiredo e Silva.

Coorientadores: Lydia Maria Lobato e Steffen Hagemann.

Tese (doutorado) – Universidade Federal de Minas Gerais, Instituto de Geociências, 2022.

Área de concentração: Geologia Econômica e Aplicada.

Bibliografia: f. 97-109.

1. Geologia econômica – Quadrilátero Ferrífero (MG) – Teses. 2. Petrologia – Quadrilátero Ferrífero (MG) – Teses. 3. Geoquímica – Quadrilátero Ferrífero (MG) – Teses. 4. Tempo geológico – Teses. I. Figueiredo e Silva, Rosaline Cristina. II. Lobato, Lydia Maria. III. Hagemann, Steffen Gerd. IV. Universidade Federal de Minas Gerais. Instituto de Geociências. V. Título.

CDU: 553(815.1)

Ficha catalográfica elaborada por Graciane Aparecida de Paula – CRB-6/3404
Biblioteca “Vitória Pedersoli”, Instituto de Geociências da UFMG

UNIVERSIDADE FEDERAL DE MINAS GERAIS

PROGRAMA DE PÓS-GRADUAÇÃO EM GEOLOGIA DO IGC-UFMG

FOLHA DE APROVAÇÃO

A INFLUÊNCIA DE FLUIDOS CAMBRIANOS EM DEPÓSITOS DE OURO OROGÊNICO ARQUEANOS, LESTE DO QUADRILÁTERO FERRÍFERO: GEOQUÍMICA, GEOCRONOLOGIA E GEOLOGIA ISOTÓPICA DOS METATURBIDITOS E ROCHAS ASSOCIADAS DO SUPERGRUPO RIO DAS VELHAS

TATIANA GONÇALVES DIAS

Tese submetida à Banca Examinadora designada pelo Colegiado do Programa de Pós-Graduação em GEOLOGIA, como requisito para obtenção do grau de Doutora em GEOLOGIA, área de concentração GEOLOGIA ECONÔMICA E APLICADA, pelo Programa de Pós-graduação em Geologia do Instituto de Geociências da Universidade Federal de Minas Gerais.

Aprovada em 13 de outubro de 2022, pela banca constituída pelos membros:

Profa. Rosaline Cristina Figueiredo e Silva - Orientadora
UFMG

Prof. Gabriel Jubé Uhlein
UFMG

Profa. Flávia Cristina Silveira Braga
UFMG

Prof. Sylvio Dutra Gomes
UFBA

GUSTAVO HENRIQUE COELHO DE MELO:38331342836
Assinado de forma digital por GUSTAVO HENRIQUE COELHO DE MELO:38331342836
Dados: 2022.11.08 21:47:59 -03'00'

Prof. Gustavo Henrique Coelho de Melo
UFOP

Belo Horizonte, 13 de outubro de 2022.

AGRADECIMENTOS

Agradeço à orientadora, Profa. Dra. Rosaline Cristina Figueiredo e Silva, por todo o suporte intelectual, condução e incentivo às etapas da pesquisa, amizade, companheirismo e e empatia, fundamentais para a conclusão desta tese. Agradeço à co-orientadora, Profa. Dra. Lydia Lobato, referência para as discussões e para o desenvolvimento dessa pesquisa. Este trabalho foi viabilizado com o apoio da Pró-Reitoria de Pós-Graduação (PRPg) e do Programa de Pós-Graduação em Geologia do Instituto de Geociências da Universidade Federal de Minas Gerais (PPGEOL/UFMG), bem como da CAPES, da FUNDEP, do Centro de Microscopia da UFMG e, sobretudo, por meio do financiamento proveniente do Projeto FAPEMIG APQ-01970-17. O presente trabalho foi realizado com apoio da Coordenação de Aperfeiçoamento de Pessoal de Nível Superior - Brasil (CAPES) – Código de Financiamento 001. Pela viabilidade e suporte ao projeto desta tese, além do apoio logístico, agradeço à Anglo Gold Ashanti e à Jaguar Minig. Agradeço ao Prof. Dr. Fabrício Caxito, pelo excepcional suporte nos estudos em geocronologia. Ao Prof. Dr. Jorge Roncato, agradeço a disponibilidade, discussões e contribuições especiais a este trabalho. Pelo acolhimento, apoio e orientação durante o período de doutorado sanduíche na Austrália, agradeço ao Prof. Dr. Steffen Hagemann. Agradeço ainda o suporte da The Univertity of Western Australia UWA, do Centre for Exploration Targeting (CET), do Centre for Microscopy, Characterisation and Analysis (CMCA), da Curtin University e do John de Laeter Centre, e dos pesquisadores Neal McNaughton, Allen Kennedy e Hao Gao pelo suporte imprescindível para a realização das análises SHRIMP. Agradeço especialmente ao Vitor Barrote, à Verônica Trevisan e à Poliany Figueiredo, pela eterna amizade, pelo acolhimento e suporte em todas as etapas do período do doutorado sanduíche. Aos colegas da PPGEOL/UFMG, agradeço o companheirismo e amizade, em especial, ao Marcelo Freimann, ao Francisco Vilela, e à Laura Wisniovsky, pela incrível troca de experiências e incentivos. Agradeço aos amigos da equipe geológica da DF+ Engenharia pelo apoio e incentivo, em especial, ao Silas Salgado, à Elisabete Nascimento, ao Lázaro Marcelino e ao Fernando Pacheco. Agradeço aos eternos amigos geológicos Joana Magalhães, Dora Atman, Daniel Galvão, Matheus Kuchenbecker, Adriana Freitas, Cristiany Pereira, Fernando Prezotti, Henrique Persequini e Samuel Hayden. À minha irmã geológica Mônica Mendes, um agradecimento mais que especial. À Ana Eliza, Lara, e Ju agradeço o enorme incentivo e amizade imensurável. Agradeço à minha família, em especial ao Marcelo e à minha mãe, pelo amor, confiança e apoio incondicional, fundamentais ao longo de todas as etapas deste trabalho.

RESUMO

Os depósitos Arqueanos de ouro orogênico do leste do Quadrilátero Ferrífero, uma das principais províncias metalogenéticas no mundo, são hospedados principalmente em sequências clásticas metassedimentares que compõem o *greenstone belt* Rio das Velhas (GBRV), com idade de cerca de 2,7 Ga. Os principais corpos mineralizados nessa região associam-se ao Lineamento Córrego do Sítio, uma marcante feição estrutural de aproximadamente 15 km de extensão na direção NE-SW. As rochas hospedeiras compõem sequências turbidíticas, reconhecidas como Associação Ressedimentada, representadas pela alternância entre metagrauvacas e metapelitos, em associação a diques e *sills* metamáficos. Os principais corpos de minério, denominados Carvoaria, Laranjeiras e Cachorro Bravo, apresentam características petrográficas semelhantes, sendo a arsenopirita o principal sulfeto e bertierita e stibnita os sulfossais com ouro associado, em veios ou disseminado. No depósito Pilar, a leste do Lineamento Córrego do Sítio, a mineralização hospeda-se no Grupo Quebra Osso, que compreende rochas ultramáficas (talco xistos), e em rochas metamáficas e metapelíticas, descritas como carbonato-albita-clorita-quartzo xisto, quartzo-clorito xisto e xisto carbonáceo, e nas BIF's, do Grupo Nova Lima. Dados U-Pb robustos obtidos *in situ* (SHRIMP) em cristais de monazita hidrotermal nos diferentes depósitos sugerem uma persistente modificação de idade Ediacarana-Cambriana (~510 e 540 Ma), possivelmente relacionada ao estágio de colapso do Orógeno Araçuaí, sobre as rochas Arqueanas hospedeiras das mineralizações. Embora seja evidenciada uma marcante impressão exercida por fluidos hidrotermais Cambrianos, a assinatura geoquímica de elementos traços e terras raras não indica perturbação considerável em relação à assinatura sedimentar original, semelhante aos padrões de folhelhos arqueanos. Análises isotópicas de Nd indicam a importância dos Complexos TTG como áreas-fonte dos metaturbiditos do SGRV, com idades modelo T_{DM} de 3,0 a 3,2 Ga e εNd (2.7 Ga) levemente negativo (-1 a -3).

Palavras-chave: ouro orogênico; *greenstone belt* Rio das Velhas; metaturbidito; monazita hidrotermal; depósito Córrego do Sítio; depósito Pilar.

ABSTRACT

The Archean orogenic gold deposits of the eastern sector of the Quadrilátero Ferrífero, one of the main metallogenetic provinces in the world, are hosted mainly by metasedimentary clastic sequences that make up the Rio das Velhas greenstone belt (RVGB). The mineralized bodies in this region are associated with the Córrego do Sítio Lineament, a remarkable NE-SW structural feature of about 15 km in length. The host rocks compose turbiditic sequences, recognized as the Ressedimented Association, represented by metagrawackes and metapelites, in association with metamafic dikes and sills. The main ore bodies, named Carvoaria, Laranjeiras and Cachorro Bravo have similar petrographic characteristics, with arsenopyrite as the predominant sulfide and bertiherite and stibnite sulfossalts with associated gold, in veins or disseminated. In the Pilar deposit, east of the Córrego do Sítio Lineament, the mineralization is hosted by the Quebra Osso Group, which comprises ultramafic rocks (talc schists), and in metamafic and metapelitic rocks, described as carbonate-albite-chlorite-quartz schist, quartz-chlorite schist and carbonaceous schist, and by the BIF's, of the Nova Lima Group. Robust U-Pb geochronological data obtained in situ (SHRIMP) in hydrothermal monazite crystals in different deposits suggest a persistent modification of Ediacaran-Cambrian age (~ 510 and 540 Ma), possibly related to the collapse stage of the Araçuaí Orogen, on the Archean rocks that host the mineralizations. Although the strong Cambrian imprint by hydrothermal fluids is observed, the geochemical signature of rare earth elements does not indicate considerable disturbance in relation to the original sedimentary signature. Isotopic Nd analysis indicate the importance of TTG Complexes as source areas for RVGB metaturbidites, with TDM model ages of 3.0 to 3.2 Ga and de direção NE-SW εNd (2.7 Ga) = -1 to -3.

Keywords: orogenic gold; Rio das Velhas *greenstone belt*; metaturbidite; hydrothermal monazite; Córrego do Sítio deposit; Pilar deposit.

LISTA DE ILUSTRAÇÕES

LISTA DE TABELAS

SUMÁRIO

1 INTRODUÇÃO

Greenstone belts Arqueanos alojam os principais depósitos de ouro orogênico, responsáveis por aproximadamente 20% da produção acumulada mundial (Roberts, 1988; Groves et al., 1995; De Wit, 1997). No Brasil, um dos mais importantes terrenos geológicos que abriga depósitos desta natureza é o Quadrilátero Ferrífero (QF), que contempla aproximadamente 40 % do ouro produzido no Brasil (Lobato et al., 2001; Vial et al., 2007; Lobato et al., 2014) e ocupa uma área de aproximadamente 7000 km2 na porção sul do cráton São Francisco (Almeida, 1967). A região do QF compreende complexos granito-gnáissicos Arqueanos e Proterozoicos, o greenstone belt Arqueano Rio das Velhas (RVGB), com extensão para noroeste, identificada como greenstone belt de Pitangui, e os Supergrupos Minas e Espinhaço, de idade Proterozoica. Apesar de sua enorme importância tanto histórica quanto geológica, em termos dos depósitos de ouro de classe mundial que hospeda (Lobato et al., 2001), os processos responsáveis pela mineralização aurífera, a idade das mineralizações em veios (do tipo lode) e sua relação com as diversas estruturas do QF são ainda questões em aberto e campos promissores para a pesquisa acadêmica (Lobato et al., 2014; Roncato et al., 2015; Ribeiro et al., 2015; Martins et al., 2016; Morales et al., 2016; entre outros).

Os depósitos de ouro estão localizados em todos os níveis estratigráficos do Grupo Nova Lima (RVGB) e são comumente interpretados como relacionados aos estágios finais de deformação e metamorfismo arqueano (e.g. Lobato et al., 2007). As formações ferríferas bandadas (FFB ± chert ferruginoso) e o conjunto de rochas denominadas “lapa seca” (rochas hidrotermais quartzo-carbonáticas com sulfeto, mica branca e albita) constituem as principais hospedeiras dos depósitos auríferos (Lobato et al., 2001). Entretanto, rochas vulcânicas, máficas e ultramáficas, vulcanoclásticas e sequências metassedimentares clásticas hospedam um conjunto significativo de depósitos de ouro, sendo as últimas de grande importância na porção nordeste do QF, por exemplo, no depósito Córrego do Sítio (CdS).

Groves et al. (2003) ressaltam a importância da aplicação de métodos geocronológicos e sistemas isotópicos robustos no entendimento da gênese de depósitos de ouro orogênico e sua associação aos estágios dos ciclos tectônicos. Dessa forma, no QF, a idade da mineralização aurífera tem sido objeto de grande discussão em diversos trabalhos (e.g. Noce et al., 2007; Lobato et al. 2007), que demonstraram, inclusive, possíveis registros de influência do evento Brasiliano (ca. 530 Ma) sobre depósitos arqueanos (ca. 2.7 Ga; e. g. Alkmim e Marshak,1998; Baltazar e Zucchetti, 2007; Martins et al., 2016). Tais registros foram ainda identificados em associação a depósitos lode de ouro paladiado (Jacutinga), que compõem o cinturão PGB

(Platiniferous Gold–Palladium belt), que compreende terrenos paleoproterozoicos (Supergrupo Minas) e mesoproterozoicos (Supergrupo Espinhaço), como descrito, por exemplo, nos trabalhos de Cabral et al. (2009; 2013; 2015) e Cabral e Zeh (2015).

Neste contexto, a presente tese de doutorado tem como objetivo principal realizar estudos que permitam adquirir novos dados isotópicos e geocronológicos sobre os depósitos auríferos de Córrego do Sítio e Pilar, hospedados no greenstone belt Rio das Velhas na região nordeste do Quadrilátero Ferrífero. Estes dados poderão evidenciar possíveis contribuições da circulação de fluidos hidrotermais provenientes do estágio de colapso do sistema orogênico Ediacarano-Cambriano Araçuaí (530 Ma - 480 Ma; Alkmim et al., 2006; Pedrosa-Soares et al., 2011) sobre esses depósitos, além de fornecer informações sobre as fontes dos sedimentos do RVGB e a possível influência destas nas mineralizações auríferas.

Esta tese insere-se como parte do projeto de cooperação técnica-científica entre a empresa de mineração Anglo Gold Ashanti (AGA), a Fundação de Desenvolvimento da Pesquisa (FUNDEP) e a Universidade Federal de Minas Gerais (UFMG). Este projeto conta ainda com recursos concedidos através do projeto Fluidos hidrotermais em jazidas de ouro e ferro no distrito mineral do Quadrilátero Ferrífero, Minas Gerais, Brasil junto à Fundação de Amparo à Pesquisa do Estado de Minas Gerais (FAPEMIG APQ-01970-17). Parte da tese foi desenvolvida na The University of Western Australia, na cidade de Perth, através do programa de Doutorado Sanduíche, ofertado pela Coordenação de Desenvolvimento Pessoal (CAPES).

Os dados produzidos durante o desenvolvimento desta tese estão expostos na forma de artigos científicos nos capítulos 4 e 5.

1.1 Localização da área de estudo

O conjunto de depósitos auríferos de Córrego do Sítio, propriedade da Anglogold Ashanti Córrego do Sítio Mineração-AGABM, e o depósito Pilar, operado pela Jaguar Mining Inc. localizam-se a aproximadamente 35 km a sudoeste do município de Santa Bárbara e 120 km de distância de Belo Horizonte, Minas Gerais. O acesso principal pode ser realizado pelas rodovias federal BR 381, estadual MG 381 e MG 436 (Figura 1).

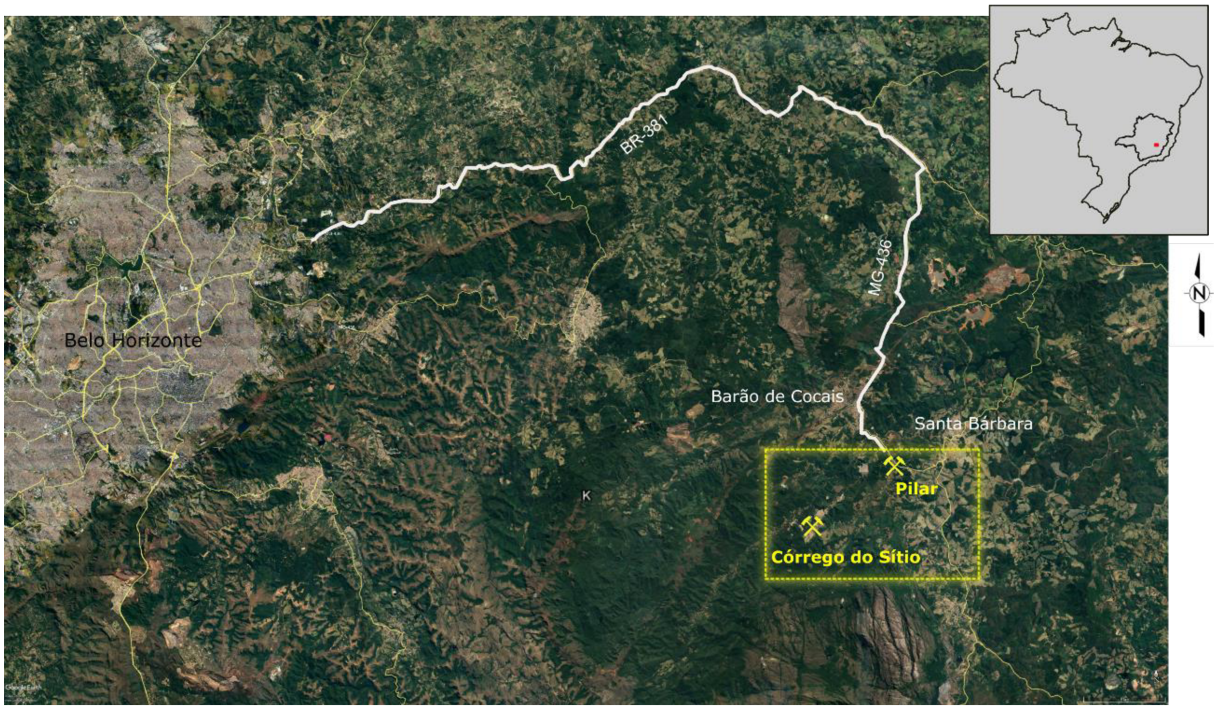

Figura 1: Mapa de localização da área de estudo, englobando os depósitos de Córrego do Sítio e Pilar, com acessos a partir de Belo Horizonte (Google Maps, acesso em janeiro de 2022).

1.2 Objetivos

Este trabalho tem como objetivo principal o estudo da idade e natureza dos diversos eventos que afetaram os sistemas hidrotermais atuantes no Supergrupo Rio das Velhas, o controle da mineralização aurífera e proveniência dos metaturbiditos desta unidade. Este estudo foi conduzido principalmente em corpos de minério associados ao lineamento aurífero Córrego do Sítio (Lima, 2012), uma estrutura regional NE-SW que controla significantes depósitos de ouro na porção leste do QF. Foram também analisadas amostras do depósito Pilar, localizado a leste do Lineamento Córrego do Sítio.

Uma das principais questões abordadas nesta tese é a investigação da influência de fluidos hidrotermais sobre as mineralizações hospedadas nas sequências Arqueanas do *Greenstone Belt* Rio das Velhas, principalmente os fluidos possivelmente relacionados ao magmatismo decorrente do colapso Cambro-Ordoviciano do Orógeno Araçuaí-Ribeira (Pedrosa-Soares e Wiedemann-Leonardos, 2000; Valeriano et al., 2016; Tupinambá et al., 2013). Esse registro vem sendo abordado em alguns trabalhos recentes sobre regiões diversas do QF, em sequências do Grupo Nova Lima, Supergrupo Rio das Velhas (Martins et al., 2016), bem como em itabiritos Paleoproterozoicos da Formação Cauê, que hospedam depósitos auríferos (e.g. Cabral et al., 2006; Cabral et al., 203). Estudos realizados por Rosiere et al. (2021) mostram ainda que pulsos de fluidos Cambrianos, interpretados a partir de idades de

minerais hidrotermais desenvolvidos em formações ferríferas bandadas podem ser associados a alterações em depósitos de ferro da Formação Cauê.

Para o desenvolvimento dessa tese foram aplicados modernos métodos químicos, isotópicos e geocronológicos com o objetivo de fornecer dados para balizar as interpretações sobre a natureza, idade e fonte dos depósitos auríferos do *greenstone belt* Rio das Velhas, especialmente, aqueles ligados aos pacotes metaturbidíticos desta unidade.

2 METODOLOGIA

2.1 Caracterização petrográfica e geoquímica dos litotipos mineralizados em ouro

A caracterização petrográfica e geoquímica dos litotipos mineralizados foi realizada para fornecer as bases de conhecimento mineralógico, textural e estrutural das rochas estudadas e para identificação das amostras que seriam mais aplicáveis aos métodos U-Pb e Sm-Nd. Esta caracterização se deu através das seguintes etapas:

- Coleta de amostras nos corpos mineralizados em ouro de Cachorro Bravo (CB), Carvoaria (CV), Laranjeiras (LJ), localizados no depósito de Córrego do Sítio, e no depósito de Pilar (PL);

- Estudo petrográfico, através de microscópio óptico de luz transmitida e refletida dos principais litotipos que compõem os depósitos estudados e caracterização dos aspectos mineralógicos e texturais. Esta etapa foi desenvolvida nos laboratórios de Metalogenia do Centro de Pesquisa Manoel Teixeira da Costa (CPMTC) na UFMG;

- Petrografia de detalhe em Microscópio Eletrônico de Varredura (MEV), com utilização do MEV acoplado ao software Mineral Liberation Analyzer (MLA), instalado no Centro de Microscopia da UFMG. Durante o período de Doutorado Sanduíche, os estudos petrográficos foram conduzidos por MEV (TESCAN VEGA3), acoplado a sistema analisador espectrométrico de energia dispersiva EDS (Energy Dispersive Spectrometer) do tipo Oxford Instruments X-Max 50 com software AZtec® e INCA®, instalados no Centre for Microscopy, Characterization and Analysis (CMCA) da The University of Western Australia (UWA).

- Caracterização geoquímica de rocha total de amostras dos litotipos metassedimentares que hospedam ouro. As amostras foram preparadas em britador e pulverizadas em moinho de discos nos laboratórios de preparação de amostras do CPMTC-IGC-UFMG e enviadas ao laboratório SGS Geosol, onde foram analisadas via ICP-MS (Induced Coupled Plasma – Mass Spectrometry) após fusão com metaborato / tetraborato de lítio e digestão com ácido nítrico diluído.

2.2 Análises isotópicas Sm-Nd

Dezesseis amostras foram encaminhadas para o Laboratório de Geocronologia e Isótopos Radiogênicos da Universidade do Estado do Rio de Janeiro (LAGIR-UERJ) para análises de isótopos Sm-Nd. As razões isotópicas foram obtidas por espectrômetro de massa de ionização térmica (TIMS - *Thermal Ionization Mass Spectrometry*) TRITON-Finnigan. A metodologia completa de análise encontra-se no Capítulo 5, como parte do segundo artigo produzido para esta tese.

2.3 Geocronologia U-Pb *in situ* (SHRIMP)

2.3.1 Preparação de amostras

Nesta etapa de trabalho, a preparação das amostras objetivou a realização de análises diretamente nos cristais de minerais hidrotermais identificados em lâmina delgada polida na etapa de petrografia, via microscópio óptico e eletrônico de varredura. O método *in situ* de análises dispensa os procedimentos de dissolução dos cristais e separação química em laboratório limpo necessários em outras técnicas de análise isotópica. Além disso, esta técnica permite a caracterização textural dos minerais que compõem os litotipos estudados, essencial para a elucidação sobre as relações entre os cristais dos minerais hidrotermais. Os procedimentos adotados são descritos a seguir:

- Identificação de cristais de monazita em Microscópio Eletrônico de Varredura (MEV). Em uma etapa inicial, o mapeamento mineralógico foi realizado com utilização do MEV acoplado ao software *Mineral Liberation Analyzer* (MLA), instalado no Centro de Microscopia da UFMG. Tal procedimento permitiu a seleção de amostras com cristais de monazita de dimensões compatíveis às análises *in situ* (> 10 μm). Dessa forma, foram selecionadas amostras dos corpos mineralizados Cachorro Bravo (CB) e Carvoaria (CV). As lâminas delgadas polidas destas amostras e metalizadas com carbono foram ainda mapeadas (Figura 2), com utilização do equipamento de MEV TIMA (TESCAN *Integrated Mineral Analyser*), instalado no John de Laeter Centre, Curtin University, Australia;

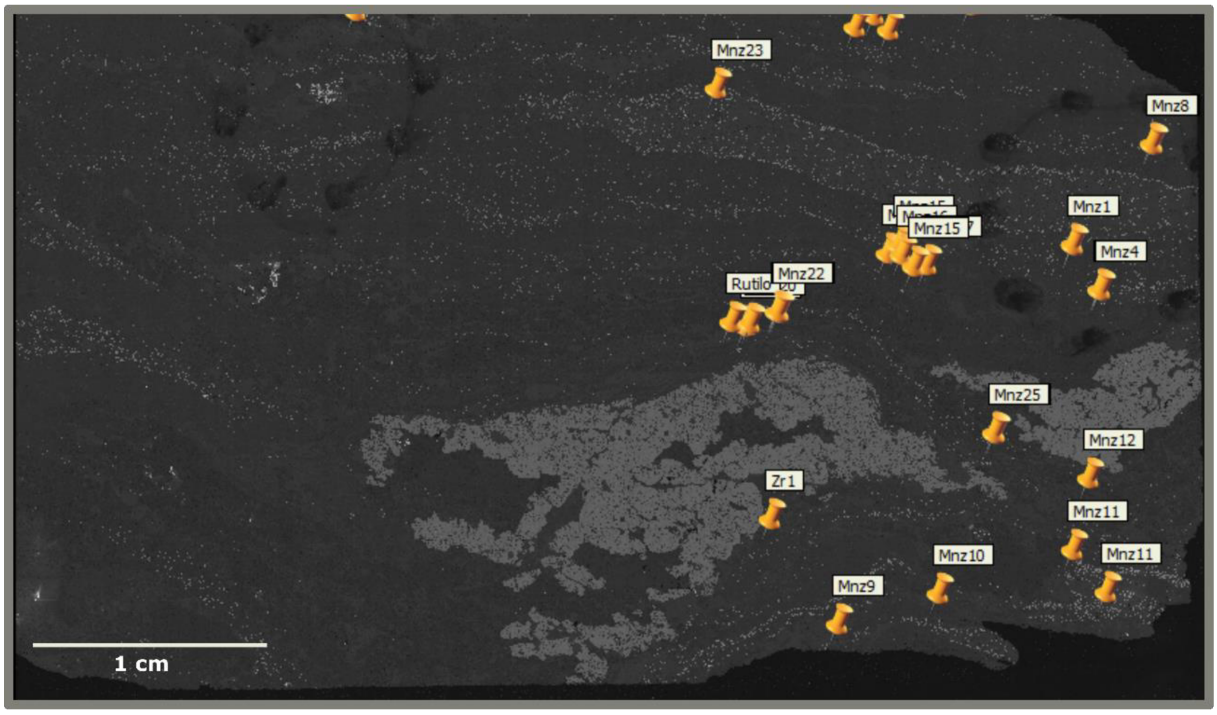

Figura 2: Mapeamento mineralógico de seção polida (amostra CB-01), com utilização do equipamento de MEV TIMA (TESCAN Integrated Mineral Analyser). Mnz – cristais de monazita; Zr -zircão.

- Identificação de cristais de monazita hidrotermal a partir de espectros geoquímicos produzidos pelo sistema de analisador espectrométrico de energia dispersiva EDS (*Energy Dispersive Spectrometer*) do tipo Oxford Instruments X-Max 50, acoplado ao MEV (TESCAN VEGA3), com software AZtec® e INCA®, instalados no Centre for Microscopy, Characterization and Analysis (CMCA) da University of Western Australia (UWA). Espectros com ausência ou com baixo pico de Th foram selecionados, como exemplificado na Figura 3, em conjunto com critérios texturais dos cristais de monazita, como proposto por Schandl e Gorton (2004) e Grand'Homme (2016);

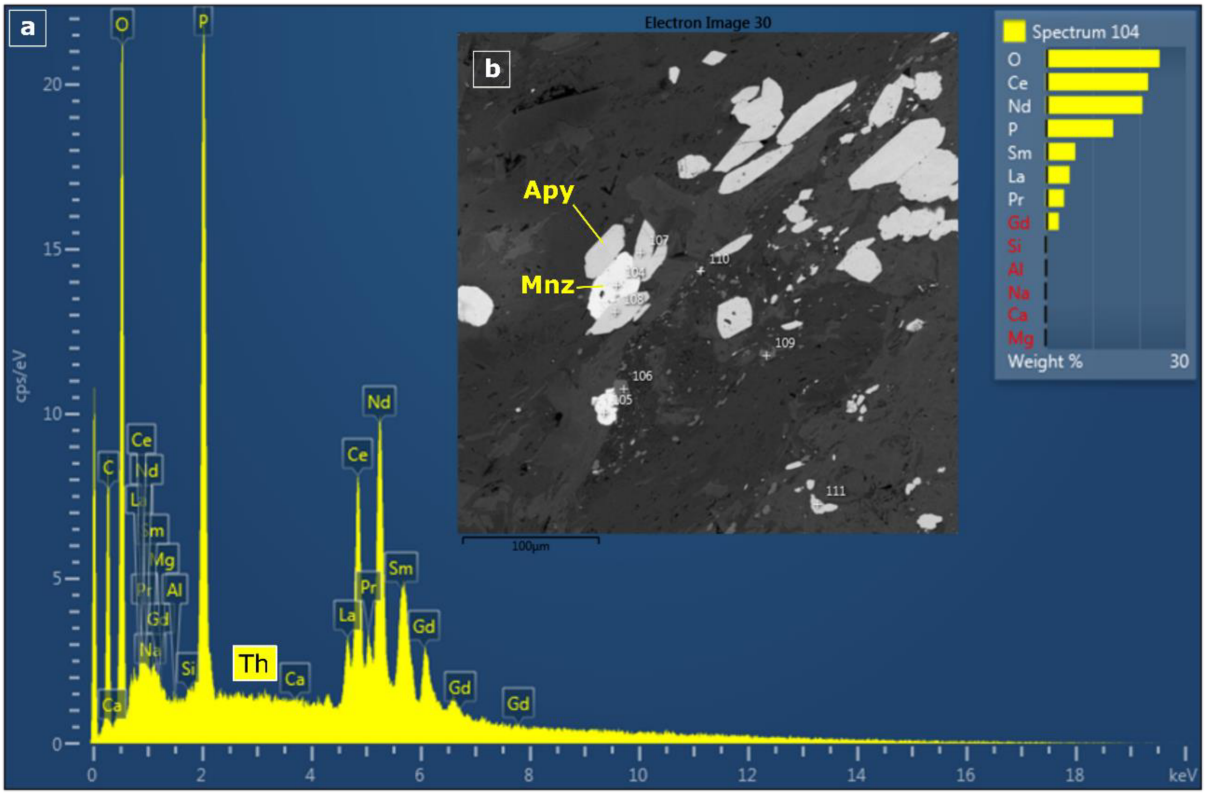

Figura 3: (a) Espectro EDS de (b) monazita (Mnz) hidrotermal associada a arsenopirita (Apy) em imagem de elétrons retroespalhados (*back scattering*).

- Seleção e marcação dos cristais de monazita identificados em MEV, através de microscópio óptico (Figura 4A);

- Microperfuração das lâminas polidas (Figura 4B), onde os cristais de monazita foram marcados, com utilização de brocas vazadas de ponta diamantada de 2 e 3 mm de diâmetro, seguindo os procedimentos de Rayner e Stern (2002) e Rasmussen e Fletcher (2010). Os discos milimétricos (*plugs*) recortados das lâminas polidas foram transferidos e afixados em placa de vidro (Figura 4C) e cobertos por resina epóxi em um molde de teflon de 2,5 mm de diâmetro (Figura 4D). Após secagem, os *mounts* produzidos foram retirados dos moldes (Figura 4E), polidos, limpos e revestidos com carbono para novo procedimento de imageamento por microscopia óptica e eletrônica de varredura;

- Produção de imagens de elétrons secundários (SE - *Secondary Electrons*) e de elétrons retro-espalhados (BSE – *Back-Scattered Electrons*) em MEV modelo TESCAN VEGA3, instalado do CMCA-UWA. As imagens BSE serviram de base para escolha dos *spots* a serem analisados por SHRIMP (*Sensitive high-resolution ion microprobe*);

2.3.2 Geocronologia por isótopos U-Pb (SHRIMP) aplicada em cristais de monazita.

A principal vantagem da utilização das microssondas iônicas para análises isotópicas é que as análises podem ser realizadas *in situ*, utilizando apenas porções micrométricas de cada cristal e, desta forma, configurando uma técnica não destrutiva onde o mesmo cristal ou grão mineral pode ser analisado diversas vezes e para diversos sistemas isotópicos. Os procedimentos seguidos para as análises e tratamento dos dados são descritos a seguir.

- Os *mounts* foram cobertos com ouro (8-10 nm de espessura; Figura 4F) juntamente com *mounts* de cristais padrão e inseridos no *rack* do SHRIMP 48 horas antes da análise para melhores condições de vácuo na fonte;

- As análises U-Pb foram realizadas no laboratório SHRIMP II do John de Laeter Centre, Curtin University;

- Ciclos de oito e de seis escaneamentos foram realizados para cada análise do espectro isotópico, caracterizado pelas massas $^{202}LaPO_2$, $^{203}CePO_2$, ^{204}Pb, ^{204} Background, $^{205.8}NdPO_2$, ^{206}Pb, ^{207}Pb, ^{208}Pb, ^{232}Th, $^{245}YCeO$, ^{254}UO, $^{264}ThO_2$, e $^{270}UO_2$. O padrão principal French, além dos padrões Z2234 e Z2908, foram também analisados;

- Os dados gerados foram reduzidos utilizando programa Squid 2.5 (Ludwig, 2009) e os gráficos foram preparados usando o *software* Isoplot 3 (Ludwig, 2003).

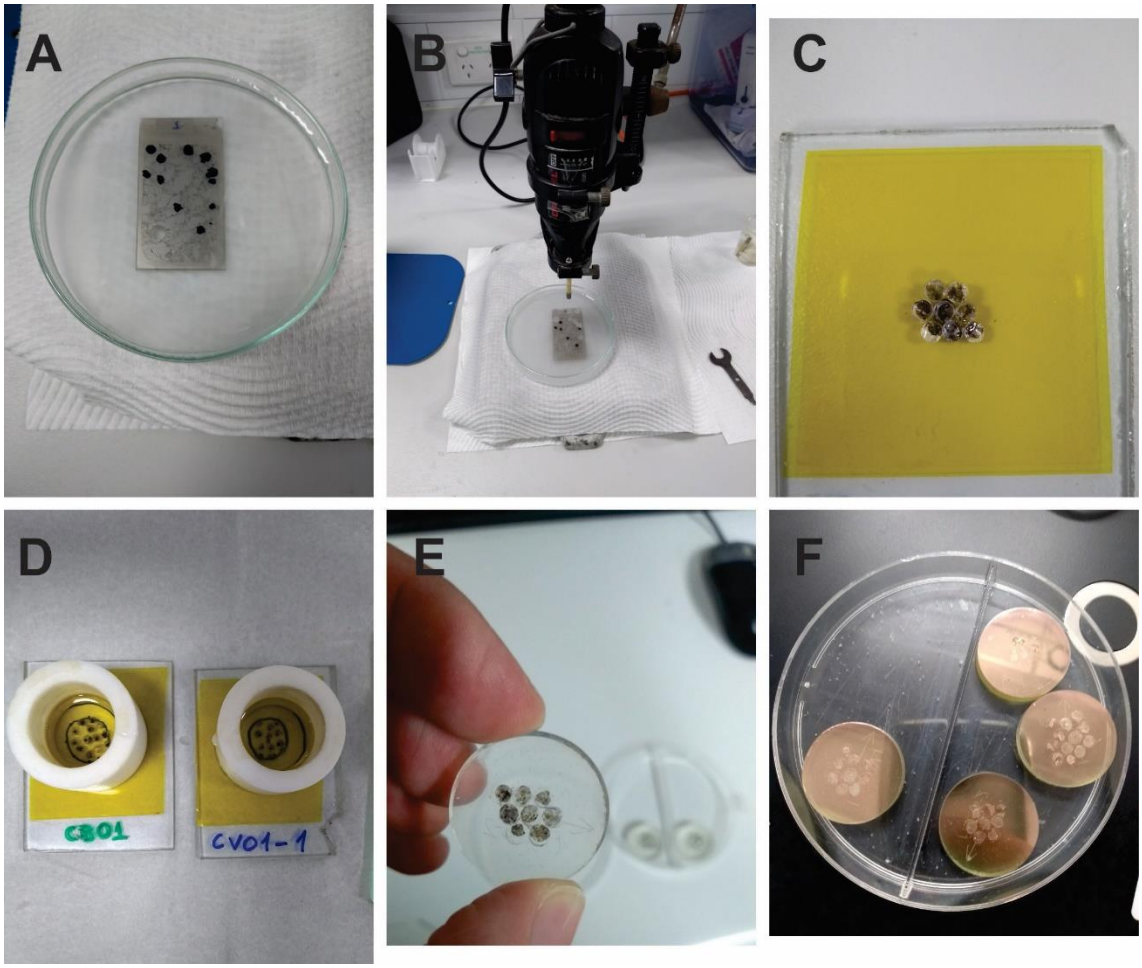

Figura 4: Imagens ilustrativas do processo de preparação dos *mounts* com discos retirados de lâminas delgadas para análise no SHRIMP. A - Lâmina polida delgada com marcação dos locais reconhecidos via MEV e microscopia ótica onde ocorrem os minerais de interesse; B – Furadeira de bancada utilizada no processo de microperfuração; C - Colocação dos testemunhos da microperfuração em lâmina de vidro com fita dupla face e do molde para preparação do *mount*; D – Colocação da mistura resina epóxi + endurecedor sobre as lâminas de vidro; E – Resultado de um *mount* em resina epóxi após secagem; F – *Mounts* cobertos por camada nanométrica de ouro para assegurar condutividade durante as análises SHRIMP.

3 CONTEXTO GEOLÓGICO

A geologia do Quadrilátero Ferrífero, situado a sul do cráton São Francisco (Almeida, 1977) reúne três unidades tectonoestratigráficas principais (Figura 5 e Figura 6; Dorr, 1965; 1969; Ladeira, 1991; Baltazar e Silva, 1996; Zucchetti e Baltazar, 1998; Lobato et al., 2001, 2005; Zucchetti e Baltazar, 2000; Baltazar e Zucchetti, 2007):

- Terrenos granito-gnáissicos Arqueanos;

- Sequências metavulcanossedimentares Arqueanas do Supergrupo Rio das Velhas (SGRV);

- Sequências supracrustais sedimentares clásticas e químicas do Supergrupo Minas e Grupo Itacolomi.

Os terrenos Arqueanos de composição trondhjemítica-tonalítica-granodiorítica (TTG) compõem o embasamento cristalino e são representados pelos complexos Bação, Belo Horizonte, Caeté, Santa Bárbara e Bonfim (Teixeira et al., 2000). Esses complexos são expostos na forma de domos, os quais se encontram em contatos tectônicos em relação às sequências *greenstone* do SGRV. A evolução tectonomagmática desses terrenos apresenta caráter polifásico (Figura 6) durante os eventos Santa Bárbara (3220–3200 Ma), Rio das Velhas I (RV I, 2930–2900 Ma) e Rio das Velhas II (RV II, 2800–2770 Ma). O Complexo Santa Bárbara, embasamento do setor leste do Quadrilátero Ferrífero, onde se situam os depósitos de ouro de Córrego do Sítio, representa o pulso magmático inicial, em 3212 ± 9 e 3210 ± 8 Ma (Lana et al., 2013).

O Supergrupo Rio das Velhas (Loczy e Ladeira, 1976), previamente denominado Série Rio das Velhas (Dorr et al., 1957), é composto por sequências metavulcanossedimentares arqueanas formadas entre 2,80 e 2,78 Ga (Baltazar e Zucchetti, 2007).

O primeiro trabalho de divisão estratigráfica do SGRV foi proposto por Dorr et al. (1957), ao definir os grupos Nova Lima, inferior, e Maquiné, superior. O Grupo Nova Lima constitui-se por uma sequência metavulcanossedimentar, e o Grupo Maquiné por uma sequência metassedimentar clástica. Schorscher (1978) introduziu na base do SGRV o Grupo Quebra Ossos, definido a partir da descrição de fluxos komatiíticos intercalados à formação ferrífera bandada. Ladeira (1980) dividiu o Grupo Nova Lima em três unidades: metavulcânica (basal), metassedimentar química (intermediária) e metassedimentar clástica (superior).

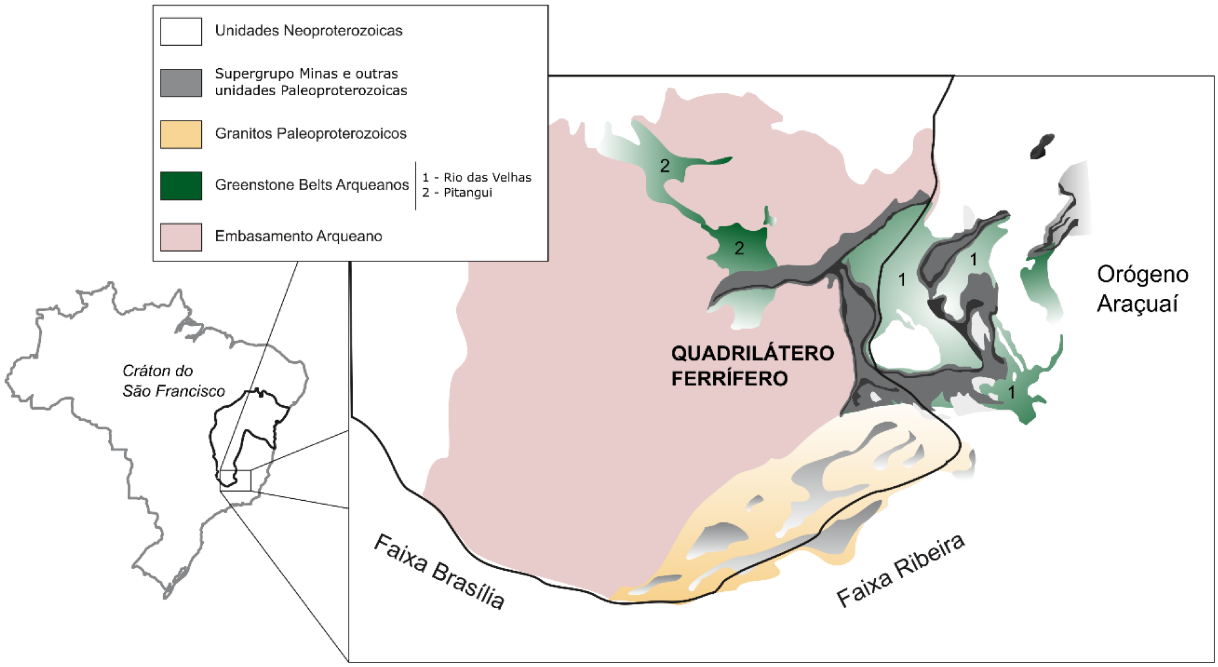

Figura 5: Contexto tectônico regional do Quadrilátero Ferrífero, na região sudeste do Cráton São Francisco. Modificado de Alkmim (2004) e Alkmim (2018).

A divisão litoestratigráfica proposta passou por significativas mudanças após as definições de Dorr et al. (1957). Baseado em associações de litofácies descritas por Pedreira e Silva (1996) e Baltazar e Pedreira (1996, 1998), o mapeamento do *greenstone belt* Rio das Velhas foi realizado segundo abordagem de Eriksson et al. (1994) calcada na estratigrafia de sequências aplicada para terrenos arqueanos. Trata-se de uma abordagem mais moderna quando comparada ao empilhamento litoestratigráfico clássico, que é sistematicamente aplicada no mapeamento de outros *greenstone belts* ao redor do mundo, como os de Barberton e Pietersburg na África do Sul (De Wit, 1991), e no bloco de Pilbara na Austrália (Krapez, 1993).

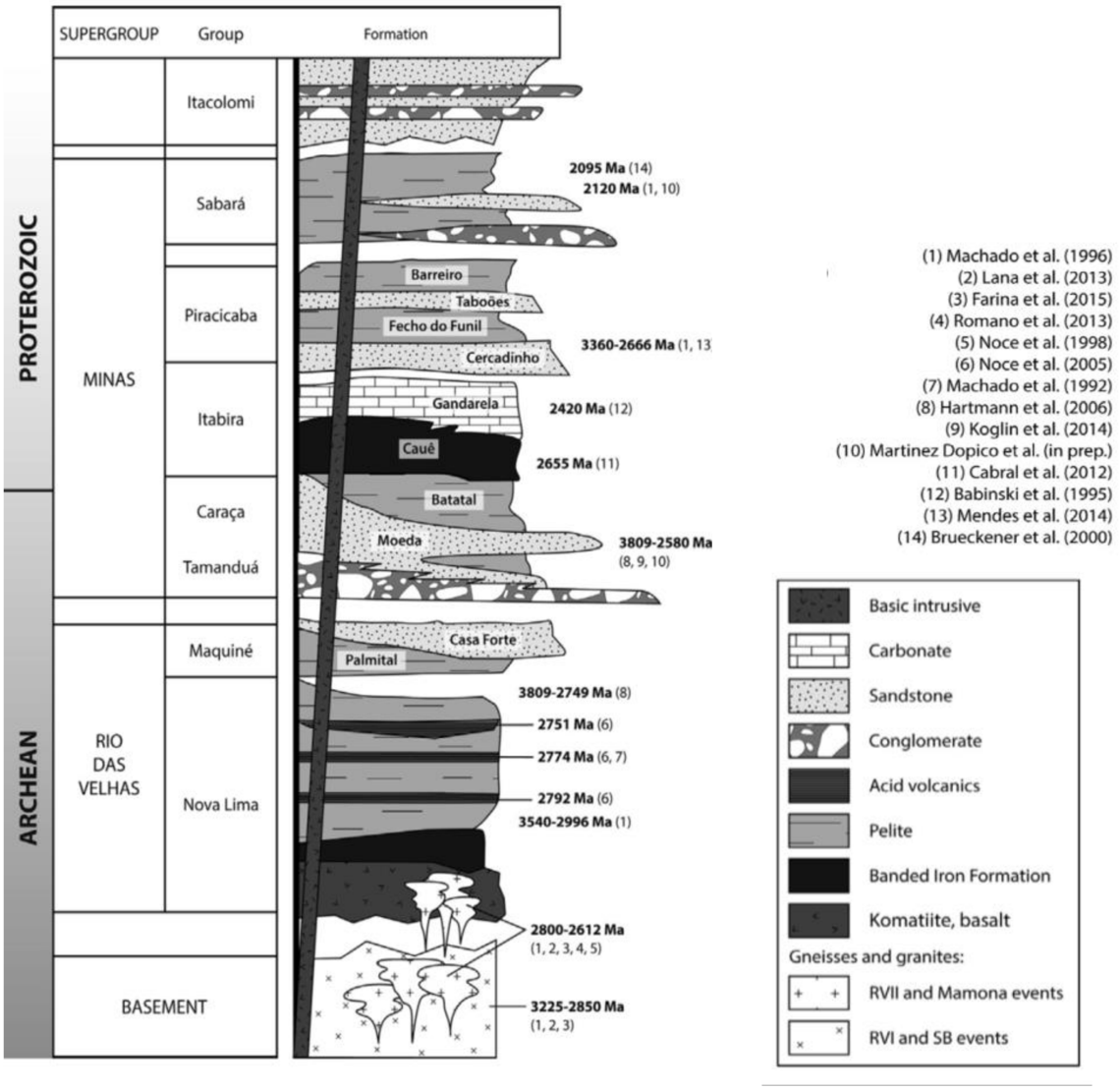

Figura 6: Estratigrafia e idades (de acordo com as referências indicadas na Figura) das sequências supracrustais do Quadrilátero Ferrífero. RVI – evento Rio das Velhas I; RVII evento Rio das Velhas II; SB – evento magmático Santa Bárbara. Retirado de Farina et al. (2016).

A partir da individualização e descrição das sete associações de litofácies da Figura 7, Baltazar e Zucchetti (2007) propuseram um modelo evolutivo do *greenstone belt* Rio das Velhas através da definição de três blocos tectônicos (Figura 8) e quatro ciclos sedimentares, considerando trabalhos anteriores, tais como Baltazar et al. (1994), Pedreira e Silva (1996), Baltazar e Pedreira (1996, 1998) e Zucchetti e Baltazar (2000). Os quatro ciclos deposicionais individualizados, relacionados com configurações tectônicas específicas, são:

- *Ciclo 1:* deposição das associações vulcânica máfica-ultramáfica (I) e vulcanossedimentar química (II) em regime tectônico extensional relacionado a abertura de bacia oceânica;

- *Ciclo 2:* deposição da associação clasto-química sedimentar (III), das grauvacas distais relacionadas à associação ressedimentada (V) e da associação costeira (VI) em estágios finais do regime extensional da bacia oceânica em transição para o início do desenvolvimento da fase de subducção;

- *Ciclo 3:* deposição das associações vulcanoclástica (IV) e ressedimentada (V) em fase orogênica do regime tectônico, com formação de arcos de ilhas;

- *Ciclo 4:* deposição da associação não-marinha em bacia do tipo *back-arc foreland*.

A Figura 7 mostra as diversas associações de litofácies identificadas por Baltazar e Zuchetti (2007) para o *greenstone belt* Rio das Velhas. Esses autores individualizaram quatro blocos denominados Caeté, Nova Lima, Santa Bárbara e São Bartolomeu (Figura 8), com estratigrafias distintas (Figura 9). Embora identificada uma proeminente falha de empurrão entre os blocos Nova Lima e Caeté, estes foram unificados, com base em semelhanças litológicas entre essas unidades.

As unidades que compõem o bloco Santa Bárbara, caracterizam-se pelo *trend* de direção NE-SW e mergulhos suaves a moderados para SE. No bloco São Bartolomeu e no setor sul do bloco Nova Lima-Caeté, as camadas apresentam um *trend* de direção NW-SE, com mergulhos para NE, com exceção do sinclinal Andaimes, de direção E-W. No setor norte do bloco Nova Lima-Caeté, as unidades são dobradas, com plano axial NE-SW, com mergulho para SE, e obliteradas por um grande sistema de falhas transcorrentes E-W (Lobato et al., 2001a).

O Lineamento Córrego do Sítio insere-se no contexto do bloco Santa Bárbara, porção leste do QF, que compreende o Supergrupo Arqueano Rio das Velhas subdividido, da base ao topo, no Grupo Quebra Osso, grupos Nova Lima e Maquiné, metamorfisados sob fácies xisto verde a anfibolito baixo. O Grupo Quebra Osso compõe-se principalmente por metakomatiitos. O Grupo Nova Lima é representado por metabasaltos toleíticos e rochas metassedimentares clastoquímicas das Formações Vigário da Vara, Santa Quitéria e Córrego do Sítio. O Grupo Maquiné compreende rochas metassedimentares siliciclásticas das formações Palmital e Casa Forte.

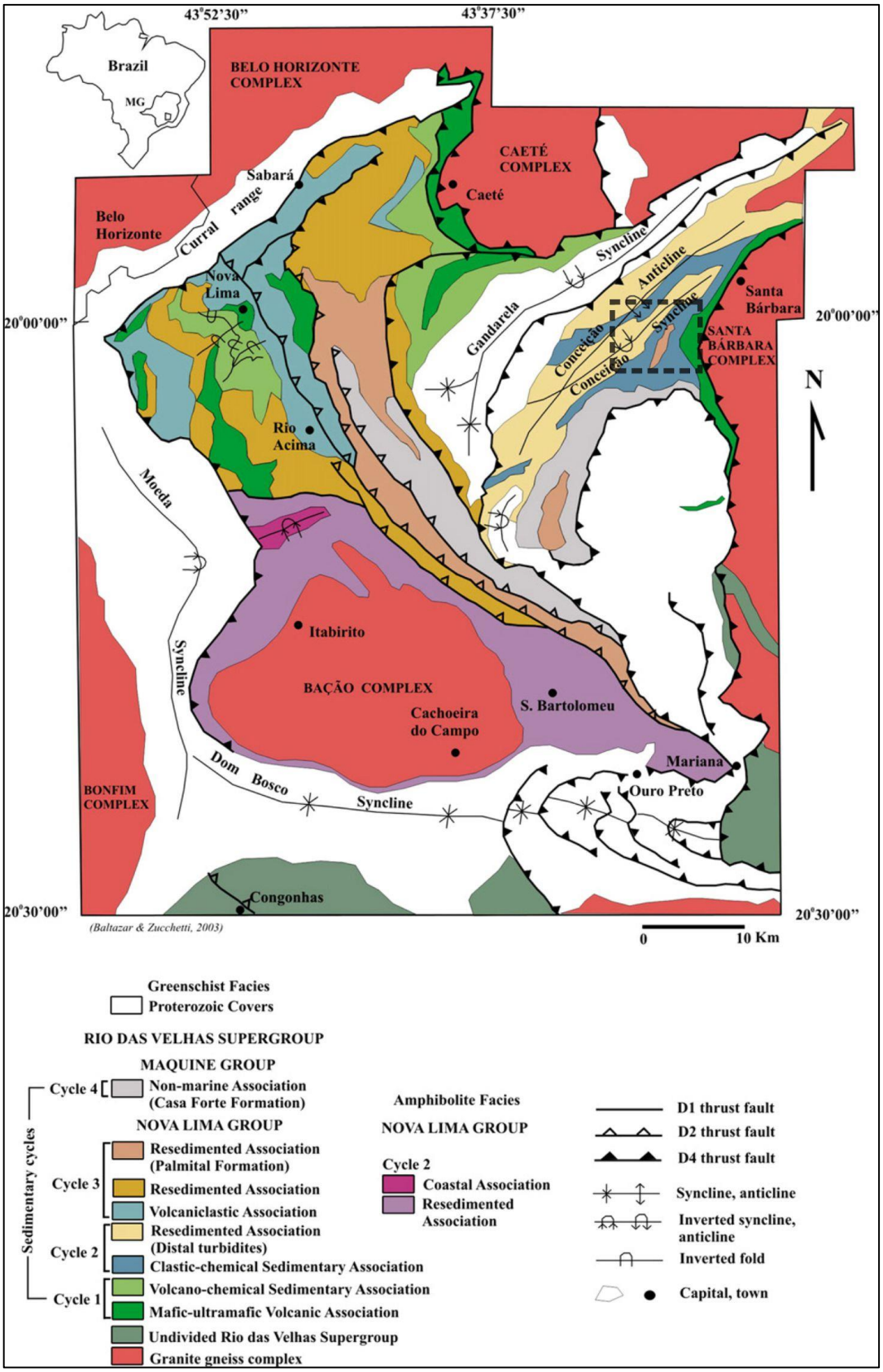

Figura 7: Mapa geológico simplificado do Quadrilátero Ferrífero com as associações de litofácies do Supergrupo Rio das Velhas (Baltazar e Zucchetti, 2007). O retângulo tracejado destaca a área de pesquisa.

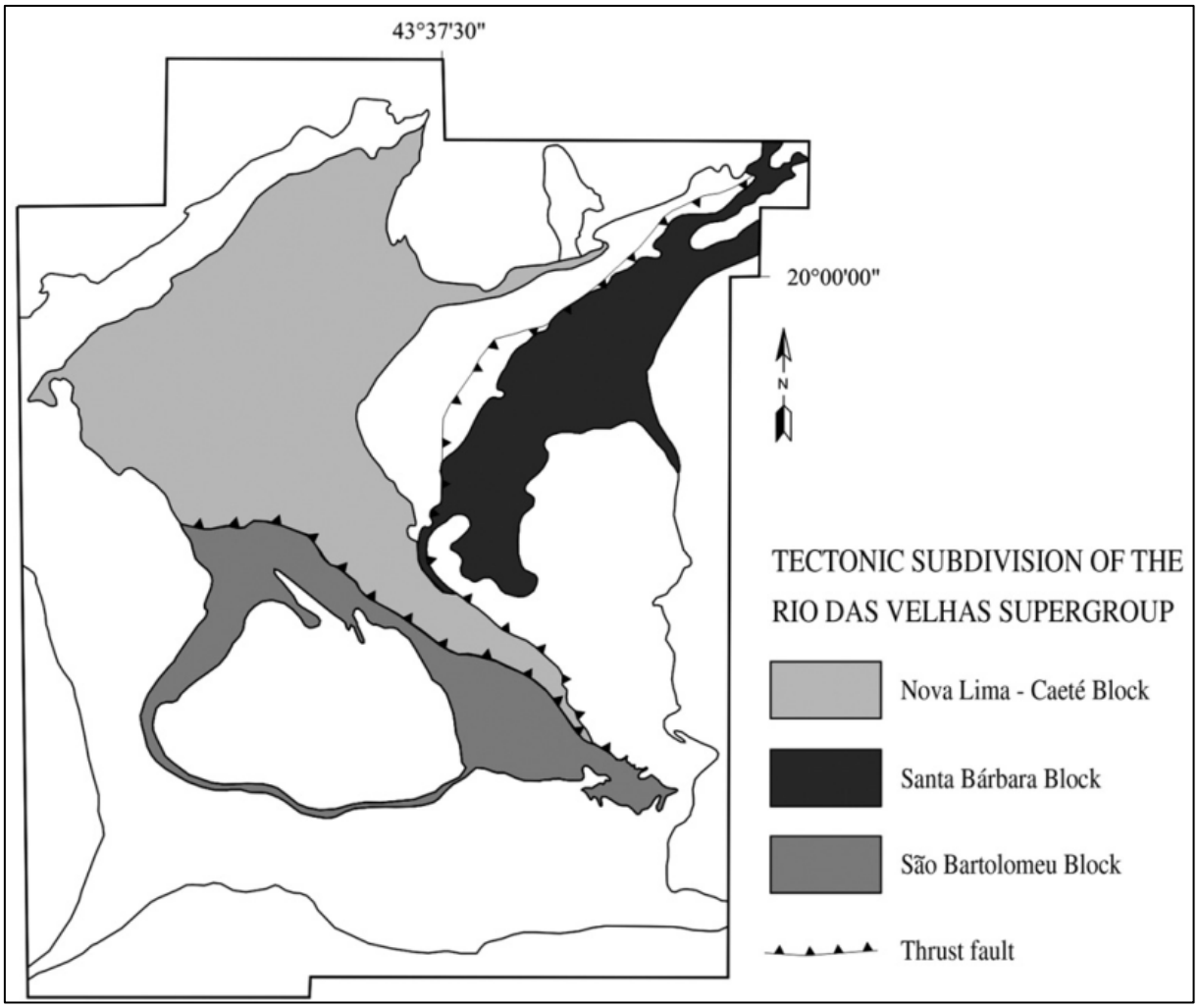

Figura 8: Domínios litoestruturais do Supergrupo Rio das Velhas no Quadrilátero Ferrífero (Baltazar and Zucchetti, 2007).

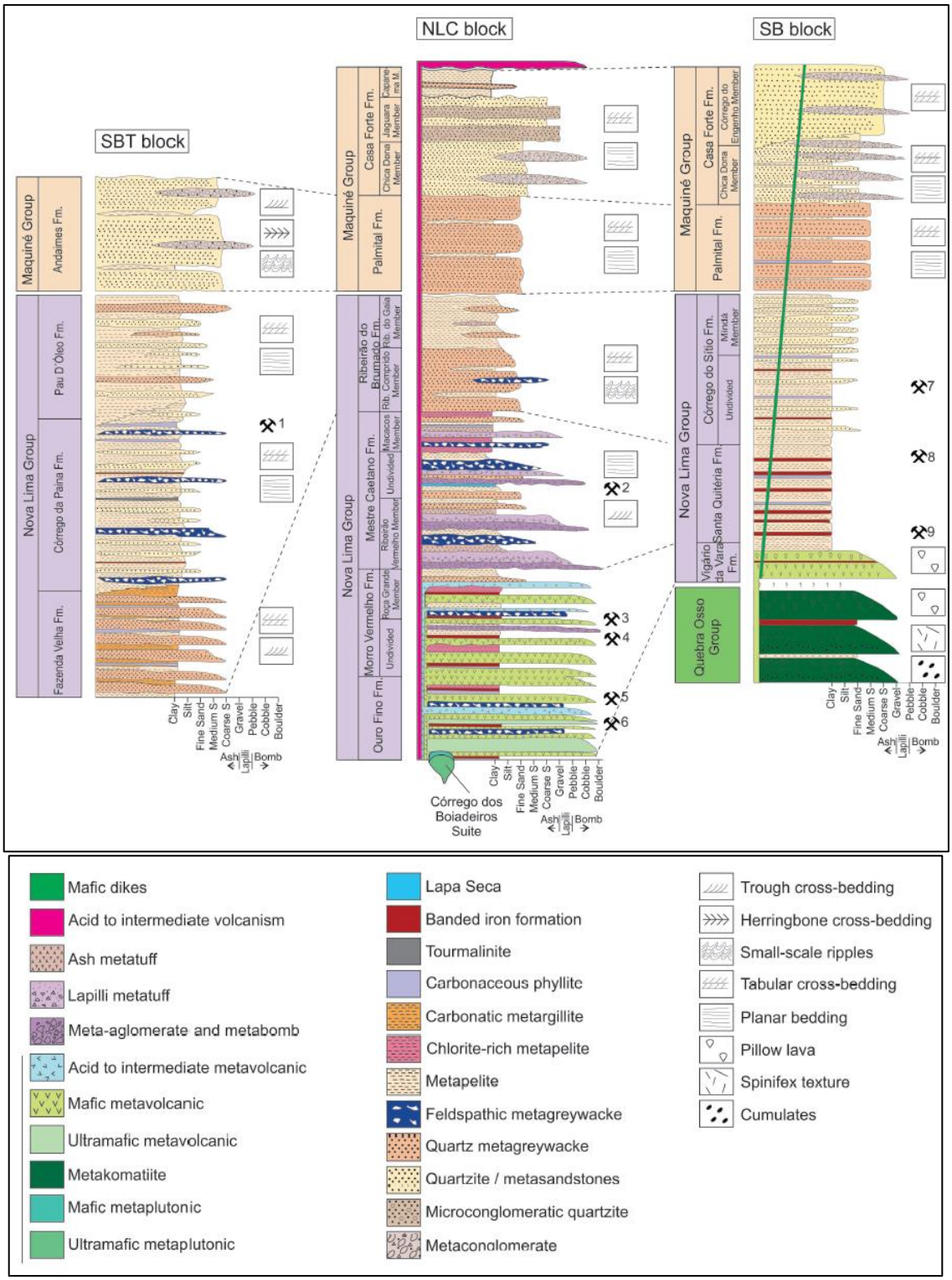

Figura 9: Colunas estratigráficas do Supergrupo Rio das Velhas, correspondentes aos três blocos tectonoestratigráficos do Greenstone Belt do Rio das Velhas: SBT – Bloco Santa Bárbara; NLC – Bloco Nova Lima – Caeté; SB – Bloco São Bartolomeu. Jazidas de ouro: 1- Santa Izabel (Complexo Paciência); Ouro Fino e Cata Branca; 2- Morro Velho; 3- Roça Grande; 4- Cuiabá e Lamego; 5- Juca Vieira; 6- Raposos; 7- Córrego do Sítio; 8- Santa Quitéria; 9- Pilar. Retirado de Araújo et al. (2020).

A noroeste do QF, terrenos arqueanos de grau metamórfico xisto verde superior a anfibolito inferior compõem o *greenstone belt* de Pitangui (GBP; Figura 5), interpretado como

a continuação do GBRV, em termos de litoestratigrafia (e.g. Lobato e Pedrosa-Soares, 1993; Alkmim e Noce, 2006; Romano, 2007; Romano et al., 2013; Pinto e Silva, 2014). Em proposta mais recente, Brando Soares et al. (2017) classifica o GBP em uma sequência composta por uma unidade inferior de rochas ultramáficas e máficas, metavulcânicas intercaladas a formações ferríferas bandadas (BIFs) e metaturbiditos; uma unidade média de metaturbiditos intercalados a rochas metavulcânicas intermediárias e, subordinadamente, BIFs e quartzitos; e uma unidade superior composta por quartzitos e metaconglomerados polimíticos. As unidades inferior e média são correlatas às sequências de litofácies dos ciclos I, II e III do Grupo Nova Lima de Baltazar e Zucchetti (2007). A unidade superior correlaciona-se ao Grupo Maquiné.

O Supergrupo Minas representa uma sequência Paleoproterozoica de rochas sedimentares plataformais em contato discordante com o Supergrupo Rio das Velhas e se subdivide nos grupos Caraça, Itabira, Piracicaba e Sabará (Dorr, 1969). Os principais trabalhos, com dados geocronológicos sobre esta sequência, são apresentados na Figura 6.

O Grupo Caraça, subdividido nas formações Moeda e Batatal, compõe-se de conglomerados e quartzitos de sequência clástica basal, aluvial a deltaica ou marinha. O Grupo Itabira representa a sedimentação química na Bacia Minas e se subdivide nas formações Cauê e Gandarela. A Formação Cauê destaca-se pelo expressivo volume de formações ferríferas, com corpos de minério de ferro que hospeda. O Grupo Piracicaba compõe-se de rochas sedimentares clásticas (pelíticas e psamíticas) e químicas em contato erosivo com o Grupo Itabira. O Grupo Sabará corresponde a uma sequência *flysch* composta por metagrauvacas, filitos carbonáceos, metadiamictitos, metaconglomerados e rochas metavulcânicas félsicas a intermediárias. O Grupo Itacolomi corresponde à sequência de topo do Supergrupo Minas e se encontra em contato discordante angular e erosivo sobre o Grupo Sabará. Trata-se de sequência molássica, composta por quartzito, metarcósio e metaconglomerado.

O Quadrilátero Ferrífero registra uma complexa história de deformação, descrita em diversos trabalhos como eventos polifásicos desde Dorr (1969) com, no mínimo, três grandes eventos deformacionais (e. g. Alkmim e Marshak, 1998).

Modelos tectônicos e de deformação para o QF têm sido propostos desde Dorr (1969), com base em pelo menos três principais eventos tectono-metamórficos compressivos intercalados a eventos extensionais (e.g. Alkmim e Marshak, 1998; Baltazar e Zucchetti, 2007 ; Baltazar e Lobato, 2020). Apesar de diversas controvérsias sobre a importância de cada um dos eventos na estruturação do Quadrilátero Ferrífero, a maioria dos autores concorda com a ocorrência dos três eventos compressivos principais. Além da importância na estruturação e no

metamorfismo na fácies xisto verde, esses eventos condicionaram a percolação de fluidos hidrotermais que foram importantes na geração dos depósitos minerais do Quadrilátero Ferrífero (Baltazar e Lobato, 2020).

Baltazar e Zucchetti (2007) descrevem três eventos que geraram estruturas compressionais e metamorfismo regional na fácies xisto-verde nas rochas do Quadrilátero Ferrífero, além dos eventos distensivos que ocorrem entre eles, caracterizando cada ciclo. Baltazar e Lobato (2020) sintetizam os eventos orogênicos e as fases de deformação correspondentes, conforme a Tabela 1.

O evento Arqueano Rio das Velhas (ca. 2,7 Ga), responsável pela inversão das bacias Nova Lima e Maquiné, com deformação associada de caráter compressivo (eixo N-S), cujas estruturas desenvolvidas são consideradas como condicionantes da mineralização de ouro nos principais depósitos (Baltazar e Lobato, 2020). Segue-se um evento distensivo, associado à Orogenia Minas, durante o Arqueano tardio e o Paleoproterozoico, com sedimentação das rochas do Supergrupo Minas (Chemale et al., 1994). Em cerca de 2,0 – 2,2 Ga, durante a Orogênese Riaciana, são geradas novas estruturas compressivas de direção NE-SW e transporte de massa para NW. As principais estruturas dessa fase são os sinclinais regionais da Serra da Moeda, Curral, Dom Bosco, Santa Rita e Gandarela (Figura 7). A Orogênese é seguida por uma fase de colapso orogenético que pode ter originado as estruturas em domo-e-quilha do Quadrilátero Ferrífero (Alkmim e Marshak, 1998). O último evento teria ocorrido no Neoproterozoico, durante a Orogênese Brasiliana e teria gerado zonas de cisalhamento de direção NE-SW, lineação de estiramento mergulhando para ESE, dobras apertadas a isoclinais com vergência para W e foliação S-C indicando movimento reverso de topo para W (Baltazar e Lobato, 2020).

Tabela 1 - Síntese da evolução estrutural do Rio das Velhas e sequências Proterozoicas no Quadrilátero Ferrífero. (Retirado de Baltazar e Lobato, 2020).

Tectonic Event	Phase	Regimen	Tectonic Transport	Main Structures
Rio das Velhas orogeny	D1[1]	Compressive, simple shear	NNE to SSW	NNW-striking, dextral transcurrent shear zone; ENE plunging, tight to isoclinal, 'z' intrafolial folds. E-striking, S-verging transpressive shear zone; S-verging tight to isoclinal folds. Inversion of the Nova Lima basin.
	D2[1]	Compressive, simple shear	ENE to WSW	NNW-striking thrust shear zones. Reactivation of D1 shear zones. NW-verging, ENE-plunging tight to isoclinal folds. ENE-plunging stretching/mineral lineation. Inversion of the Maquiné basin.
Minas orogeny	D3[2]	Compressive, simple shear	SE to NW	NE-striking, NW-verging thrusts. NW-verging tight to open folds. Stretching and mineral lineations plunging towards SE. EW- striking crenulation cleavage. Inversion of the Minas and Sabará basins.
	DE[2]	Extensional	WNW to ESE	Uplift of granite- gneissic basement as domes. Normal faults around the domes. Intermontana Itacolomi basins.
Araçuaí orogeny	D4[3]	Compressive, simple shear	E to W	NS-striking, W-verging thrusts. W-verging tight to isoclinal folds and open, normal folds. Stretching and mineral lineations plunging towards ESE. NS-striking crenulation cleavage. Inversion of the Itacolomi basin.

3.1 Depósitos Auríferos

Os depósitos de ouro do *greenstone belt* arqueano Rio das Velhas, no Quadrilátero Ferrífero (Figura 10), são comumente associados ao Grupo Nova Lima em todos os seus níveis estratigráficos (Lobato e Vieira, 1998), na base do Supergrupo Rio das Velhas. São classificados como do tipo *lode-gold* orogênicos no sentido de Groves et al. (1998), apresentando características similares a outros depósitos de mesmo tipo que ocorrem pelo mundo, em outros crátons Arqueanos.

Os depósitos auríferos localizados na extensão NW do Quadrilátero Ferrífero (e.g. minas Faina, Turmalina e São Sebastião; Figura 10), hospedam-se em sequências metavulcanossedimentares, englobadas no *Greenstone Belt* de Pitangui, as quais são consideradas como cronocorrelatas ao Grupo Nova Lima, do Supergrupo Rio das Velhas (e. g. Romano et al., 2013; Brando-Soares et al., 2017). Entretanto, trabalhos recentes sugerem evoluções tectono-magmáticas distintas para esses cinturões baseadas em diferenças entre assinaturas geoquímicas das rochas máficas (Verma et al., 2017), e entre idades das fontes das rochas metassedimentares (ca. 2694 Ma; Melo-Silva et al., 2020).

As mineralizações auríferas são hospedadas por formações ferríferas bandadas, metacherts, rochas metavulcânicas ultramáficas, máficas e félsicas e metassedimentares (i.e.

metapelitos, metagrauvacas e metaconglomerados), e são controladas estruturalmente por zonas de cisalhamento e de charneiras de dobras, associadas às estruturas compressivas desenvolvidas no Arqueano (Baltazar e Zucchetti, 2007). Esses autores descrevem mineralizações controladas por estruturas de direção NW, com vergência para SW, em escala regional. Em escala de depósito, os corpos auríferos são confinados a estruturas de segunda e terceira ordens, relacionadas a zonas de cisalhamento do tipo *strike–slip* e dobras redobradas. Na escala dos corpos de minério, observa-se uma grande variedade de estruturas com mineralização associada, incluindo interseções de falhas e dobras. Corpos de alto teor, geralmente, constituem zonas de charneira em forma de charuto, podem ser boudinados e interrompidos. O *plunge* dos corpos de minério é geralmente subparalelo à direção NW, mas pode estar transposto por estruturas posteriores.

Esses depósitos têm sua formação relacionada aos estágios tardios de deformação e metamorfismo do *greenstone belt* Rio das Velhas. O minério desenvolveu-se durante a deformação compressiva à transpressiva ao longo do orógeno Arqueano (e.g. Lobato e Vieira, 1998; Lobato et al., 2001, 2007; Junqueira et al., 2007; Martins Pereira et al., 2007; Ribeiro-Rodrigues e Lobato, 1999; Ribeiro-Rodrigues et al., 2000; Baltazar e Zucchetti, 2007; Vial et al., 2007). Uma idade de mineralização de 2672 ± 14 Ma foi obtida por datação U-Pb SHRIMP, em cristais de monazita hidrotermal associadas a pirita aurífera nas jazidas Morro Velho e Cuiabá (Lobato et al., 2007). Recentemente, Martins et al. (2016) obteve outra idade U-Pb SHRIMP em monazitas do depósito Lamego, nas proximidades do depósito de classe mundial Cuiabá (Figura 10), em 2730 ± 42 Ma; porém, estes autores obtiveram também uma idade U-Pb em xenotima no mesmo depósito em 518,5 ± 9 Ma, reacendendo o debate sobre a importância dos diversos ciclos tectônicos no condicionamento e geração dos depósitos auríferos.

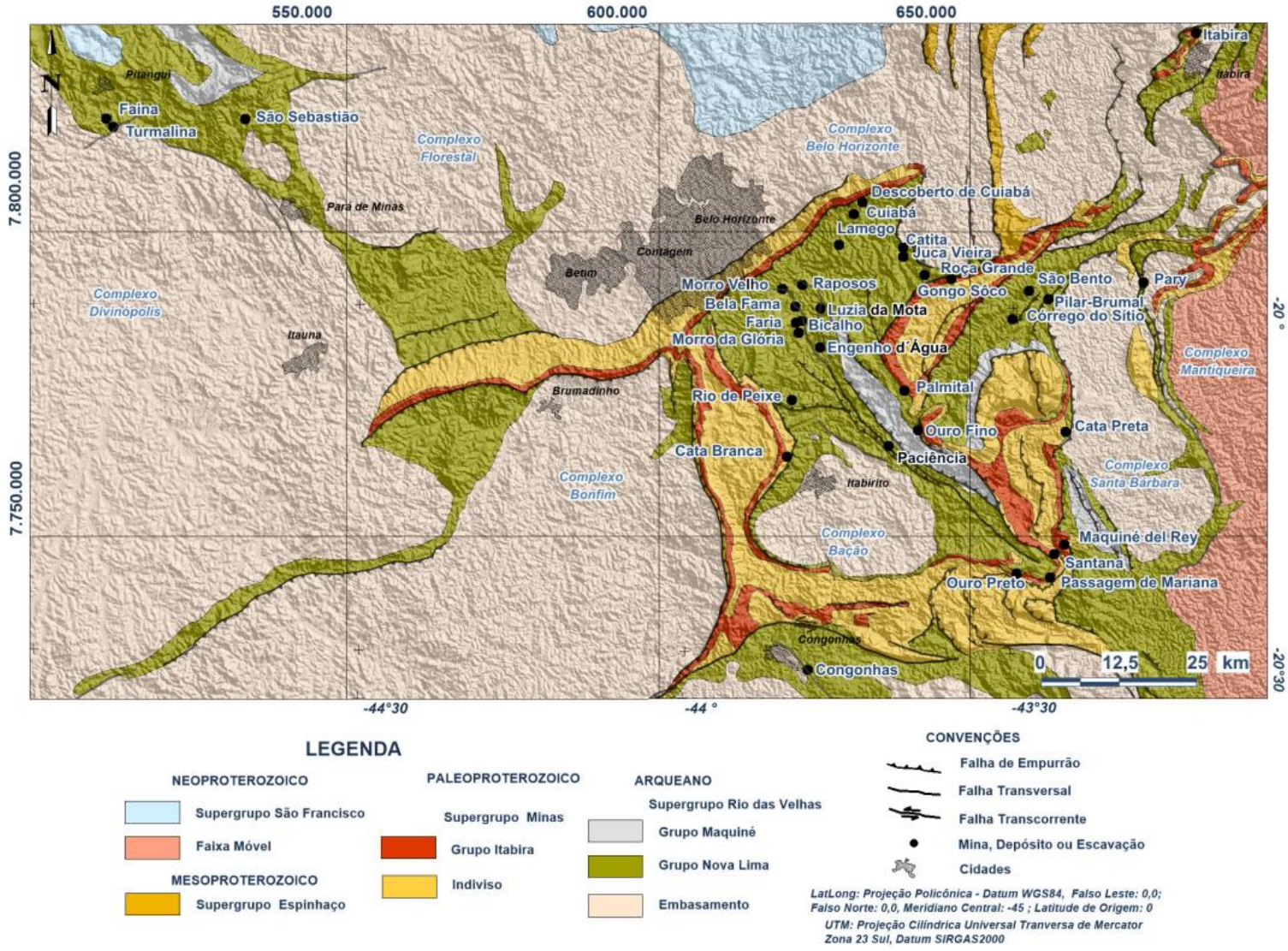

Figura 10: Depósitos, minas e escavações auríferos hospedados no Supergrupo Rio das Velhas, Quadrilátero Ferrífero e arredores. Retirado de Lobato e Costa, 2018 (baseado nos mapas elaborados por Dorr, 1969; Zucchetti e Baltazar 1996; Pinto e Silva 2014)

3.1.1 Lineamento Aurífero Córrego do Sítio

A área de pesquisa deste trabalho está inserida no contexto da borda leste do Quadrilátero Ferrífero (Figura 7), onde são encontradas mineralizações auríferas do tipo *lode*, hospedadas nos metaturbiditos e xistos do Grupo Nova Lima e associadas a lineamentos estruturais de direção NE-SW. Essas mineralizações compõem importantes corpos de minério, tais como Cachorro Bravo, Laranjeiras, Cristina, Rosalino, Grota Funda, Carvoaria, entre outros (Figura 11; Lima, 2012; Sequeto-Pereira et al., 2013; Roncato et al., 2015). Lima (2012) propôs a denominação Lineamento Aurífero Córrego do Sítio para o conjunto de depósitos nessa região, relacionados ao alinhamento NE-SW, com aproximadamente 15 km de extensão, e que possuem mineralizações auríferas com características litoestratigráficas semelhantes. O Lineamento Aurífero Córrego do Sítio engloba as zonas de cisalhamento Córrego do Sítio, Cristina e São Bento-Donana (Figura 11).

De acordo com Porto (2008) e Lima (2012), na área do Lineamento Córrego do Sítio aflora uma sequência metassedimentar turbidítica metamorfisada em fácies xisto verde, composta pela alternância entre grauvacas e filitos, caracterizando ciclos incompletos de Bouma (1983). Diques e *sills* metamáficos apresentam-se subparalelos ou discordantes à sequência.

De acordo com Porto (2008) e Lima (2012), na área do Lineamento Córrego do Sítio aflora uma sequência metassedimentar turbidítica metamorfisada em fácies xisto verde, composta pela alternância entre grauvacas e filitos, caracterizando ciclos incompletos de Bouma (1983). Diques e *sills* metamáficos apresentam-se subparalelos ou discordantes à sequência.

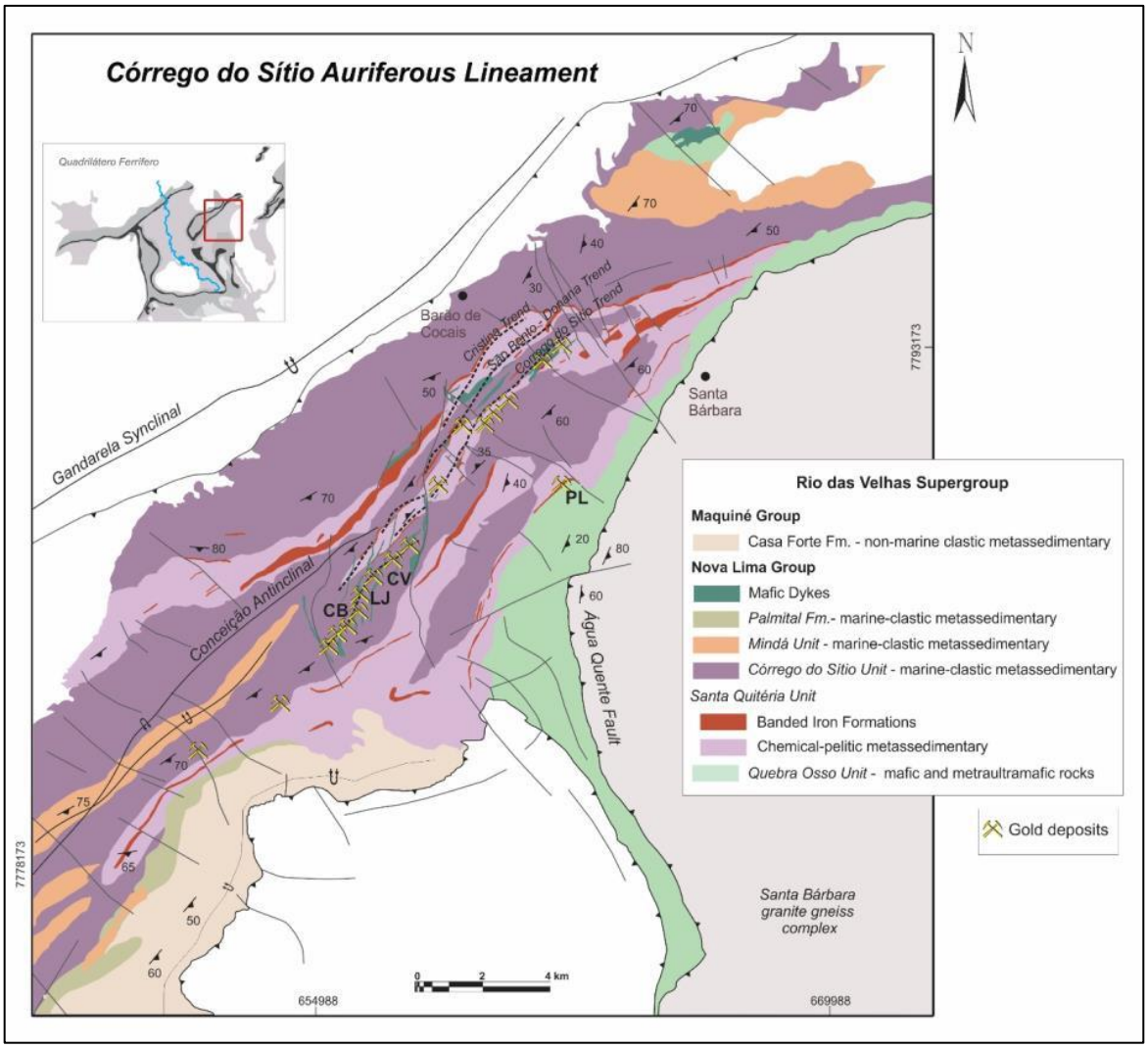

Figura 11: Mapa geológico com os principais depósitos auríferos associados ao Lineamento Córrego do Sítio (CdS) – Cachorro Bravo (CB); Laranjeiras (LJ); Carvoaria (CV) e o depósito de Pilar (PL), observados na área de pesquisa (figura original a partir de dados de Lobato et al., 2005, Lima, 2012 e Sequetto-Pereira et al., 2013).

Lima (2012) subdivide a Unidade Córrego do Sítio, no sentido de Zucchetti e Baltazar (1998), nas sequências Superior, Intermediária e Inferior (Figura 12):

- Unidade Córrego do Sítio Superior: metagrauvacas com lentes de filitos carbonosos subordinados, caracterizando ciclos de Bouma incompletos. O acamamento apresenta granodecrescência normal ou invertida.

- Unidade Córrego do Sítio Intermediária: metapelitos carbonosos com xistosidade anastomosada, venulações quartzo-carbonáticas, de espessuras milimétricas a métricas e microdobramentos, localmente transpostos segundo o plano axial de dobras assimétricas. Esta unidade destaca-se pela mineralização em veios de quartzo-carbonato que contêm ouro, sulfetos e sulfossais disseminados. O contato superior e o inferior são bruscos.

- Unidade Córrego do Sitio Inferior: metapelitos carbonosos intercalados a camadas de metagrauvaca, com ciclos de Bouma incompletos, camadas e lentes métricas-decamétricas de formação ferrífera bandada subordinadas, com raras camadas magnéticas, e intercalações de xisto carbonoso.

O Lineamento Córrego do Sítio encontra-se no contexto do Anticlinal Conceição (Dorr et al., 1969), uma dobra homoclinal de direção NE-SW, com mergulho para SE. Essa megaestrutura está localizada entre o sistema de falhas Fazendão (direção NNW-SSE), a leste, e o sinclinal Gandarela, (direção NE-SW) a oeste, relacionado ao sistema de falhas Fundão-Cambotas (Figura 13). A estruturação desse setor do Quadrilátero Ferrífero se deu em regime transpressivo, com inversão estratigráfica (Chemale Jr. et al., 1994).

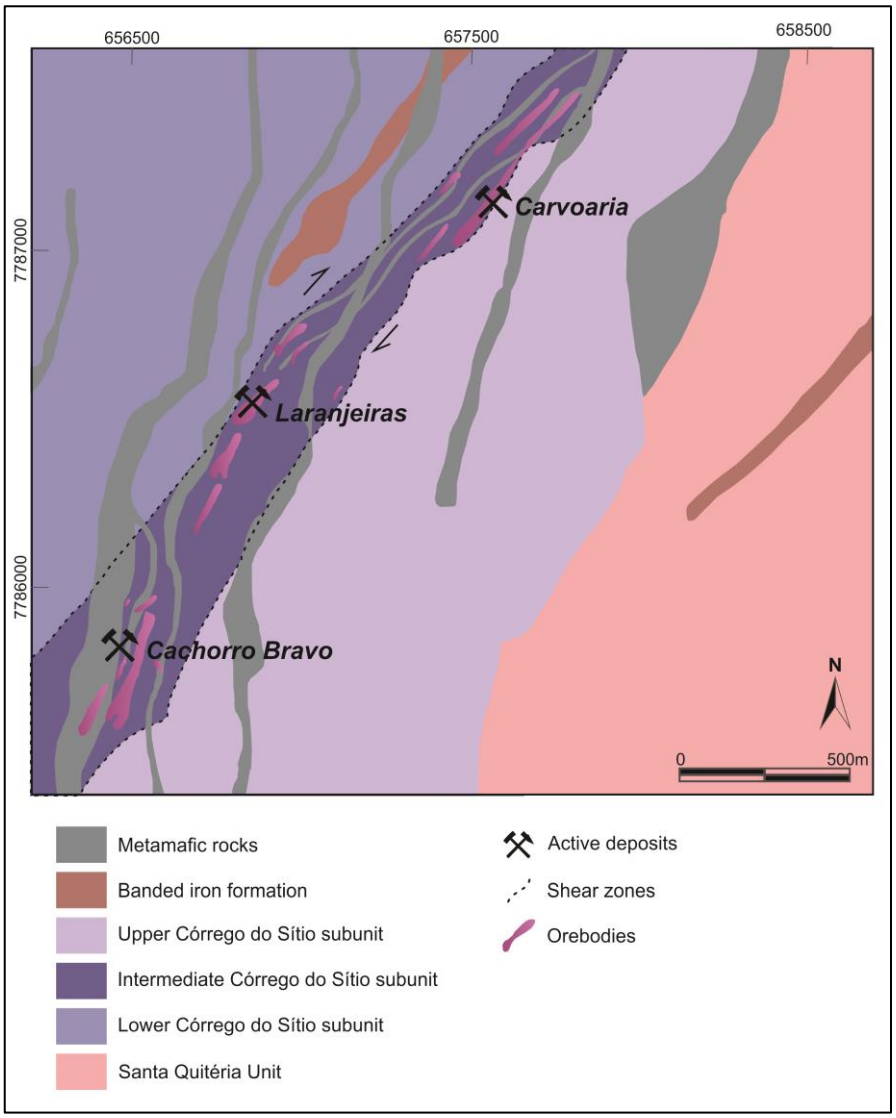

Figura 12: Mapa geológico do setor central do Complexo de depósitos auríferos Córrego do Sítio, com os principais depósitos ativos: Cachorro Bravo, Laranjeiras e Carvoaria. Modificado de Sequetto-Pereira et al. (2013).

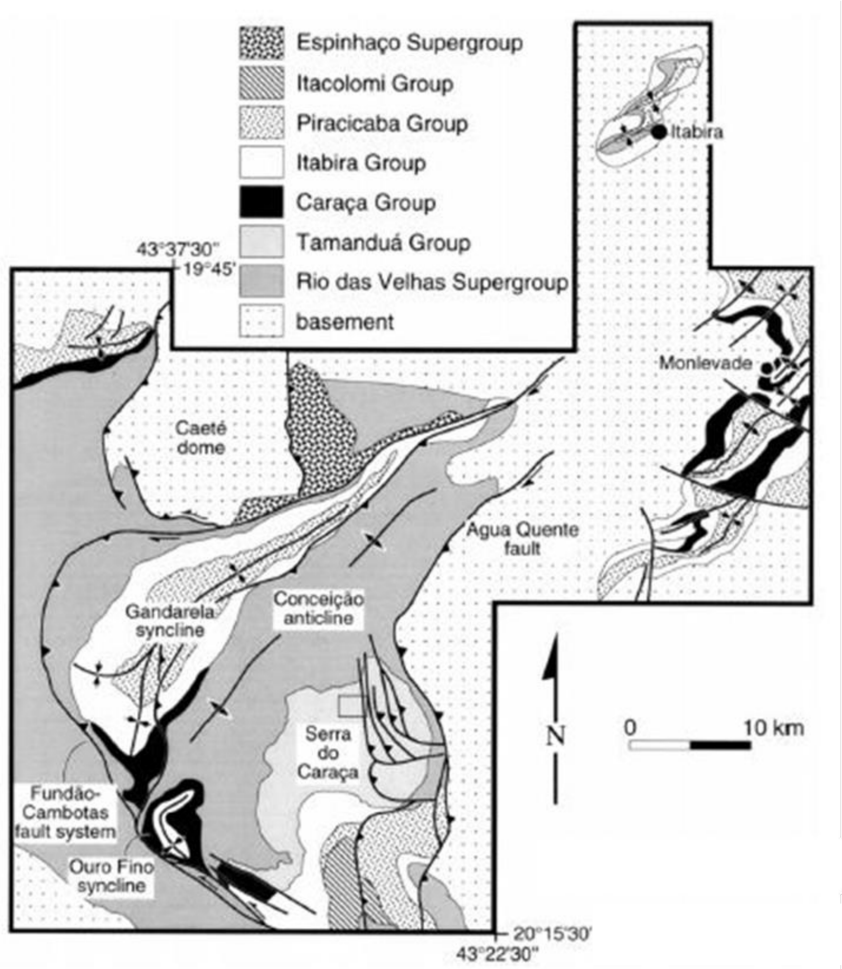

Figura 13: Mapa geológico da porção nordeste do Quadrilátero Ferrífero e e contexto estrutural regional onde se insere o Lineamento Córrego do Sítio (Alkmim e Marshak, 1998).

3.1.2 Depósito Pilar

O depósito Pilar, de propriedade da *Jaguar Mining Inc*., situado no Complexo Mineiro de Caeté, localiza-se a leste do Lineamento Córrego do Sítio (Figura 11 e Figura 14), na porção nordeste do Quadrilátero Ferrífero, entre o embasamento Arqueano composto por granito-gnaisses do Complexo Santa Bárbara e o Supergrupo Rio das Velhas.

O depósito está situado entre as rochas granito-gnáissicas arqueanas do Complexo Santa Bárbara, em sua porção leste, e pelo Supergrupo Rio das Velhas, a oeste, que mostram uma configuração estratigraficamente invertida com as rochas mais antigas, representadas pelo Grupo Quebra Osso, sobre os litotipos mais jovens do Grupo Nova Lima (Figura 15 e Figura 16). O Grupo Quebra Osso é representado por rochas ultramáficas xistificadas e talcificada, tais como talco xisto, clorita-talco xisto e serpentinito. O Grupo Nova Lima compreende rochas sedimentares, vulcânicas e vulcanoclásticas, deformadas e metamorfisadas na fácies xisto verde, intrudidas por diques de rochas máficas e entrecortadas por veios de quartzo. As rochas do Grupo Quebra Osso, identificadas na porção central da área, estão posicionadas na base da

coluna estratigráfica da área e estão em contato tectônico, por zonas de empurrão, com as rochas do Grupo Nova Lima em sua unidade inferior (Ladeira, 1980).

Na região de Santa Bárbara, ocorrem zonas de empurrão representadas pelo sistema de falhas reversas e de empurrão denominado de Água Quente (Figura 13; Dorr, 1969). Esse sistema se encontra a leste da área do depósito e é um dos responsáveis pela estruturação atual deste setor do Quadrilátero Ferrífero, onde as rochas mais antigas foram sobrepostas sobre as mais jovens (Ferreira Filho et al., 2001). Este conjunto litológico apresenta-se intensamente hidrotermalizado e intemperizado.

A mineralização hospeda-se nas rochas ultramáficas (talco xistos) do Grupo Quebra Osso, e em rochas metamáficas e metapelíticas (carbonato-albita-clorita-quartzo xisto, quartzo-clorita xisto e xisto carbonoso), e nas BIF's, do Grupo Nova Lima. Essas sequências são intersectadas por veios de quartzo ± carbonato (Silva, 2007; Rios Guerrero, 2016; Pressaco e Sepp, 2018).

Trata-se de sequência dobrada (isoclinal) invertida, limitada por zonas de cisalhamento e falhamento inverso, que cortam unidades do Supergrupo Rio das Velhas. Os corpos mineralizados são concordantes às estruturas principais, segundo a direção NE-SW, em uma geometria *stratabound*, com ouro em bandas de sulfetos maciços, que ocorrem em grãos dispersos, em junções e em agregados granulares de formato irregular dispostos ao longo e substituindo carbonatos de ferro nas BIF's.

Arsenopirita e pirrotita são os minerais de sulfeto mais importantes nos corpos mineralizados. Pirita, calcopirita, galena e esfalerita estão comumente presentes como minerais acessórios. As zonas mineralizadas podem ser hospedadas ainda por xistos metavulcânicos que ocorrem na borda leste do depósito Pilar (Silva, 2007; Rios Guerrero, 2016; Pressaco e Sepp, 2018).

A mineralização aurífera apresenta-se de forma disseminada na formação ferrífera (BIF), associada aos sulfetos (arsenopirita e pirrotita), em zona de charneira do dobramento e associada à zona de cisalhamento, ou como ouro livre nos veios de quartzo-carbonáticos.

Passos (1999) caracteriza as feições de alteração hidrotermal na área do depósito como relacionadas a processos tardios, associadas aos veios quartzo-carbonáticos. A Tabela 2 sintetiza as zonas de alteração hidrotermal reconhecidas para as rochas metaultramáficas, metamáficas e metassedimentares.

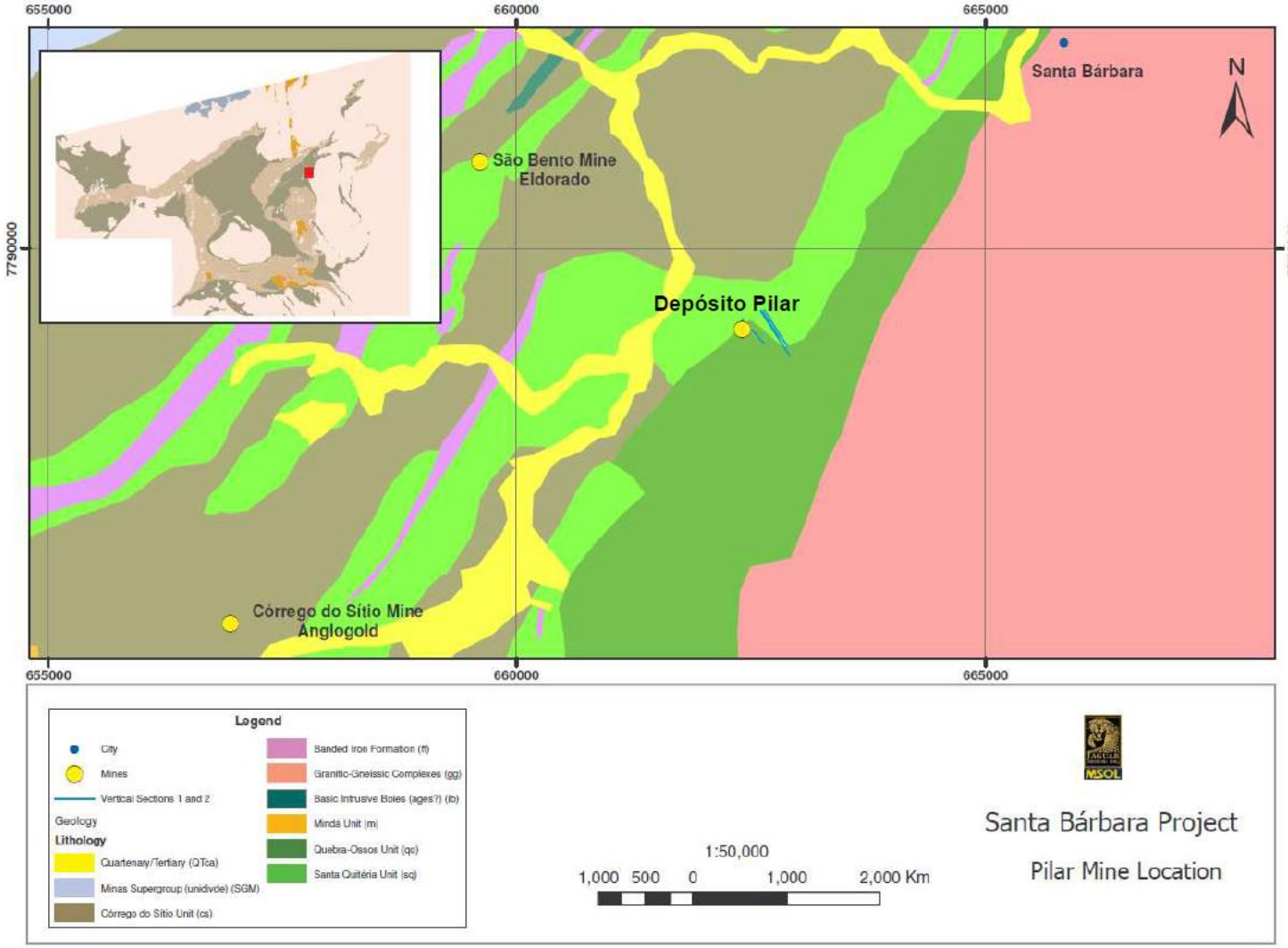

Figura 14: Mapa geológico da região de Santa Bárbara/Barão de Cocais com a localização do depósito Pilar. Retirado de Silva (2007). Baseado em MSOL/Jaguar Mining Inc. (2005).

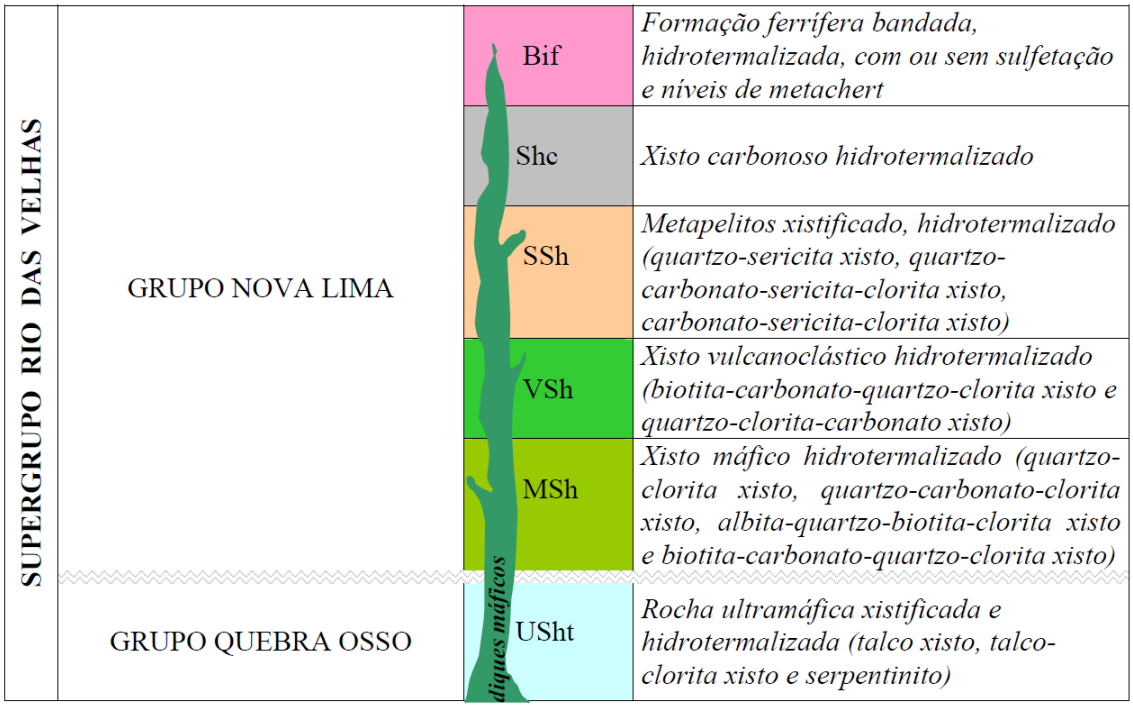

Figura 15: Estratigrafia do Depósito Pilar (Silva, 2007)

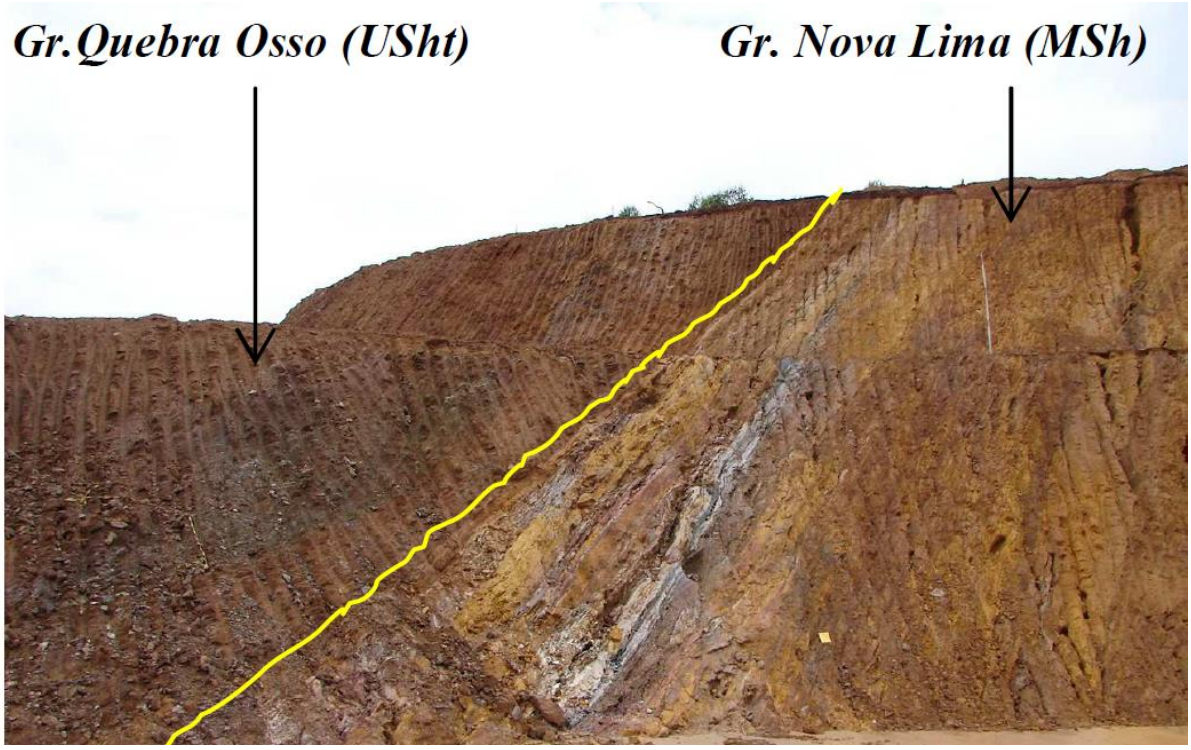

Figura 16: Contato entre o Grupo Quebra Ossso e o Grupo Nova Lima, em exposição na área do depósito Pilar (Silva, 2007).

Tabela 2: Síntese das paragêneses das zonas de alteração hidrotermal para o Depósito Pilar (Passos 1999).

Zona de Alteração Hidrotermal	Rochas Sedimentares	Rochas Máficas	Rochas Ultramáficas
Pré-alteração	?	Tremolita/actinolita+clorita+ plagioclásio+titanita+ epidoto	Serpentina+tremolita/actinolita+clorita+talco
Zona da Clorita	?	Clorita+plagioclásio+biotita+ carbonato ± tremolita/actinolita	Talco+clorita+dolomita+ quartzo
Zona do Carbonato	Ankerita/dolomita+muscovita+ quartzo+clorita ± turmalina	Dolomita/calcita+clorita+albita+ quartzo±biotita±sericita±pirita	Talco+dolomita±pirita
Zona da Sericita	Muscovita+cloritóide+dolomita /ankerita+clorita+quartzo	Dolomita±muscovita±biotita ±clorita+albita	?
Formação Ferrífera			
Zona do Stilpnomelano	Siderita±ankerita+estilpnomelano+quartzo+clorita+sulfetos		
Zona do Carbonato	Siderita+ankerita+quartzo±sulfetos		

4 ARTIGO I – EDIACARAN – CAMBRIAN FLUID FLOW IN ARCHEAN OROGENIC GOLD DEPOSITS: evidence from U-Pb shrimp hydrothermal monazite ages of the metaturbidite-hosted Córrego do Sítio and Pilar deposits, Quadrilátero Ferrífero, Brazil

Tatiana Gonçalves Dias[1], Rosaline Cristina Figueiredo e Silva[1], Lydia Maria Lobato[1,2], Fabricio de Andrade Caxito[1], Steffen Hagemann[3], João Orestes Schneider Santos[4], Vitor Barrote [5,6]

1 – Programa de Pós-Graduação em Geologia, Instituto de Geociências, Universidade Federal de Minas Gerais (IGC-UFMG), Belo Horizonte, MG, Brazil.

2 – HydroFluids&Minerals (HF&M)

3 – Centre for Exploration Targeting, University of Western Australia, Perth, WA, Australia

4 – Universidade do Estado do Amazonas, Manaus, AM, Brazil

5 – Freie Universität Berlin, Institut für Geologische Wissenschaften, Geochemie, Malteserstr. 74-100, 12249, Berlin, Germany

6 – ISOTOPIA Lab, School of Earth, Atmosphere and Environment, Monash University, Wellington Rd, Clayton, VIC 3800, Australia

Artigo publicado na revista *Journal of South American Earth Sciences*, https://doi.org/10.1016/j.jsames.2022.103844

ABSTRACT

Archean orogenic gold deposits are hosted in the Rio das Velhas greenstone belt in the eastern sector of the Quadrilátero Ferrífero, Southern São Francisco Craton region, southeastern Brazil. These include the gold deposits along the NE-trending Córrego do Sítio lineament, stretching for some 15 km, and the Pilar deposit, object of the present study. These deposits occur in an area close to boundary of the São Francisco craton, which is commonly interpreted to have preserved the Archean and Paleoproterozoic crust from the effects of Ediacaran-Cambrian Araçuaí orogenic front. The gold deposits were formerly interpreted as exclusively Archean (ca. 2.7 Ga). However, recent geochronological data suggest the imprint of late Ediacaran-Cambrian Brasiliano Orogeny in host rocks of these deposits, as structural modification or hydrothermal alteration assemblages that postdates Archean mineralization. To elucidate those issues, contextual (thin section) in-situ U-Pb SHRIMP dating was conducted on hydrothermal monazite crystals from the Carvoaria and Cachorro Bravo deposits of the Córrego

do Sítio lineament and from the Pilar gold deposit. Hydrothermal monazite in mineralized metapelites from Carvoaria yielded a U-Pb Discordia with intercepts at 2,514 ± 22 Ma and 555 ± 19 Ma. Three younger, age-equivalent crystals are concordant and yield a U-Pb Concordia age of 539 ± 9 Ma, identical within uncertainties to the lower intercept age. Monazite from the Cachorro Bravo deposit yielded U-Pb Concordia ages of 551 ± 10 Ma and 510 ± 11 Ma. Monazite from the veined (silicified) sulfide-schist from the Pilar deposit is depleted in U, precluding the calculation of robust U-Pb ages, and disclosed a mean $^{208}Pb/^{232}Th$ average age of 508.2 ± 6.4 Ma. These results reinforce the proposal of a strong Cambrian imprint related to the final stages of the Brasiliano orogenic event, affecting Archean gold deposits throughout the Quadrilátero Ferrífero. Consequently, the results point to the importance of mapping Brasiliano-related structures that control the spatial arrangement of the gold deposits, such as the Córrego do Sítio lineament, consisting of an important exploration target. This major NE-SW trending strike-slip shear zone hosts several gold deposits and might represent an Archean structure reactivated during the Brasiliano Orogeny that possibly led the large volume of Ediacaran-Cambrian post-collisional hydrothermal fluids among the east sector of the Quadrilátero Ferrífero.

Keywords: gold deposits, U-Pb SHRIMP geochronology, hydrothermal monazite, Archean greenstone belt

4.1 Introduction

World-class orogenic gold deposits of the Quadrilátero Ferrífero (QF) region, eastern Brazil, are hosted in the Archean (2.8-2.7 Ga) Rio das Velhas greenstone belt, which consists of one of the most important metallogenetic provinces of the world (Figura 17; Lobato et al., 2001a). Orogenic gold deposits make up an important type of mineralization, which provide approximately a third of the world's reserves (Frimmel, 2008). In the QF (Figura 17), this type of deposit is mainly associated with banded iron formation (BIF) and quartz-sulfide veins (lode-type) located in major structures such as shear zones and fold hinges (Lobato et al., 2001 a, b; Martins et al., 2016).

Despite the historical and geological significance of the QF province, some aspects of the genesis, timing and structural control of the gold mineralization on the Rio das Velhas greenstone belt are not yet completely understood. The deposits occur in all stratigraphic levels and units of the Nova Lima Group (Lobato & Vieira, 1998), and are thought to be related to the late stages of Archean deformation and metamorphism (e.g. Lobato et al., 2001, 2007; Noce et

al., 2007; Junqueira et al., 2007; Martins Pereira et al., 2007; Baltazar & Zucchetti, 2007; Vial et al., 2007). Although the Quadrilátero Ferrífero region occurs in an atypical configuration, crosscut by the accepted limit of the southern tip of the Archean/Paleoproterozoic São Francisco Craton and the thrust fronts of the Ediacaran/Cambrian Araçuaí Orogen to the west, the main gold deposits are classically interpreted as related to Archean mineralization (e.g. Lobato et al., 2001a, b; Araújo et al., 2020; Baltazar and Lobato, 2020). However, recent geochronological data suggest the influence of a Ediacaran – Cambrian orogeny event in structuring of host rocks of some of the gold deposits, as indicated by an U-Pb age of 518.5 ± 9 Ma, obtained on xenotime crystals from mineralized mafic volcanic rocks from the Lamego deposit, although an expressive hydrothermal alteration record, and the possibility of having reached the gold deposits, has not been confirmed at this time (Martins et al., 2016), as suggested by Figura 18.

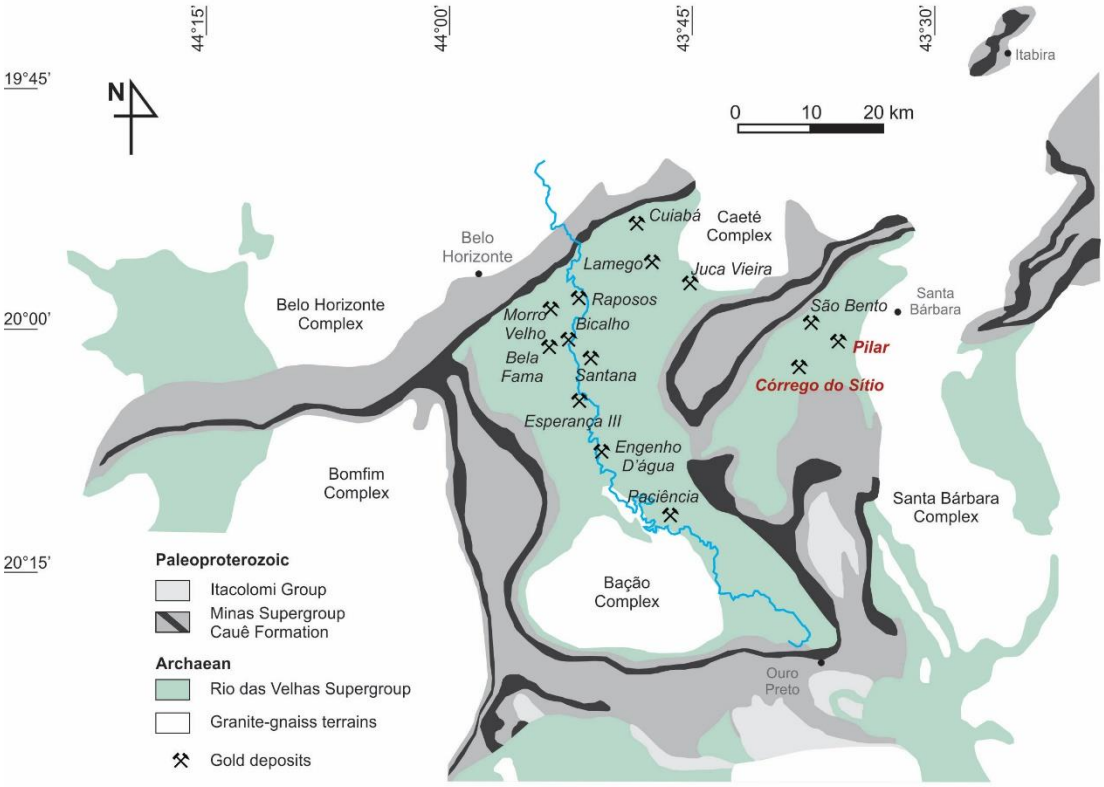

Figura 17: Simplified map of the Rio das Velhas hosted main gold deposits in the Quadrilátero Ferrífero province. Based on Dorr (1969), Alkmim & Marshak (1998), Lobato et al. (2001). The studied deposits are in red.

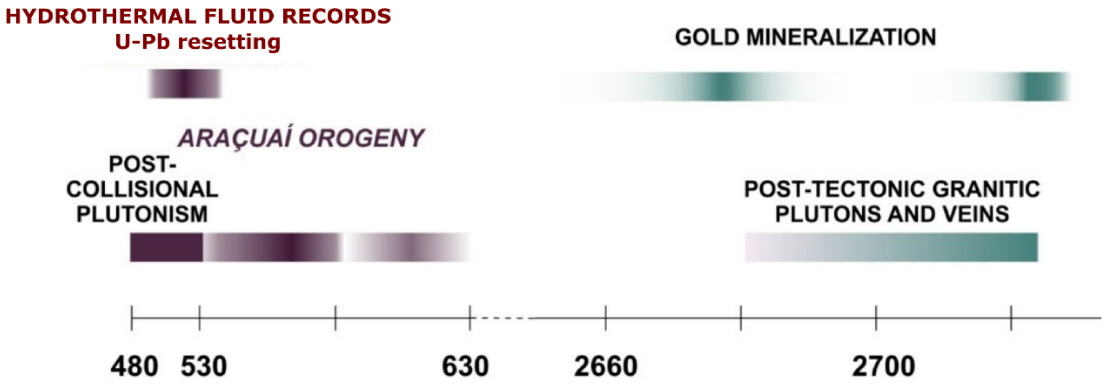

Figura 18: Simplified chronology of evolution of the QF showing relationship between igneous activity, gold mineralization Archean age, and the intensive generation of hydrothermal fluid related to the Ediacaran-Cambrian Orogeny. Modified after Lobato et al. (2001a).

Although gold deposits related to Archean terrains are commonly associated with a single hydrothermal event, they may have been formed at different periods during the supercontinent cycle (Groves et al., 1998). For example, recent studies in vein-hosted gold deposits related to the Statherian Capricorn Orogen, at the southern margin of the Pilbara Craton in Western Australia, demonstrate that gold occurrences in this domain show different radiometric ages, with peaks at ca. 1.7 and 2.4 Ga (U-Pb SHRIMP; Fielding et al., 2018). This emphasizes that, in the absence of robust, precise and accurate radiometric ages of both host rocks and mineralization, even spatially related gold deposits with similar characteristics must be treated separately. Radiometric data can provide insights to correlate the deformational, metamorphic and mineralization processes in a regional tectonic framework. Hence, a detailed radiometric study can be applicable to elucidate the tectonic evolution of the Rio das Velhas greenstone belt and associated gold mineralization in southeastern Brazil.

In order to obtain precise and accurate radiometric ages that can be used to link the evolution of gold deposits with regional events, when it is not possible to apply methods directly on ore minerals, such as sulphides, detailed petrographic information is necessary to characterize which datable accessory minerals can be used for this task. One major difficulty is that datable minerals are commonly very fine (< 10 μm long) and show irregular habits, with exquisite shapes oriented in the foliation planes, making physical separation by standard crushing, sieving, gravimetric and magnetic methods very difficult. Alternative sample preparation methods were proposed for cases where petrographic information is crucial to establish the paragenetic and textural correlations between datable gangue minerals and ore minerals, allowing *in-situ* ion microprobe study of delicate accessory minerals in thin sections (Rayner and Stern, 2002; Rasmussen and Fletcher, 2010).

The techniques of *in-situ* dating of minerals directly on thin sections require small volumes of sample. This method has the advantage of not being invasive and destructive as the time-consuming mineral separation techniques from ground rock matrix and avoid potential contamination by exogenous grains and allows retaining petrographic and textural information. In fact, retaining the petrographic and paragenetic information (i.e., contextual dating) is essential to demonstrate the genetic relationship between ore-generating hydrothermal events and datable minerals, since the original surface of the sample is preserved. The high spatial resolution and small quantity of sample required for ion microprobe analyses allow the analysis of individual, irregularly shaped, <10 μm-long crystals, which would be very hard to separate through standard techniques.

When it comes to hydrothermal ore deposits, or even major pulses of hydrothermal and metamorphic events, monazite is one of the most reliable geochronometers for U-Pb dating, due its high blocking temperature at ca. 700°C (Schandl & Gorton, 2004). In this study, we present the first SHRIMP (Sensitive High Ion MicroProbe) U-Pb in-situ dating of hydrothermal monazite in distinct mineralized orebodies of the Córrego do Sítio and Pilar orogenic gold deposits, hosted by Archean sequences encompassed in the Rio das Velhas greenstone belt, located in the eastern sector of the QF. The results reinforce the discussion about the importance of Ediacaran-Cambrian events on mobilizing young fluids over existing Archean mineralization.

4.2 Geological Setting

4.2.1 Regional context of the QF region

The QF province encompasses an area of about 7,000 km^2 in the southern São Francisco Craton. It marks the eastern border of the craton with the Ediacaran-Cambrian west-verging thrust-and-fold belt of the Araçuaí Orogen (Alkmim et al., 2006; Endo et al., 2020). It comprises three main units (Fig. 11; Dorr et al., 1957): (i) Archean metamorphic complexes composed of TTG suites and high-K granites; (ii) typical greenstone belt sequences of the Rio das Velhas Supergroup (Rio das Velhas greenstone belt); and (iii) metasedimentary rocks of the Paleoproterozoic Minas Supergroup.

The Archean TTGs are represented by dome-shaped structures, such as the Bação, Belo Horizonte, Caeté, Santa Bárbara, and Bonfim complexes, which typify the crystalline basement (Teixeira et al., 2000). This TTG crust presents a tectonomagmatic polyphase evolution, recognized in the Santa Bárbara (3,220–3,200 Ma), Rio das Velhas I (RV I, 2,930–2,900 Ma)

and Rio das Velhas II (RV II, 2,800–2,770 Ma) events. In the eastern sector of the QF, the basement is represented by the Santa Bárbara Complex, interpreted to have been the first magmatic pulse in the evolution of the southern São Francisco Craton dated at 3,212 ± 9 and 3,210 ± 8 Ma (Lana et al., 2013).

The Rio das Velhas Supergroup (RVSG; Loczy & Ladeira, 1976), previously known as Rio das Velhas Series (Dorr et al., 1957), encompasses Archean metavolcanosedimentary sequences formed from 2.80 to 2.78 Ga (Baltazar & Zucchetti, 2007). The first proposals of stratigraphic subdivisions for the Rio das Velhas greenstone belt were put forward by Dorr et al. (1957), with the establishment of the lower Nova Lima and the upper Maquiné groups. Schorscher (1978) further proposed the Quebra Ossos Group at the base of the Rio das Velhas Supergroup, which is composed of komatiitic flows interlayered with BIF.

According to Ladeira (1980), the Nova Lima Group is comprised, from the base to the top, of metavolcanic, chemical metasedimentary and clastic metasedimentary units. It hosts the major auriferous deposits of the QF. Following the proposals of Pedreira & Silva (1996), Baltazar & Pedreira (1996, 1998) and Zucchetti & Baltazar (2000), Baltazar & Zucchetti (2007) proposed a subdivision of the Rio das Velhas greenstone belt based on the concept of sequence stratigraphy applied to Archean terrains (after Eriksson et al., 1994). Accordingly, seven lithofacies associations developed during four sedimentary cycles (Figura 19), in a tectonic configuration controlled by the Nova Lima–Caeté, Santa Bárbara and São Bartolomeu tectonic blocks.

- Cycle 1 (2.80 – 2.78 Ga) comprises basal mafic-ultramafic volcanism and deposition of a chemical volcanosedimentary association in an initial extensional stage with oceanic basin development.

- Cycle 2 is related to the deposition of a clastic-chemical-sedimentary association, the distal turbidites of the resedimented association that occur in the eastern sector of the QF, and the coastal association at the final extensional stages and initial subduction stages.

- Cycle 3 is composed of a volcanoclastic and a resedimented association during the orogenic phase, in an island arc setting.

- Cycle 4 comprises a non-marine association and deposition in foreland-basin settings.

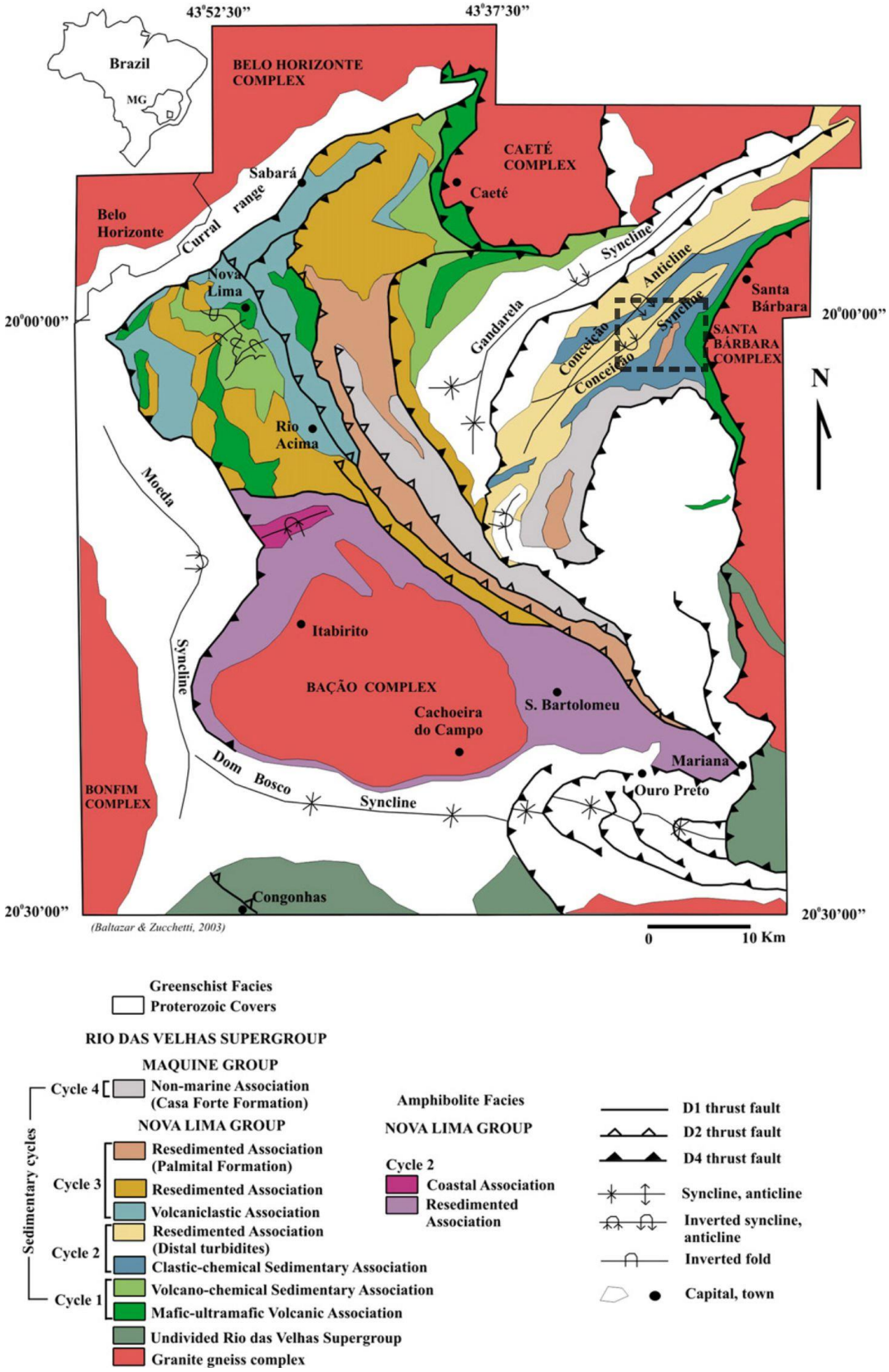

Figura 19 : Lithofacies associations of the Rio das Velhas Supergroup (Baltazar & Zucchetti, 2007). Studied area is highlighted in the dashed square.

The metasedimentary sequence of the Minas Supergroup (Dorr, 1969; Babinski et al., 1991; Renger et al., 1995) overlies the Rio das Velhas Supergroup, and is composed of both clastic and chemical rocks (Alkmim and Marshak, 1998). This unit is well represented in the ridges that design the outstanding "quadrangle" shape of the QF.

Different models of deformation and tectonic development of the QF have been proposed since Dorr (1969), which suggests a multiphase model, with at least three main compressive tectonic–metamorphic events intercalated with extensional events (e. g. Alkmim & Marshak, 1998; Baltazar & Zucchetti, 2007; Baltazar & Lobato, 2020).

The first compressional episode is related to the NE-SW tectonic transport in the Archean (ca. 2.7 Ga). The second event, of extensional nature, was responsible for the Minas Supergroup sedimentation in the late Archean and Paleoproterozoic (Chemale et al., 1994).

The second compressional event, around 2.2 – 2.0 Ga, is characterized by the development of NW-verging compressive structures related to the Transamazonian Orogeny. The major regional structures of the QF, such as the Serra da Moeda, Curral, Dom Bosco, Santa Rita and Gandarela regional synclines, are also thought to be developed during this orogeny. The Transamazonian Orogeny was followed by an orogenic collapse phase, which was responsible for the dome-and-keel features of the QF (Alkmim & Marshak, 1998).

A last compressive event is responsible for the development of N-S trending shear zones, E to ESE-plunging stretching lineations, tight to isoclinal west verging folds and S-C structures with reverse top-to-W displacement. The trend of those structures is parallel to the Ediacaran-Cambrian Araçuaí Orogen to the east, and thus those structures are believed to have been formed during the Brasiliano Orogeny and western Gondwana amalgamation.

Despite several controversies about the importance and age of each of these events during the tectonic evolution of the QF, most authors agree with the occurrence of three main compressive events. Besides the importance for developing structures and greenschist facies metamorphism, these events might have influenced the percolation of hydrothermal fluids that were very important to the generation of the mineral deposits in the QF.

4.2.2 Geological context and gold mineralization of the Córrego do Sítio Lineament and Pilar deposits

The main gold mineralizations in Archean greenstone belts around the world are related to BIF and mafic rocks metamorphosed under upper-greenschist to middle-amphibolite facies conditions. The gold deposits are developed mainly in greenstone terranes dominated by

anastomosing sets of crustal-scale shear zones resulting in broadly linear arrays of orebodies (Groves et al., 2018). Likewise, the Rio das Velhas greenstone belt hosts several deposits, in which structural styles and the associated hydrothermal alteration control the regional distribution and the shape of gold-mineralized bodies.

The clastic metasedimentary sequences of the Resedimented Association of the Rio das Velhas greenstone belt host a significant set of gold deposits in the northeastern portion of the QF. These occur along the NE-SW trending Córrego do Sítio lineament (Figura 20; CdS), proposed by Lima (2012) to refer to all gold occurrences hosted in the metasedimentary sequences that encompass those of the Córrego do Sítio, Cristina and São Bento-Donana shear zones. In this region, the Nova Lima Group is represented mainly by the Córrego do Sítio Unit (Baltazar & Silva, 1998), which is considered by Baltazar & Zuchetti (2007) as one of the most abundant clastic metasedimentary units of the Rio das Velhas greenstone belt. This sequence is cut by NNE-striking and SE-dipping mafic dykes and sills. (Canale, 1999; Porto 2008, Lima 2012; Sequetto-Pereira et al., 2013; Ribeiro et al., 2013; Roncato et al., 2015).

The Córrego do Sítio lineament is a NE-SW trending steep to vertical-dipping structure marked by the development of shear zones with S-C fabrics, mainly visible in carbonaceous phyllites, indicating dextral shear. The S planes are subparallel to a pervasive S_{1-2} foliation with modal maxima at ca. 119/70 (dip direction). A rarely observed sericite mineral lineation indicates strike-slip to oblique movement, at ca. 45/45 (trend/plunge) (Roncato et al., 2015). The metavolcanosedimentary rocks affected by the Córrego do Sítio lineament are unformally grouped under the denomination Córrego do Sítio Unit.

The Córrego do Sítio Unit is composed of metagraywackes, quartz metagraywackes, quartzites and metapelites, besides subordinate metric-decimetric BIF layers. This association is considered by many authors (Baltazar & Silva 1998; Baltazar & Zuchetti, 2007; Porto, 2008; Lima, 2012; Roncato et al., 2015) as an incomplete Bouma (1983) turbiditic sequence. The gold mineralization is hosted in carbonaceous phyllite and in, at least, five quartz-carbonate vein systems with sulfide (arsenopyrite, pirrotite, pyrite, chalcopyrite) and sulfosalts (stibnite and berthierite; Pereira et al., 2013; Ribeiro et al., 2015).

The main deposits of the Córrego do Sítio Lineament, namely Cachorro Bravo, Carvoaria and Laranjeiras, near 10 km from the town of Santa Bárbara, Minas Gerais state, are related to the Intermediate subunit of the Córrego do Sitio Unit (Lima, 2012), distinguished by a significant zone of hydrothermal alteration on carbonaceous phyllite, with sulfide and sulfosalts in quartz-carbonate (ankerite) veins. However, there are some distinct features

between these deposits in terms of hydrothermal alteration assemblages of the host rocks, regarding the mafic dykes occurrence. The Cachorro Bravo deposit is confined by metamafic dikes, while the Laranjeiras and Carvoaria are unrelated to these igneous intrusions and show berthierite, stibnite and pyrite as a particular mineral assemblage. At Cachorro Bravo, located in the southernmost portion of the main deposits of CdS Lineament (Figura 20), the ore zone is related to intense silicification, which occurs at the stratigraphic break between metasedimentary and metamafic rocks, with quartz-carbonate-bearing veins (Roncato et al., 2015). Studies by Ribeiro et al. (2013) recognized that the ore-forming fluids are mainly metamorphic, or magmatic, mixed with meteoric waters.

The Pilar deposit, located on the Caeté Mining Complex, is located east of the Córrego do Sítio Lineament (Figura 20), between the Archean basement composed of granite-gneisses of the Santa Barbara Complex and the Rio das Velhas Supergroup. The mineralization is hosted in the supracrustal sequence of the Rio das Velhas Greenstone Belt, from base to top; in the Quebra Osso Group (Schorscher, 1978), which comprises ultramafic rocks (talc schists), and in metamafic and metapelitic rocks, described as carbonate-albite-chlorite-quartz schist, quartz-chlorite schist and carbonaceous schist, and in BIF's, of the Nova Lima Group. These sequences are intersected by quartz ± carbonate veins (Rios Guerrero, 2016; Pressaco & Sepp, 2018).

The gold mineralization at the Pilar deposit is hosted by a folded sequence in a stratabound geometry, with gold-bearing in bands of massive sulfides, that occur in scattered grains, in seams, and in irregular-shaped granular aggregates disposed along and replacing iron carbonates-rich bands of the BIFs. Arsenopyrite and pyrrhotite are the most important sulphide minerals in the mineralized bodies. Pyrite, chalcopyrite, galena and sphalerite are commonly present as accessory minerals. Furthermore, the mineralized zones can be hosted by a distinct stratigraphic package of meta-volcanic schists occurring at the eastern border of the Pilar deposit (Rios Guerrero, 2016; Pressaco & Sepp, 2018).

4.2.3 Structural Setting

The designation Córrego do Sítio auriferous structural lineament was proposed by Lima (2012), that comprise NE-SW direction shear zones, with associated gold mineralization. In its SW extension (Figura 20), the Córrego do Sítio lineament comprises six deposits, where the Cachorro Bravo and Carvoaria are included. Four deformation episodes, at least, are recognized in the Córrego do Sítio Lineament (Roncato et al., 2015), which affected the compositional and gradational banding S_0. The first event D1 produced a progressive foliation $S_{1\text{-}2}$, striking NNE,

and dipping to ESE, reflected in tight, asymmetric, isoclinal and disharmonic, kink folds. The D2 structures comprise a crenulation cleavage and a spaced crenulation cleavage S_3, which strikes NNE crosscutting the S_{1-2}. The D3 episode formed large-scale, open folds, which distorted S_0, S_{1-2} and S_3. Parallel fractures, spaced from centimetres to metres along with open folds or subordinate kink folds with high angle vertical axial plane, striking mainly towards NW, refers to the D4 event.

The vein systems framework In the Córrego do Sítio Lineament is intimately related to the set of structural elements. As detailed by Ribeiro et al. (2015), the veins are classified as: V1 veins – quartz-ankerite-pyrite-berthierite-gold – parallel to the main regional foliation S_n,; V2 veins – quartz-ankerite-pyrite – related to the extensional crenulation cleavage S_{n+1}, and rarely gold mineralized; V3 veins – quartz-ankerite – oriented according S_{n+3} fractures, free of sulfides and sulfosalts; V4 veins – quartz-calcite – with restricted occurrence, linked to metamafic dikes and sills, with no preferential orientation.

The Pilar deposit is related to an inverted isoclinal fold, striking ENE and dipping to SSE, limited by shear zones and inverse faulting, moving to the N-S direction towards the south of the mine property. At the deposit scale, at least three different orientations of faults are recognized. The earliest fault is correlated to the northeasterly-striking regional thrust fault, which delineates the Nova Lima Group different sequences interfaces. This thrust fault is cross-cutted by a northerly set of faults, which is striking approximately 020° and dip steeply to the east. The third set of faults are oriented in an east-west orientation and have subvertical dips (Rios Guerrero, 2016; Pressaco & Sepp, 2018).

4.3 Previous geochronological data

Radiometric data obtained from hydrothermal monazite associated with gold-bearing sulfides constrain the age of the giant Cuiabá and Morro Velho gold deposits (Figura 30) at ca. 2,672 ± 14 Ma (U-Pb SHRIMP; Lobato et al., 2007). However, in the nearby Lamego deposit (Figura 30), while monazite crystals yielded a similar Archean age (2,730 ± 42 Ma) using the same method, a Cambrian age at 518.5 ± 9 Ma was yielded by xenotime crystals (Martins et al., 2016), suggesting the imprint of the Ediacaran-Cambrian Brasiliano Orogeny. This highlights the importance of distinct phases of the orogenic cycles and associated fluid flow produced over the lode gold deposits. Gonçalves et al. (2019) suggests that fluid circulation derived from orogenic collapse-related magmatism of the Araçuaí Orogeny, represented by the the G4 (530 – 500 Ma) and G5 (520 – 480 Ma) granitoid supersuites (Pedrosa-Soares et al., 2011; Gradim et al., 2014; De Campos et al., 2016), could have imprinted similar modifications

with U-Pb ages between 515 to ca. 495 Ma, in hydrothermal minerals related to mineralized systems from the São Francisco craton and Araçuaí belt (Southern Espinhaço Range and QF).

The Brasiliano imprint in mineral deposits of the QF has also been observed on specular hematite-rich palladiferous lode gold deposits, known as Jacutinga, in Minas Gerais. These ore compose the Platiniferous Gold-palladium Belt (PGB; e.g. Cabral et al., 2006) and are hosted in itabirites of the Cauê Formation, which comprises a Paleoproterozoic banded iron formation from the Minas Supergroup. In the Itabira district, located on the far northeast of the QF (Figura 30), monazite from lode gold veins yielded an U-Pb age of 495.6 ± 2.2 Ma (uncalibrated age, U-Pb, LA-SF-ICP-MS; Cabral et al., 2015). A very similar age was recorded, through the same method, in xenotime crystals of 496.3 ± 2.0 Ma, from the Passagem de Mariana lode gold deposit, at the southernmost border of the PGB (Cabral & Zeh, 2015).

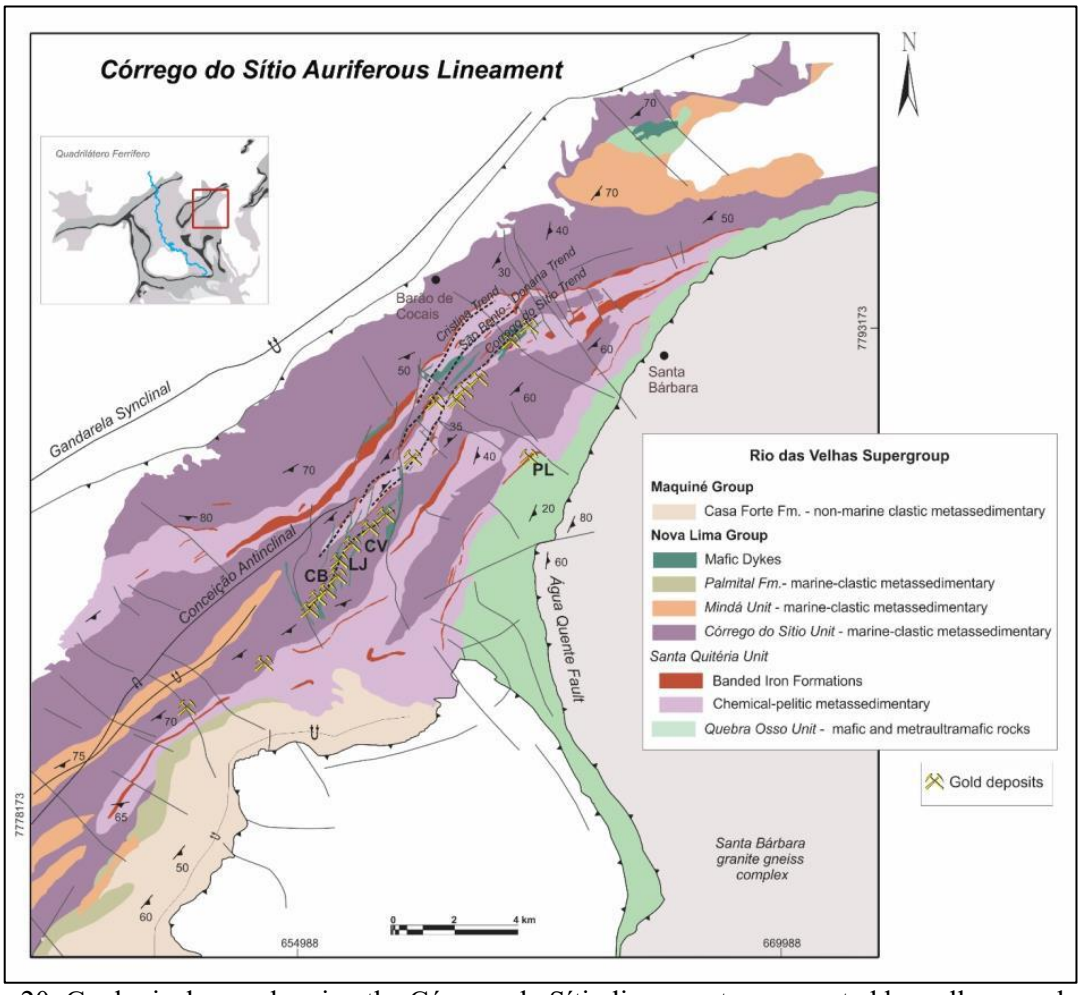

Figura 20: Geological map showing the Córrego do Sítio lineament, represented by yellow symbols on gold deposits hosted by lithofacies associations of the Nova Lima Group of the Rio das Velhas Greenstone Belt, in the northeastern sector of the Quadrilátero Ferrífero province. The main active deposits are Carvoaria (CV), Laranjeiras (LJ) and Cachorro Bravo (CB), located in the central portion of the lineament. The Pilar deposit (PL) is located east of the CdS Lineament. Based on data from Lobato et al. (2005); Lima (2012); Sequetto-Pereira et al. (2013).

4.4 Sampling and Methods

Samples of mineralized sulphidised metapelites and veined plagioclase-sericite-quartz-carbonate schist were collected from two distinct deposits of the CdS Lineament and from the Pilar deposit, respectively. Polished thin sections were prepared for each sample and analyzed using optical and scanning electron microscopy techniques.

The polished and carbon-coated thin sections were mapped using a scanning electron microscope (SEM)-based TESCAN Integrated Mineral Analyser (TIMA). Identification of hydrothermal monazite was made using a TESCAN VEGA3 SEM equipped with an energy dispersive spectrometer (EDS) system and aZtec® software, located in the Centre for Microscopy, Characterization and Analysis (CMCA) at the University of Western Australia (UWA). Hydrothermal monazite is characterized by spectra with low or flat Th contents. Textural criteria, such as the occurrence of clusters of 5 to 20 crystals within a small area, were considered in choosing representative hydrothermal monazite from thin sections (e.g. Schandl & Gorton, 2004). Monazite may also occur as anhedral grains, some of which are intergrown with sulfides (pyrite and arsenopyrite), parallel to the main foliation, as in sample CB-01. The thin sections were micro-drilled to obtain plugs of 1 and 3 mm diameters around selected monazite grains, which were embedded in epoxy mounts, with diameter of 2.5 cm. This procedure produced five mounts: one mount for the CB-01 sample (CB01-1 mount), two for CV-01 sample (CV01-1 and CV01-2 mounts), and two for Pilar sample (mounts N16-05 and N16-06). The plugs were imaged at about four or five different magnifications by SEM, using both the secondary and back-scattered electron (BSE) detectors, and by optical microscopy.

The U–Th–Pb analyses were conducted at the Sensitive High Resolution Ion MicroProbe (SHRIMP II B) at Curtin University, Western Australia, during two 24 hour-sessions.

Sets of either eight or six cycles of scans were used for each analysis of the isotopic spectrum which were formed by the masses of ^{202}LaPO2, ^{203}CePO2, ^{204}Pb, ^{204}Background, $^{205.8}$NdPO2, ^{206}Pb, ^{207}Pb, ^{208}Pb, ^{232}Th, ^{245}yCeO, ^{254}UO, ^{264}ThO2, and ^{270}UO2, using a spot size of 10 μm. French monazite (Paquette et al., 1994) was used as the main standard, for initial Pb/U and Pb/Th age calibrations. The matrix corrections are based on elemental differences between French and the monazite crystals. The Z2234 of 1026 Ma (Stern & Sanborn,1998), ideal to calibrate ratios of Th-poor monazite, was used for further calibration of the Pb/U ratio, and the Z2908 (1796 Ma) as a monitor for the ^{207}Pb/^{206}Pb ratio.

The acquired data were processed using the SQUID 2.5 software (Ludwig, 2009) and the Concordia plots were constructed using Isoplot 3.0 (Ludwig, 2003). Input errors from SQUID-treated raw data are at 1σ and the calculated Concordia ages from Isoplot are presented at the 2σ level.

4.5 Results of in-situ U-Pb SHRIMP monazite analyses

4.5.1 Córrego do Sítio Lineament

In situ U-Pb analysis were performed on samples from the Cachorro Bravo and Carvoaria deposits, Córrego do Sítio lineament, named CB-01 (Figura 21 and Figura 22) and CV-01 (Figura 24 and Figura 25), respectively. Sample CB-01 is a carbonaceous phyllite, with abundant disseminated arsenopyrite with gold inclusions. The main hydrothermal minerals include quartz, carbonate (ankerite), white mica, chlorite and accessory rutile and apatite. Minerals in trace amounts include chalcopyrite, galena, sulfosalts and tetrahedrite. Rare earth-bearing phases are dominated by hydrothermal monazite, commonly associated with arsenopyrite (Figura 22). Minor to rare allanite, bastnaesite, xenotime and thorite are also present.

Most of the analyzed monazite crystals has minute rounded quartz inclusions, yielding a characteristic sieve-like texture (Figura 22 B). Their Th contents are extremely low (7–- 99 ppm), suggesting a hydrothermal/metamorphic affiliation (e.g. Kempe et al., 2008; Grand'Homme, 2016). A slight zoning is rarely observed by contrast of shades of gray in backscattering images. Eight spots in eight distinct crystals yielded concordant U-Pb data, which allowed the calculation of two Concordia ages, of 551 ± 10 Ma and 510 ± 11 Ma, with an older outlier with a of 582 ± 17 Ma $^{206}Pb/^{238}U$ age (Figura 23).

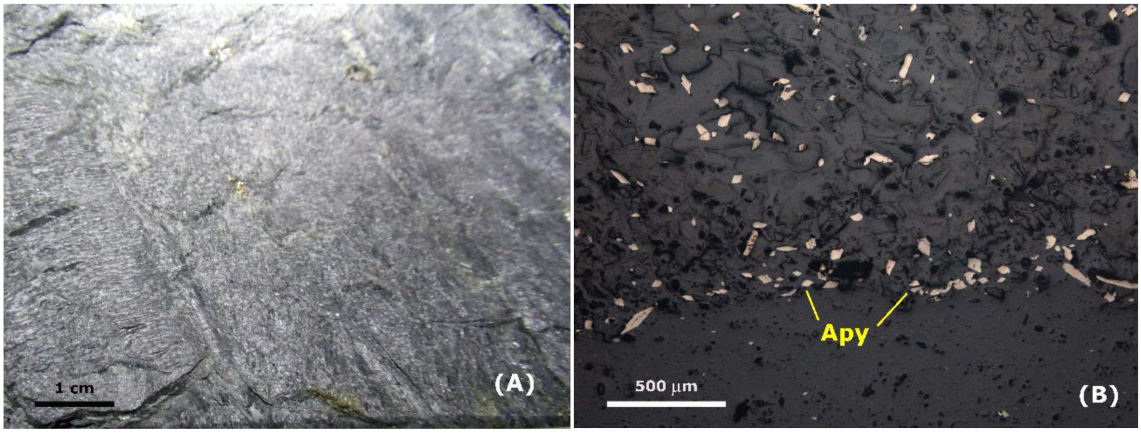

Figura 21: (A) Sampled outcrop of a mineralized zone site at Cachorro Bravo gallery; (B) Sample CB-01–- carbonaceous phyllite, with abundant disseminated arsenopyrite (reflected light).

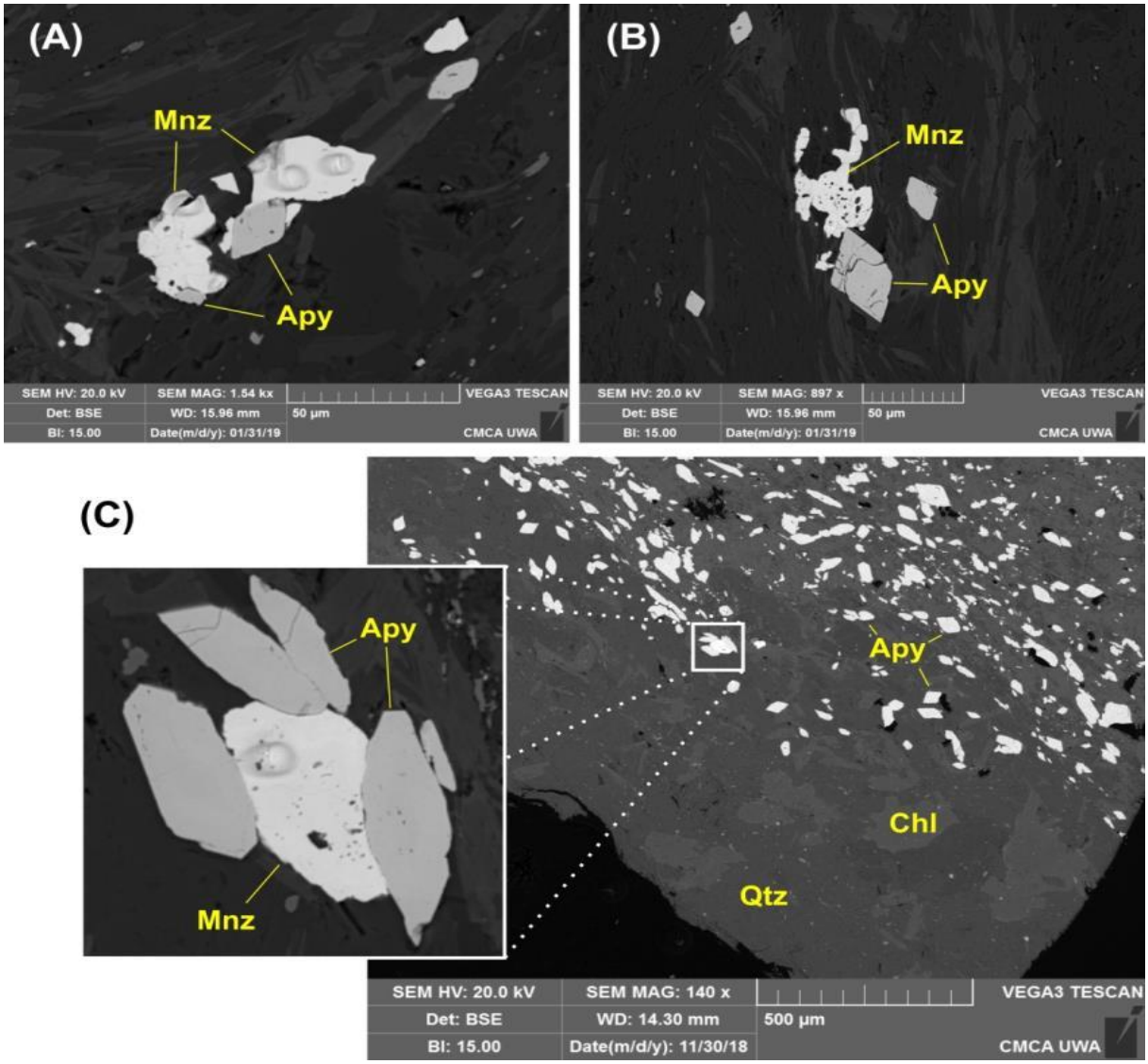

Figura 22: Representative back-scattered electron images of monazite (Mnz), sample CB01 (Cachorro Bravo orebody). The analyzed crystals are in association with arsenopyrite (Apy), the main gold-associated sulfide. (A) Smooth intergrowth of Mnz and Apy; (B) Mnz crystal in "sieve" habit, with high content in quartz inclusions, and in association with Apy; (C) Disseminated Apy in plug of thin section and detail for Mnz crystal surrounded by euhedral to subhedral Apy. The other minerals are quartz (qz) and chlorite (chl). Elliptical SHRIMP pits ca. 10 µm long and a few µm deep can be seen in the monazite crystals in (A) and (C).

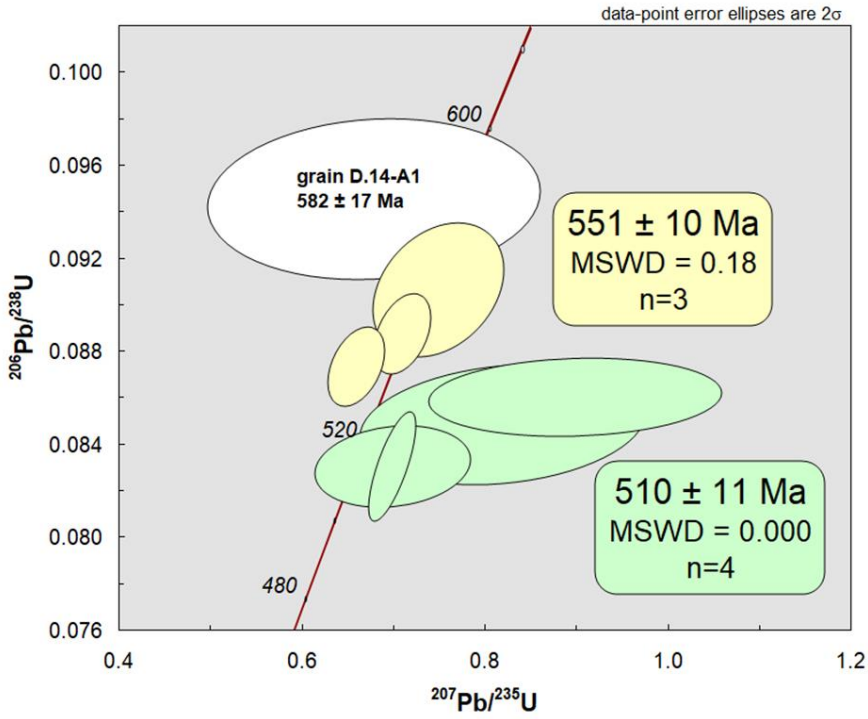

Figura 23 : Concordia diagram and plot of SHRIMP data for monazite from ore samples of the Cachorro Bravo deposit from the Córrego do Sítio lineament gold deposit (data in Table 1). Age uncertainties are at the 2σ level.

Sample CV-01 is characterized by a lower content of sulfides in relation to sample CB-01. Most of the monazites in CV-01 show a higher concentration of rounded quartz inclusions (Figura 25) in comparison to CB-01; they are elongated in the main foliation direction, generating anhedral crystals with a strong sieve aspect.

Thirteen spots in 11 different monazite grains yielded variably discordant data aligned in an array that define a Discordia regression with an upper intercept at 2514 ± 22 Ma and a lower intercept at 555 ± 19 Ma (Figura 26). The younger spots are concordant and age-equivalent, furnishing a Concordia age at 539 ± 9 Ma (MSWD = 1.5), identical within uncertainty to the lower intercept age (Figura 27). The older spot is also concordant and anchors the upper intercept at the Concordia curve in the late Neoarchean.

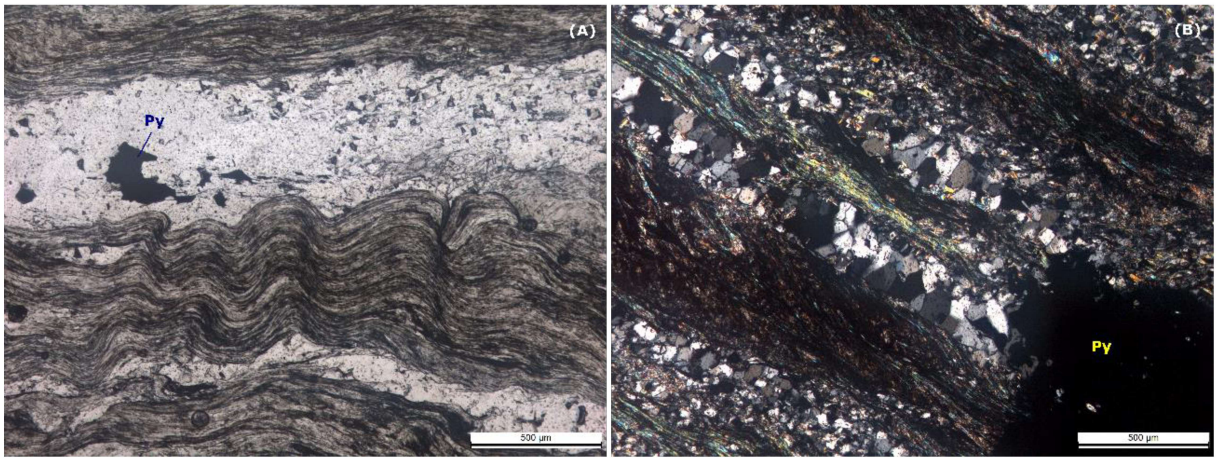

Figura 24: Photomicrograph of CV-01 sample: (A) quartz veinlets parallel to main foliation with disseminated sulfide and pyrite aggregates (Py); (B) alternating quartz and muscovite/sericite rich portions, with quartz veinlets.

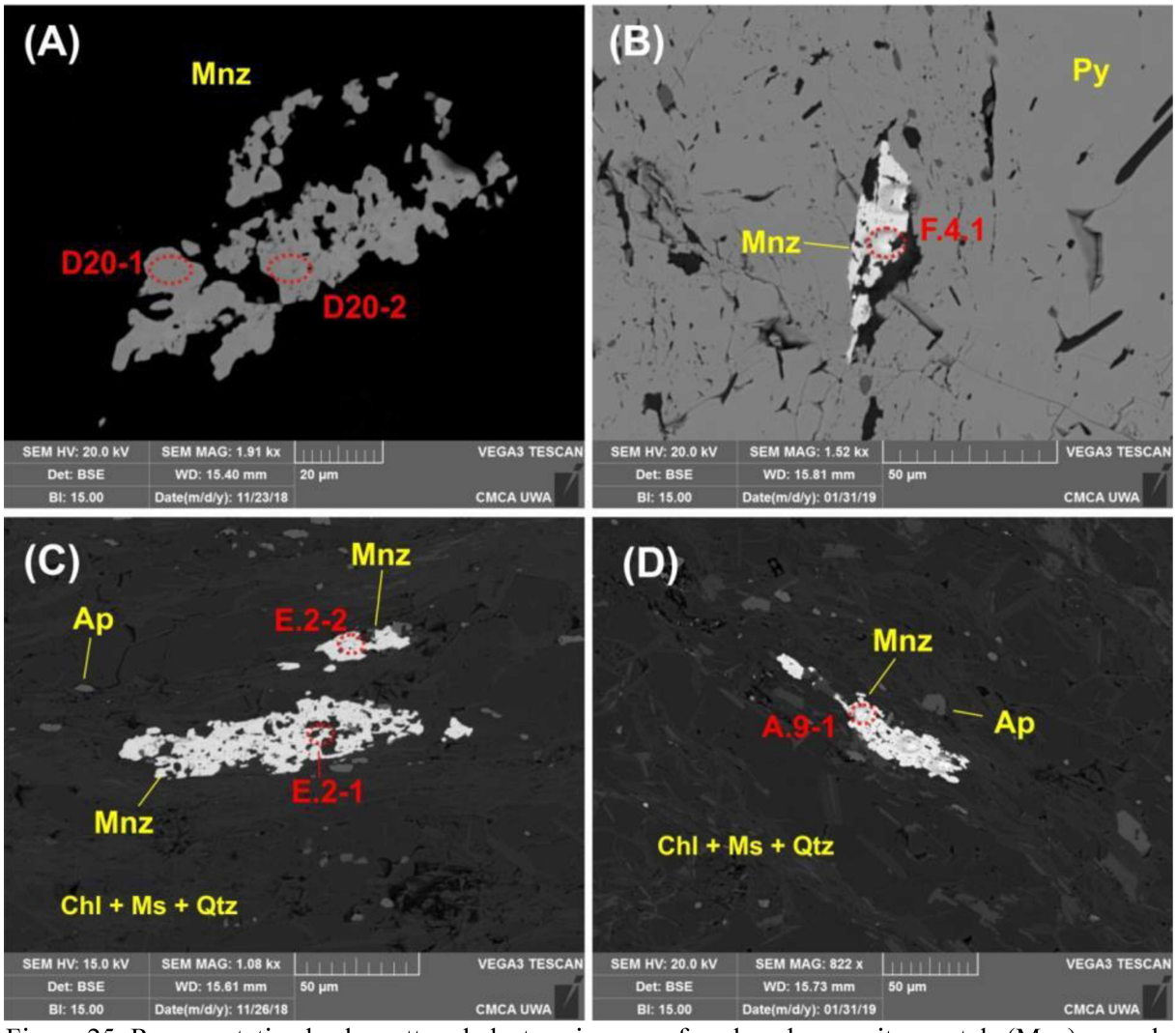

Figura 25: Representative back-scattered electron images of analyzed monazite crystals (Mnz), sample CV01 (Carvoaria ore). The red dashed ellipses represent the analyzed spots. (A) Monazite crystal with abundant rounded quartz inclusions; (B) Monazite crystal as inclusion in pyrite (Py); (C) and (D) show the monazite crystals parallel to the main foliation of the sample.

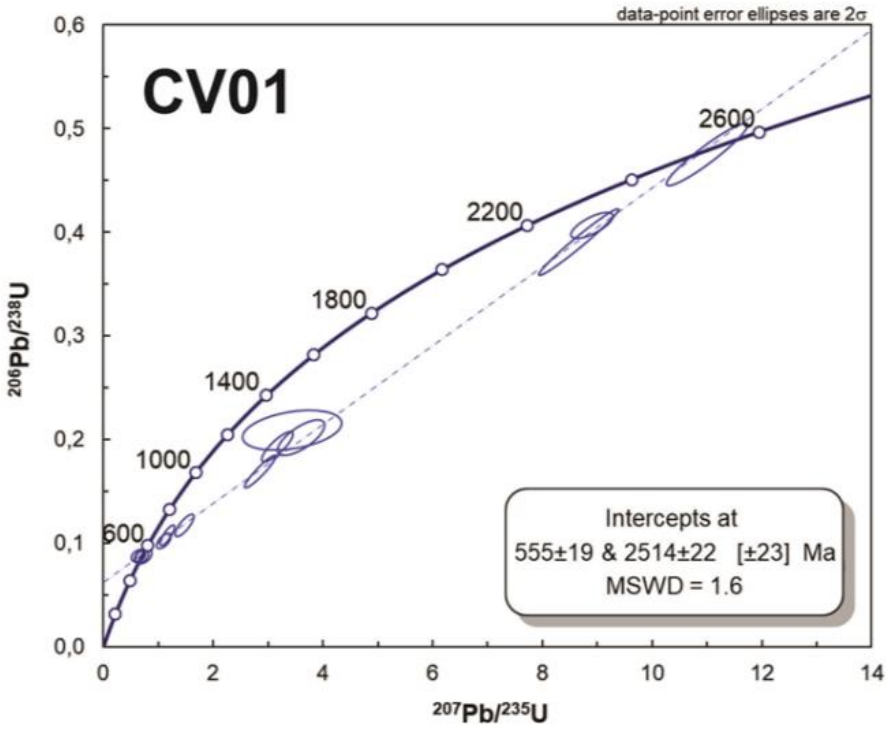

Figura 26: Plot of SHRIMP data for monazite from ore samples of the Carvoaria orebody from Córrego do Sítio gold deposit (data in Table 1). The Discordia regression yielded an upper intercept at 2,514 ± 22 Ma and a lower intercept at 555 ± 19 Ma. Uncertainties are at the 2σ level.

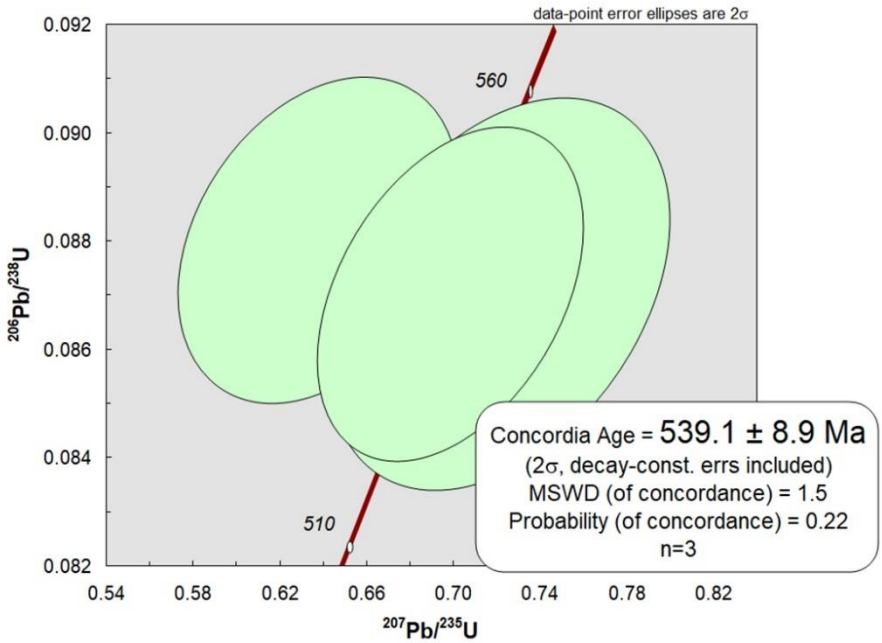

Figura 27: Plots of SHRIMP data from ore samples of the Carvoaria deposit from Córrego do Sítio lineament (data in Table 1) of the younger spots, which yielded a Concordia age of 539 ± 8.9 Ma (MSWD = 1.5).

4.5.2 Pilar Deposit

The in-situ U-Pb analyses of the Pilar deposit were performed on monazite crystals hosted in a quartz-plagioclase-veined (silicified) banded schist (Figura 28), identified as A21 BL15, which shows banding imposed by few alternating quartz ± sulphide-plagioclase veins. The rock is dominated by granoblastic plagioclase, sericite-muscovite, carbonate, sulphide minerals, with accessory chlorite, titanite,magnetite, and rutile. The veins contain coarse-grained albite crystals. Pyrrhotite, arsenopyrite, pyrite, arsenian pyrite and chalcopyrite represent the sulfide phases.

Average of U content of the 13 analyzed monazites is very low, at 22 ppm. Th content is low (average of 1536 ppm), typical of hydrothermal monazite. Monazites of this sample are more depleted in U relatively to the Cachorro Bravo (average U=464 ppm) and Carvoaria (U=286 ppm) deposits. The very low U and ^{206}Pb (1.48 ppm) precludes using ^{206}Pb/^{238}U ages. The amounts of ^{232}Th (1536 ppm) and ^{208}Pb (35 ppm) are much higher than ^{238}U and ^{206}Pb contents making the ^{208}Pb/^{232}Th ages more robust than the ^{206}Pb/ ^{238}U ages. Thirteen spots in twelve grains yielded a weighted mean ^{208}Pb/^{232}Th age of 508.2 ± 6.4 Ma (Figura 29).

Figura 28: Analyzed sulphidized quartz-plagioclase-veined (silicified) banded schist sample from Pilar deposit. (Py – pyrite crystals and aggregates).

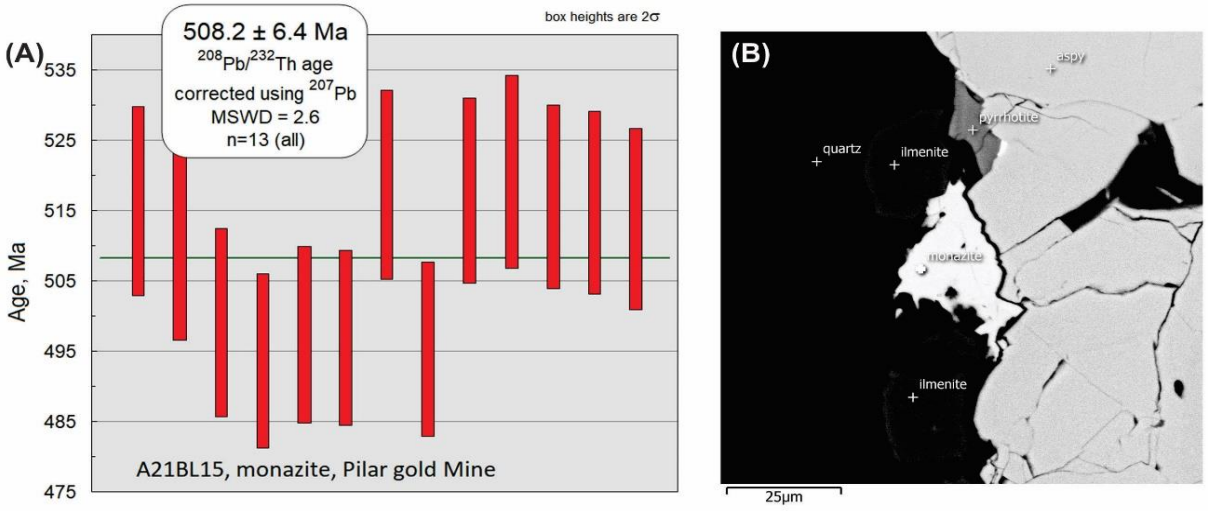

Figura 29: (A) Weighted average data of ^{207}Pb-corrected $^{208}Pb/^{232}Th$ data from monazite in ore samples of the Pilar deposit (data in Table 3), in paragenesis with arsenopyrite (aspy) as shown in the BSE image of (B).

Tabela 3: U–Th-Pb SHRIMP isotopic data (samples CB01- Cachorro Bravo and CV01- Carvoaria) from hydrothermal monazite, Córrego do Sítio gold deposits. All errors are at the 1σ level.

					Isotopic ratios									Ages				
Spot name	^{238}U	^{232}Th	$^{232}Th/^{238}U$	f206	$^{207}Pb/^{206}Pb$	err.	$^{207}Pb/^{235}U$	err	$^{206}Pb/^{238}U$	err.	err. corr.	**$^{208}Pb/^{232}Th$**	% err	$^{207}Pb/^{206}Pb$	err	$^{206}Pb/^{238}U$	err	Disc.
Cachorro Bravo	ppm	ppm		%		%		%		%			%		1σ		1σ	%
CB01-1.I.13B-1	482	95	0.203	0.83	0.055	3.5	0.66	3.8	0.0873	1.6	0.4	**13.9**	1.8	411	77	540	8	-33
CB01-1.I.13A.2	390	89	0.237	0.44	0.060	2.0	0.7	3.0	0.083	2.3	0.75	**12.9**	3.2	603	43	515	11	15
CB01-1.H2.1	583	57	0.101	4.65	0.070	15.4	0.82	15.6	0.0848	2.5	0.2	**12.1**	1.8	925	317	525	12	+45
CB01-1.H1.1	629	7	0.012	0.70	0.060	7.3	0.75	7.8	0.0906	2.6	0.3	**13.4**	4.4	609	158	559	14	+9
CB01-1.G11A.1	452	99	0.227	3.11	0.061	9.8	0.7	10.0	0.083	1.7	0.17	**13.5**	3.2	656	211	516	8	22
CB01-1.D.14B-2	281	91	0.336	2.58	0.076	14.5	0.9	14.6	0.086	1.6	0.11	**14.9**	3.3	1087	290	531	8	53
CB01-1.D.14A-1	309	28	0.093	9.23	0.053	21.6	0.68	21.9	0.0945	3.0	0.1	**13.6**	1.8	310	493	582	17	-92
CB01-1.C.22-1	589	41	0.071	0.63	0.058	3.3	0.71	3.6	0.0887	1.6	0.4	**14.0**	2.1	524	72	548	8	-5
Carvoaria																		
CV01-2.H8A.1	230	62	0.278	0.81	0.078	2.7	1.16	4.6	0.1076	3.8	0.8	**14.6**	2.9	1157	54	659	24	+45
CV01-2.E2-2	156	34	0.225	3.21	0.119	10.1	3.4	10.7	0.209	3.8	0.35	**20.2**	2.9	1945	180	1224	42	41
CV01-2.E2-1	245	35	0.148	1.31	0.129	3.4	3.60	4.9	0.2018	3.5	0.7	**17.1**	2.9	2090	61	1185	38	+47
CV01-2.D20.2	396	35	0.091	1.45	0.058	6.6	0.70	7.2	0.0871	2.9	0.4	**11.7**	3.0	537	145	538	15	-0
CV01-2.D20.1	399	37	0.095	1.89	0.053	7.8	0.6	8.3	0.088	2.8	0.33	**13.0**	3.0	315	179	543	14	-75
CV01-2.C16.1	223	56	0.258	1.23	0.119	2.0	3.17	3.7	0.1931	3.1	0.8	**16.8**	2.9	1941	36	1138	32	+45
CV01-2.C15.3	290	56	0.200	0.62	0.122	1.5	2.85	4.1	0.1690	3.8	0.9	**14.0**	2.9	1992	26	1007	35	+53
CV01-2.C15.1	260	42	0.168	1.24	0.091	2.9	1.5	4.8	0.117	3.8	0.79	**14.6**	3.0	1454	56	714	25	54
CV01-2.B23.1	204	67	0.343	1.00	0.078	3.9	1.10	4.9	0.1021	3.0	0.6	**15.9**	3.0	1147	77	627	18	+48
CV01-2.A14.1	251	78	0.321	2.46	0.060	8.2	0.72	8.9	0.0875	3.4	0.4	**13.4**	2.9	600	178	540	18	+10
CV01-1.F.4.1	319	61	0.199	0.18	0.161	0.7	8.7	3.4	0.391	3.4	0.98	**22.8**	3.8	2464	12	2126	61	16
CV01-1.E.7.1	400	49	0.126	0.12	0.168	0.9	11.00	2.8	0.4752	2.6	0.9	**27.5**	3.9	2537	15	2506	54	+1
CV01-1.A.9-1	347	35	0.104	0.10	0.159	1.2	8.90	1.8	0.4067	1.3	0.7	**19.7**	5.0	2442	21	2200	23	+12

Tabela 4: U–Th-Pb SHRIMP isotopic data from hydrothermal monazite, Pilar gold deposit.

							Isotopic ratios									Ages						
Spot Name	^{238}U	^{232}Th	$^{232}Th/^{238}U$	$^{207}corr\ ^{208}Pb$	common ^{208}Pb	$^{207}corr\ ^{206}Pb$	$^{207}Pb/^{206}Pb$	err.	$^{207}Pb/^{235}U$	err.	$^{206}Pb/^{238}U$	err.	rho	**$^{208}Pb/^{232}Th$**	**err**	$^{206}Pb/^{238}U$	err	$^{207}Pb/^{206}Pb$	err.	disc.	**$^{208}Pb/^{232}Th$**	**err.**
Pilar	ppm	ppm		ppm	% (^{207}corr)	ppm	^{204}corr	%	^{204}corr	%	^{204}corr	%		**^{207}corr**	**%**	^{204}corr	1σ	^{204}corr	1σ	%	**^{207}corr**	**1σ**
16-05A.1-1	2	830	436	18	0.21	0.13	0.10482	26.1	1.1676	27	0.0808	5.72	0.214	**0.02480**	**2.55**	501	28	1711	480	+73	**495**	**12**
16-05C.1-1	10	1270	130	29	1.51	0.61	0.17335	15.1	1.9688	16	0.0824	5.38	0.335	**0.02589**	**2.67**	510	26	2590	252	+83	**517**	**14**
16-05D.1-1	48	1396	30	33	2.95	3.44	0.04006	63.6	0.4464	64	0.0808	4.72	0.074	**0.02600**	**2.65**	501	23	-347	1642	+254	**519**	**14**
16-05F.1-1	12	1351	114	30	1.02	0.78	0.03292	168.4	0.3268	169	0.0720	7.83	0.046	**0.02491**	**2.58**	448	34	-883	4863	+156	**497**	**13**
16-05F.2-1	44	2521	59	56	0.99	3.19	0.05036	33.6	0.5829	34	0.0839	3.77	0.112	**0.02489**	**2.57**	520	19	212	779	-151	**497**	**13**
16-05G.1-1	10	1302	133	29	0.52	0.70	0.01648	292.4	0.1686	293	0.0742	8.55	0.029	**0.02500**	**2.75**	461	38	n.a.	n.a.	n.a.	**499**	**14**
16-05G.1-2	3	814	243	18	0.65	0.22	0.08799	51.2	0.9302	52	0.0767	7.04	0.136	**0.02472**	**2.57**	476	32	1382	984	+68	**494**	**13**
16-05H.1-1	6	1297	236	30	0.30	0.38	0.07331	25.7	0.8118	26	0.0803	4.67	0.179	**0.02557**	**2.76**	498	22	1023	521	+53	**510**	**14**
N16-06A.1-1	3	633	246	15	0.34	0.15	0.04312	132.1	0.3963	132	0.0667	8.20	0.062	**0.02575**	**2.58**	416	33	-161	3285	+371	**514**	**13**
N16-06E.1-1	82	3286	42	76	0.36	5.36	0.05507	16.8	0.5784	17	0.0762	3.57	0.207	**0.02591**	**2.59**	473	16	415	376	-15	**517**	**13**
N16-06E.2-1	29	2294	83	53	3.42	2.02	0.09640	45.6	1.1456	46	0.0862	6.60	0.143	**0.02587**	**2.59**	533	34	1556	856	+68	**516**	**13**
N16-06F.1-1	21	1545	76	36	0.98	1.43	0.03147	97.5	0.3324	98	0.0766	5.43	0.056	**0.02596**	**2.60**	476	25	-1015	2901	+153	**518**	**13**
N16-06G.1-1	11	1432	136	33	0.63	0.78	0.03753	76.5	0.4204	77	0.0812	5.03	0.066	**0.02609**	**2.70**	504	24	-518	2044	+205	**521**	**14**

4.6 Discussion

4.6.1 Age of the fluid flow episodes at the Córrego do Sítio and Pilar deposits

An Archean age for the orogenic gold deposits in Quadrilátero Ferrífero has been suggested, based on previous geochronological and structural evolution data. In this study, the Carvoaria deposit yields an Archean age retained in monazite crystals disclosed by the upper intercept of the Discordia with the Concordia plot. The obtained age, at 2514 ± 22 Ma, is, however younger than those obtained for the Cuiabá, Morro Velho and Lamego gold deposits, with hydrothermal monazite ages of ca. 2.7 Ma (Lobato et al., 2007; Martins et al., 2016). Unlike the latter, the 2.5 age could be linked to the opening of the Paleoproterozoic Minas platform basin imposed on the Archean paleocontinent and associated isotopic rejuvenation (e.g. Alkmim and Teixeira, 2017). This event is also marked by intrusion of the Lavras mafic dyke swarm dated (zircon U-Pb SHRIMP) at 2551 ± 9.8 Ma (Caxito et al., 2020). This set of geochronological traits is also within the context of a critical period in the geological record, in terms of global evolution of late-Archean granitoids (Laurent et al., 2014) and the passage to Proterozoic-style plate tectonics.

The monazite U-Pb SHRIMP data also reveal the presence of outstanding late Ediacaran-Cambrian ages imprinted on the Cachorro Bravo (551 Ma and 510 Ma), Carvoaria (539 Ma) and Pilar (508 Ma) orebodies. The lower intercept in the Concordia plot of the Carvoaria samples reveals a Cambrian episode of Pb loss at ca. 555 Ma (Figura 26), reinforced by the occurrence of monazite crystals which suffered total Pb lost and resetting of the U-Pb clock, yielding the Concordia age at 539 ± 9 Ma (Figura 27). At that time, the Brasiliano event may have induced total or partial transposition of structures and, consequently, the hydrothermal fluid from the post-collisional time pathways, along the Córrego do Sítio gold deposits, corroborated by the textural relationship between monazite and arsenopyrite (Figura 22). The growth of the monazite crystals according to the main foliation may denote a Cambrian age for the final shaping of the Córrego do Sítio Lineament as well. Data from the Cachorro Bravo deposits are relatively more scattered defining two main clusters at 510 ± 11 Ma and 551 ± 10 Ma, besides an outlier with a 582 ± 17 Ma $^{206}Pb/^{238}U$ age. These could either be interpreted as marking distinct episodes of fluid flow and monazite formation in the late Ediacaran to Cambrian, or as progressive Pb-loss that causes slight discordance of some spots in this area of the Concordia. The ^{208}Th-^{232}Pb of 508.2 ± 6.4 Ma (Figura 29) obtained from the Pilar deposit reinforces that the Cambrian fluid flow could have acted broadly over the QF.

4.6.2 Correlation with regional tectonic events and importance of the Cambrian collapse of the Aracuaí –Ribeira Orogen

Orogenic gold-hosting Archean to early Paleoproterozoic granite–greenstone terrains known worldwide have been reworked or overprinted by younger orogenies, which brought new complexities to unravel the structural control and timing of gold mineralization at these locations. This is the case for some of the major granite-greenstone terrains such as the ones found at the margins of the northern Yilgarn craton (Perring and McNaughton, 1990; McMillan, 1996; Vielreicher et al., 2002; Gazley, 2011; Duclaux et al., 2012; Gazley et al., 2016), the Karelian craton (Larionova et al., 2013; Molnár et al., 2016), and the North China craton (Zhang et al., 2018).

In view of the tectonic evolution and data presented in recent works (e.g. Cabral et al., 2015; Martins et al., 2016; Silveira Braga et al., 2020; Silveira Braga et al., 2021), Cambrian ages are clearly imprinted in some gold and iron deposits throughout the QF, also extending to eastern margin of the São Francisco Craton bordering the late Neoproterozoic–Cambrian Araçuaí Orogen. All of the Cambrian data for hydrothermal minerals match the development of post-collisional plutons of the Araçuaí-Ribeira Orogen (Figura 30; e. g. Noce et al., 2000; Mendes et al., 2005; Castañeda et al., 2006; Pedrosa-Soares et al. 2006, De Campos et al., 2016; Valeriano et al., 2011; 2016) and of the Eastern Brazilian Pegmatite Province (EBPP; Pedrosa-Soares et al., 2011), an important and large complex of pegmatite bodies. This body of evidence indicates an expressive hydrothermal activity and progressive cooling, at least until *ca*. 490 Ma (e. g. Gonçalves et al., 2016; Peixoto et al., 2018), developed during the orogenic collapse of the Araçuaí/Ribeira Orogen (Alkmim et al., 2006).

Gonçalves et al. (2019) presented significant U-Pb age data for hydrothermal minerals (monazite, rutile and xenotime), for samples collected along the external belt of the Araçuaí Orogen and adjoining SFC including the QF region. These data elucidate the extent of influence of fluid circulation events related to the gravitational collapse of the Araçuaí orogenic system (e.g., Alkmim et al., 2006) and its relationship with the pegmatitic provinces resulting from the post-collisional I and A-type magmatism of the G4 and G5 Suites (530–480 Ma).

Silveira Braga et al. (2020) studied iron orebodies hosted by Orisirian to early Statherian metamorphic banded iron formation in the western border of the Araçuaí Orogen, to the north of the Quadrilátero Ferrífero. The authors demonstrate that detrital zircons from the associated Lower Espinhaço Supergroup and igneous zircons from the Archean gneissic basement of the Guanhães Complex and from Statherian Borrachudos Suite include grains with 5 µm to 50 µm

wide rims with lower Th/U ratios than the cores and U-Pb SHRIMP ages from 492 Ma to 554 Ma. Silveira Braga et al. (2020) propose that uplift and decompression in the final collapse stage of the Araçuaí Orogen promoted partial melting of the Borrachudos Suite, generating pegmatite intrusions associated with magmatic-hydrothermal fluid circulation. Formation of massive magnetite bodies occurred due to contact metamorphism-metasomatism with the pegmatite bodies, followed by oxidation of magnetite to kenomagnetite, martite and crystallization of granular hematite by increased input of meteoric fluids. Thus, the hydrothermal fluid circulation related to the Cambrian collapse of the Araçuaí Orogen influenced not only the final structuring, but also the enrichment and modification of iron ore bodies in the Quadrilátero Ferrífero and vicinities (Oliveira et al., 2017; Silveira Braga et al., 2020).

The *in-situ* U-Pb SHRIMP data of hydrothermal monazite associated with gold-bearing arsenopyrite presented here brings a new panorama for the QF gold deposits, including in terms of prospective research purposes, based on robust, accurate and precise Archean and Cambrian ages. These reliable results could reveal a possibly intense influence of the inherited fluids from the collapse of the Araçuaí Neoproterozoic orogen over the host rocks. The results also indicate the importance of mapping and controlling of the Cambrian structures in spatial restructuring of the gold deposits. As monazite oriented in the main foliation in the NE-SW trending Córrego do Sítio Lineament show a strong, partial to total resetting of the U-Pb clock at 555-510 Ma, this structure can be interpreted as reactivated during the last stages of the Brasiliano Orogeny, that might have opened late Ediacaran-Cambrian fluid pathways among the east sector of the Quadrilátero Ferrífero.

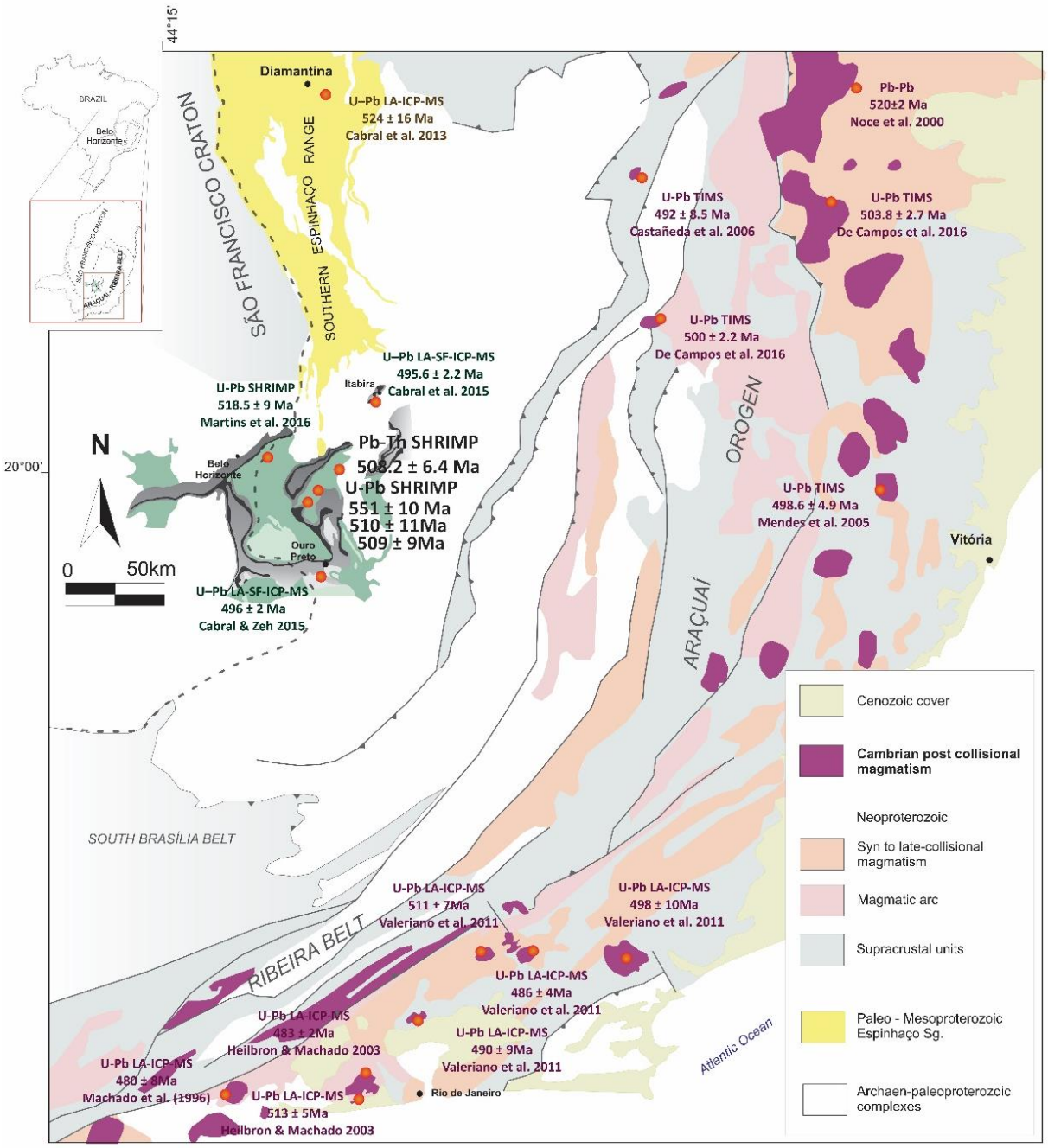

Figura 30: Simplified geologic map showing the results obtained in this work (U-Pb SHRIMP of 551 ± 10 Ma, 539 ± 9 Ma; 534.8 ± 11 Ma, 510 ± 11, and Th-Pb SHRIMP of 508.2 ± 6.4 Ma) and the compilation, for comparison, of the Ediacaran-Cambrian ages in Quadrilátero Ferrífero and along the sector of the Mantiqueira Province represented by the Araçuaí and Northern Ribeira orogens. The red points represent the location of the samples.

In sum, although the main gold mineralization event in the Quadrilátero Ferrífero region is Neoarchean, there was an important Brasiliano fluid flow event which might have partially remobilized the mineralized sections during Cambrian times. In terms of gold metallogenesis, the Brasiliano front might have strongly influenced some of the main structures that control mineralization in the eastern Quadrilátero Ferrífero area, such as the Córrego do

Sítio lineament, and might have extended at least to the region of the Lamego mine to the west (Figura 30), as shown by a similar age obtained on xenotime by Martins et al. (2016). Linking distinct structural styles at the deposit scale with the deformational ages is a hard but necessary task in future works. In this direction, it must be understood that Cambrian deformation and fluid flow might have occurred through the reworking and reactivation of ancient, Archean or Paleoproterozoic, shear zones. Cambrian fluid sources which led to monazite and xenotime crystallization are probably related to the collapse stage of the Araçuaí Orogen, accompanied by intense heat flow driven by mantle upwelling, which generated abundant I- and S-type granitic and gabbroic intrusions in the orogenic core.

4.7 Conclusions

The timing and impact of Cambrian hydrothermal fluid flow over gold and iron deposits in the QF metallogenetic province is noticeable, as ratified in this work for the Córrego do Sítio and Pilar gold deposits.

The SHRIMP U-Pb data in hydrothermal monazite crystals yielded discordant ages with intercepts at 2,514 ± 22 Ma and at 555 ± 19 Ma for the sample from Carvoaria deposit, besides robust concordant ages of 539 ± 9 for the monazite crystals that suffered total Pb loss during the Cambrian in the Carvoaria deposit, of 522.9 ± 17 Ma and 545 ± 11 Ma in the Cachorro Bravo deposit and a Th-Pb age of 508.2 ± 6.4 Ma in the Pilar deposit.

The Neoarchean upper intercept age obtained in the Carvoaria deposit is coherent, although relatively younger, with those reported for the world-class Cuiabá and Morro Velho deposits. This time lapse suggests that a disturbance in the isotopic system may have occurred, being induced by the opening of the Paleoproterozoic Minas basin over the Archean paleocontinent.

Although the concordant Archean upper intercept is retained in a variably of preserved monazite crystals, the Cambrian imprint also recorded in concordant monazites is persistent all over the QF, including within important ore deposits.

Nevertheless, there is still a lack of evidence that indicates total remobilization and development of ore at both Archean and Cambrian stages. Geochronology of ore minerals and sulfides directly related to the gold mineralizations (e.g. Re-Os dating of arsenopyrite) can be useful to further clarify those issues in future works.

ACKNOWLEDGMENTS

This study was financed in part by the Coordenação de Aperfeiçoamento de Pessoal de Nível Superior–- Brasil (CAPES)–- Finance Code 001 and the Fundação de Amparo à Pesquisa do Estado de Minas Gerais (FAPEMIG). The first author is fully financed by CAPES through scholarships granted during her thesis research and PhD sandwich program. The authors thank AngloGold Ashanti Córrego do Sítio Mineração S/A-AGA for their logistic, technical support, and for allowing the publication of data gathered from samples collected in their mines. Our acknowledgments also to Postgraduate Program of Universidade Federal de Minas Gerais (UFMG), to Centro de Microscopia UFMG, to Centre for Exploration Targeting (CET) and Centre for Microscopy, Characterisation and Analysis (CMCA) at University of Western Australia (UWA) and John de Laeter Research Centre at Curtin University. The U/Pb analyses were performed using a SHRIMP II probe at the John DeLaeter Centre of the Curtin University, Perth, Western Australia, enabled by NCRIS via AuScope. We thank Neal McNaughton for guidance and support during the preparation and analysis of the SHRIMP mounts and Allen Kennedy and Hao Gao for support during the analysis. A preliminary version of the paper was greatly improved after comments and suggestions by two anonymous reviewers.

5 ARTIGO II: PETROGRAPHY, LITHOCHEMISTRY AND SM-ND ISOTOPE SYSTEMATICS OF THE ARCHEAN CÓRREGO DO SÍTIO METATURBIDITE-HOSTED GOLD DEPOSITS, QUADRILÁTERO FERRÍFERO, MINAS GERAIS, BRAZIL.

Tatiana Gonçalves Dias[1], Rosaline Cristina Figueiredo e Silva[1], Lydia Maria Lobato[1,2], Fabricio Caxito[1], Claudio de Morisson Valeriano[3], Steffen Hagemann[4]

1- Programa de Pós-Graduação Em Geologia, Instituto de Geociências, Universidade Federal de Minas Gerais (IGC-UFMG), Belo Horizonte, MG, Brazil

2 - HydroFluids&Minerals (HF&M), Brazil

3 - Rio de Janeiro State University–- UERJ–- Rio de Janeiro (RJ), Brazil

4 - Centre for Exploration Targeting, University of Western Australia, Perth, WA, Australia

Artigo submetido ao periódico *Journal of South American Earth Sciences*

ABSTRACT

The Córrego do Sítio (CdS) Lineament represents extensive Archean lode-gold deposits hosted mainly in a metamorphosed turbiditic sequence of the Rio das Velhas Greenstone Belt. It comprises a series of orebodies, where arsenopyrite is the predominant gold-associated sulfide, closely related to the NE-SW trending shear zone which controls the behavior of the hydrothermal alteration observed in wall rocks. Lithogeochemistry data of metapelites suggest that the original sedimentary features have been preserved from significant hydrothermal modifications, especially rare earth elements data and incompatible element ratios which are similar to Archean Shale composition. Nd isotopic signatures, with TDM of 3.0-3.2 Ga and slightly evolved εNd (2.7 Ga) of -1 to -3 suggest that the Tonalite–trondhjemite–granodiorite (TTG) complexes of the Quadrilátero Ferrífero can be the main source areas of the metaturbidites. Lack of correlations of elements concentrated in mafic and ultramafic rocks such as Cr and Ni with the Nd isotope features, and Au contents suggest that metavolcanic successions such as the Quebra Ossos Group were not an important source for both the sedimentary rocks and associated gold. Although the metaturbidite samples preserve most of the original sedimentary geochemical and isotopic features, sedimentary processes were probably not important or definitive in concentrating gold, which is mainly of hydrothermal origin as suggested by the close spatial association with arsenopyrite.

5.1 Introduction

In the Quadrilátero Ferrífero (QF), one of the largest metallogenetic provinces in Brazil, gold deposits are greenstone-hosted within the Rio das Velhas Supergroup (RVSG), and mostly related to banded iron formation (BIF) and quartz-sulfide veins (lode-type) controlled by regionally remarkable shear zones and fold hinges (Lobato et al., 2001). However, clastic metasedimentary sequences also host important deposits, mainly in the eastern portion of the QF (Porto, 2008, Lima, 2012, Roncato et al., 2015).

Important questions to be addressed in Archean greenstone belts concern the provenance of the metaturbidites associated with gold deposits. In those deposits, gold occurs both concentrated by hydrothermal processes and dispersed throughout the rock groundmass (e.g. Cox et al., 1995; Bierlen et al., 1998; Ugarkar et al., 2015). Sedimentary processes could have enriched those rocks in gold, or alternatively, gold contents are exclusively linked to hydrothermal concentration. As TTG granite-gneissic complexes and juvenile ultramafic rocks occur in greenstone belts, both could be tested as possible sources for gold enrichment in metaturbidites of the same greenstone belts, using modern and robust geochemical and isotopic tools.

To address those issues, whole-rock Sm-Nd isotope data is presented for metaturbidites of the Archean Rio das Velhas greenstone belt (RVGB) along with novel geochemical and petrographic data. This data is used to resolve the provenance of the metaturbidites of the Córrego do Sítio (CdS) and shed light on the sources and processes of gold enrichment in the RVGB. The main objective is to characterize the provenance and source areas of the CdS metaturbidites and then to assess the importance of TTG versus ultramafic sources in gold provenance.

5.2 Geological Setting

Besides the metallogenetic significance, in terms of volume and diversity of commodities, the QF is one of the most important Archean-Paleoproterozoic provinces in Brazil, with about 7000 km^2 in extension in the southern São Francisco Craton.

Three main units are described in this region (Dorr et al., 1957): the Archean metamorphic complexes are composed of TTG suites and high-K granites (3.2-2.7 Ga); the typical greenstone belt sequence of Archean Rio das Velhas Supergroup (RVSG, ca. 2.7 Ga); and the metasedimentary sequence of the Paleoproterozoic Minas Supergroup (ca. 2.5-2.0 Ga).

Northwest of the QF, Archean terrains of higher greenschist to lower amphibolite facies make up the Pitangui greenstone belt (GBP), interpreted as an extension of the RVGB, in terms of lithostratigraphy (e.g. Lobato & Pedrosa-Soares, 1993; Alkmim and Noce, 2006; Romano, 2007; Hasui, 2012; Romano et al., 2013; Pinto and Silva, 2014).

The RVSG (Loczy & Ladeira, 1976), previously known as Rio das Velhas Series (Dorr et al., 1957), is considered as composed of Archean metavolcanosedimentary sequences formed at around 2.80 to 2.78 Ga (Baltazar & Zucchetti, 2007), subdivided at first into the lower Nova Lima and upper Maquiné Groups (Dorr et al., 1957). The Quebra Ossos Group (Schorscher, 1978) was proposed as in the bottom of the RVSG and represents komatiitic flows interlayered with BIFs.

The Nova Lima Group, which contains the major auriferous deposits of the QF, comprises, from bottom to top, a metavolcanic unit, a chemical metasedimentary unit and a clastic metasedimentary unit (Ladeira, 1980).

Baltazar & Zucchetti (2007), after Pedreira & Silva (1996), Baltazar & Pedreira (1996, 1998) and Zucchetti & Baltazar (2000), elucidated an evolution of the Rio das Velhas greenstone belt (RVGB) based on sequence stratigraphy applied to Archean terrains, as proposed by Eriksson et al. (1994). This model is considered a modern approach when compared to the classical lithostratigraphy, which is systematically applied to mapping survey of other greenstone belts around the world, such as the Barberton and Pietersburg, in South Africa (De Wit, 1991), and Pilbara block in Australia (Krapez, 1993). In this view, the RVGB was subdivided into seven lithofacies associations, developed during four sedimentary cycles (Figura 31), as follows, controlled by Nova Lima–Caeté, Santa Bárbara and São Bartolomeu tectonic blocks.

- Cycle 1 (2.80 – 2.78 Ga) was responsible for the mafic-ultramafic volcanism and deposition of a chemical volcano-sedimentary association related to an initially extensional stage with oceanic basin development.
- Cycle 2 is related to the deposition of the clastic-chemical-sedimentary association, the distal turbidites of the resedimented association, which occurs in the eastern sector of the QF, and the coastal association during the final extensional stage and initial subduction stage.
- Cycle 3 refers to the deposition of volcaniclastic and resedimented associations, during the orogenic phase, which was responsible for the development of island arcs.

- Cycle 4 comprises the non-marine association deposition in a retro-arc foreland-basin.

Deformation and tectonic development models of the QF have been proposed since Dorr (1969), which suggests a multiphase model, with at least three main compressive tectonic–metamorphic events intercalated with extensional events (e. g. Alkmim & Marshak, 1998; Baltazar & Zucchetti, 2007; Baltazar & Lobato, 2020).

Baltazar & Zucchetti (2007) proposed three events which were responsible for the development of compressional structures and greenschist facies metamorphism, besides the extensional phases that took place between them, according to each sedimentary cycle. The first episode is related to the NE-SW tectonic transport during the Neoarchean (ca. 2.7 Ga). The second event, between the late Neoarchean and Siderian, was responsible for the Minas Supergroup sedimentation (Chemale et al., 1994).

Around 2.0 – 2.2 Ga, the development of compressive structures with NE-SW trend and vergence to the NW is related to the Transamazonian or Minas Orogeny, represented by the Serra da Moeda, Curral, Dom Bosco, Santa Rita and Gandarela regional synclines.

The Transamazonian Orogeny was followed by orogenic collapse, which was responsible for the dome-and-keel feature of the QF (Alkmim & Marshak, 1998). Shear zones with N-S trend, stretching lineations with plunge toward ESE, tight to isoclinal west verging folds and S-C structures with reverse top-to-W displacement are assigned to this last event, which occurred in the Neoproterozoic, during the Brasiliano Orogeny.

Despite several controversies about the importance of each of these events in the QF structuring, most authors agree with the occurrence of the three main orogenic events. Besides the importance in structuring and development of greenschist facies metamorphism, these events influenced the percolation of hydrothermal fluids that were very important for the generation of mineral deposits in the QF (e.g. Lobato et al., 2007, Martins et al., 2016).

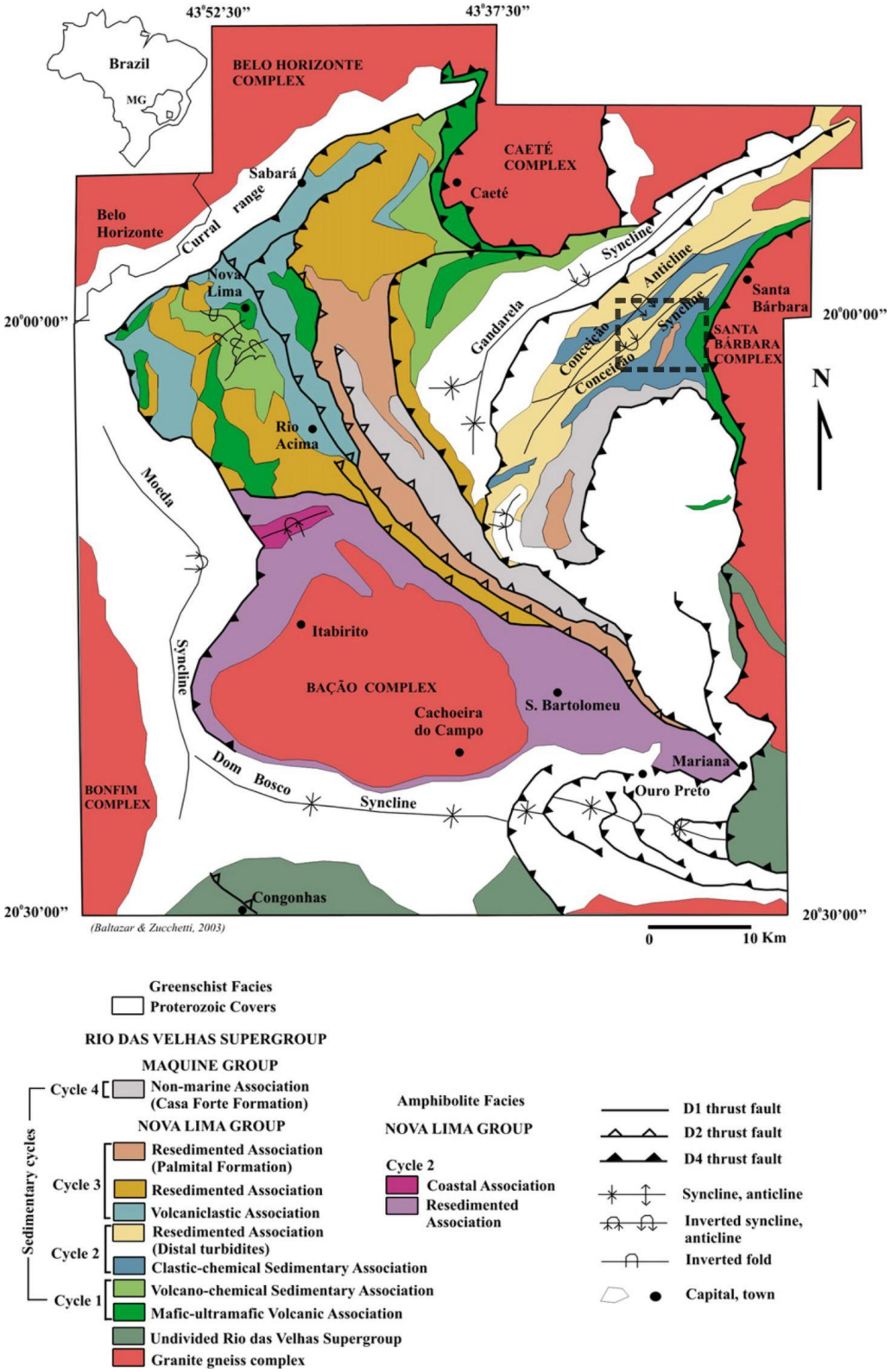

Figura 31: Lithofacies associations of the Rio das Velhas Supergroup (Baltazar & Zucchetti, 2007). Studied area is highlighted by the dashed rectangle.

5.2.1 Geology of the Córrego do Sítio Lineament

Several gold occurrences and deposits are related to the Córrego do Sítio structural lineament (CdS Lineament, Lima, 2012) in the northeastern sector of the QF, a dextral-sense strike-slip shear zone with NE-SW trend. Canale (1999), Lima (2012) and Roncato et al. (2015) associated different families of planar and linear structures of the CdS Lineament deposits as the results of four deformational phases, regarding the progressive Archean deformation within the context of the QF structural evolution (Marshak and Alkmim, 1989; Chemale et al., 1994; Baltazar and Zucchetti, 2000; Baltazar and Zucchetti 2007; Baltazar and Lobato, 2020).

The D1 phase, related to the S_1 regional schistosity (S_1 = 100-120/45-55, azimuth of dip direction/dip angle), overlaps the primary structures of the sedimentary bedding (S_o), highlighted by compositional variation and typical gradational bedding of the metaturbidites in the study area. The S_{m1} mylonitic foliation is progressive and parallel to S_1, commonly related to the mineralized areas, with characteristic boudinage and silicification. The S_2 crenulation cleavage (S_2= 280-320/40-65), attributed to the D2 phase, is responsible for the transposition of the S_1 foliation. The subhorizontal lc_2 lineation developed along the NE-SW trend. The D3 phase, of ductile character, is responsible for metric folding with NE–SW trace of axial surfaces. These mesofolds are related to changes in direction of S1 dip, from SE to NW. Modifications in the geometry of the ore bodies from the Cachorro Bravo deposit were recorded by Lima (2012) as conditioned by these structures. Closely spaced subvertical fractures of WNW-ESSE direction represent the D4 phase.

The D1 and D2 phases of the progressive Archean deformation are described by Baltazar and Lobato (2020) as responsible for the stages of the gold mineralization placing in the Nova Lima Group, referred as Type 1 (phyrrotite-dominated) and Type 2 (pyrite and arsenopyrite-dominated), respectively.

Locally, the Nova Lima Group is represented by the Córrego do Sítio Unit (Baltazar & Silva, 1998), which is considered by Baltazar & Zuchetti (2007) as one of the most abundant metasedimentary units of the Rio das Velhas Greenstone Belt as a part of the resedimented lithofacies association.

The Córrego do Sítio unit is made up mainly of graywackes, quartz graywackes, sandstones and siltstones, showing planar cross-bedding, plane and trough bedding, among other structures, arranged in cycles with abrupt basal contact between them. This association is considered by many authors (Baltazar & Silva 1998; Baltazar & Zuchetti, 2007; Porto, 2008;

Lima, 2012) as made up of incomplete Bouma turbiditic sequences (Bouma, 1983), which overlie the BIFs, the main host rocks of the gold mineralizations in the QF.

The rocks of the Upper and Lower portions of the Córrego do Sítio unit are characterized by their essentially psammitic composition, with greywacke predominating over lenses of sericitic and/or carbonaceous metapelites, besides horizons of heterogeneous BIFs containing magnetite, carbonates and quartz. The Intermediate subunit, where carbonaceous schists predominate, holds the main gold mineralization and the most important deposits (Cachorro Bravo, Laranjeiras and Carvoaria; Figure 2; Lima, 2012). The Córrego do Sítio Lineament contain other minor deposits (Cristina, Rosalino and Grota Funda), excavations and geochemical anomalies to the northeast (Sangue de Boi, Descoberta, Santana, Barra Feliz, Anomalia 1 and Santa Quitéria) and the southwest (Saracura and Serra Redonda).

David (2006) identified in a first integrated isotopic work, through isotopic studies for Pb, Sr and Nd systems, these host rocks as the sources of the mineralizing fluids in a polycyclic process with hydrothermal and metamorphic events, at 2.2 Ga, 2.0 Ga and at 600 Ma.

A swarm of metamafic dikes and sills, which has uncertain age, is remarkable in the Córrego do Sítio Lineament region. Tabular metagabbro dykes occur mainly in the NE-SW direction (Figure 2), dipping to SE. (Lima, 2012; Roncato et al., 2015).

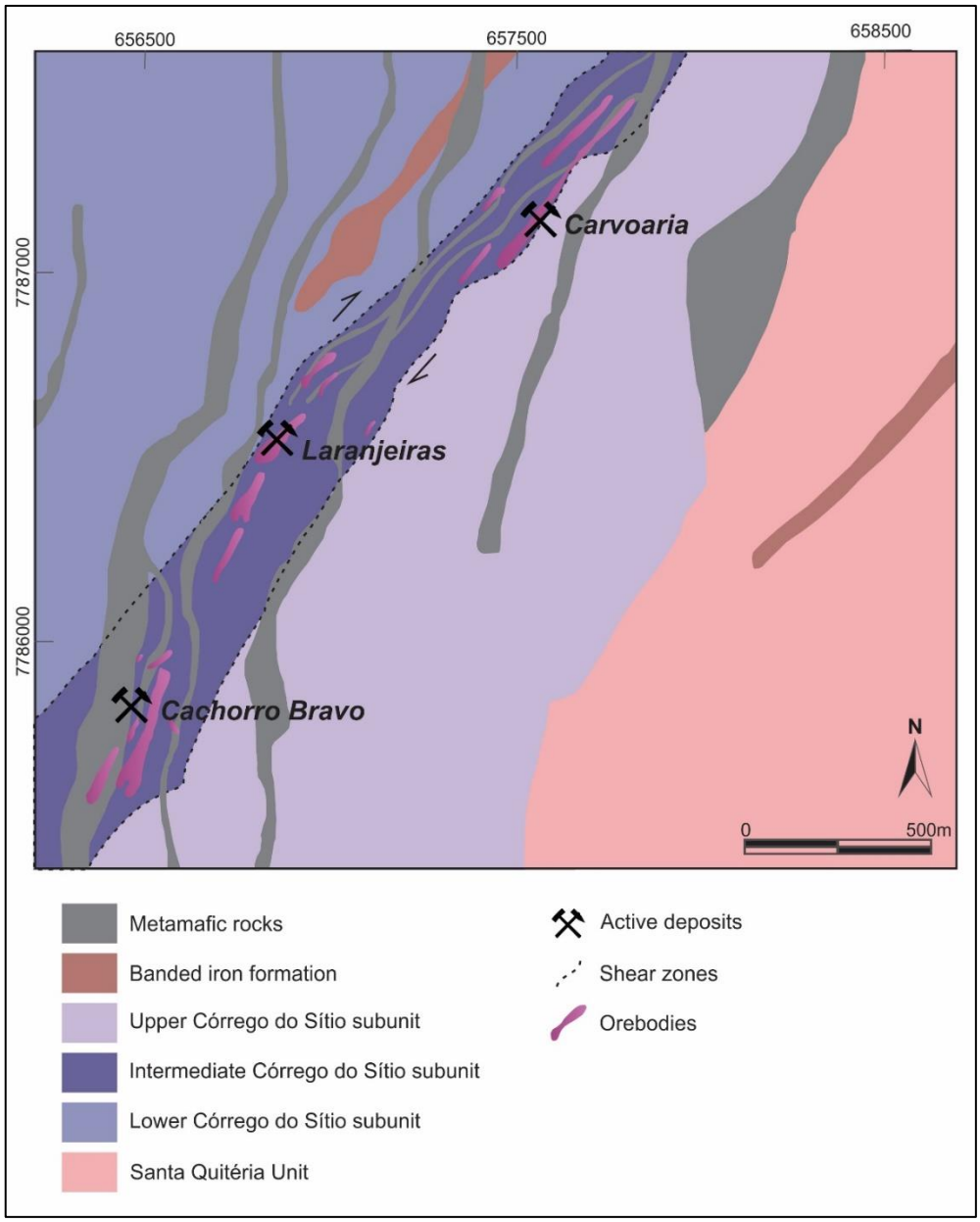

Figure 32: Geological map of the central sector of the Córrego do Sítio Lineament, with the main active deposits (modified from Sequetto-Pereira et al., 2013).

5.2.2 Gold Mineralization and hydrothermal alteration

Disseminated gold-sulfide ores associated with gold–quartz and gold–antimony minerals vein are known in orogenic areas of different ages worldwide, including turbidite-hosted deposits (e.g Hamsay et al., 1998; Kovalev et al., 2014).

The mineralization observed in the study area, which is hosted exclusively by the Intermediate Córrego do Sítio subunit, occurs mainly as disseminated sulfide-associated ore in metaturbidite lithotypes and/or in quartz-carbonate-sulfide ± sulfosalts veins (Lima, 2012, Ribeiro et al., 2015, Roncato et al., 2015, Dias et al., 2022), at least for the main deposits Cachorro Bravo, Laranjeiras and Carvoaria. These veins are correlated to specific deformation

events in a varied distribution, with free gold in quartz, gold inclusions in pyrite, pyrrhotite and in sulfosalts and are hosted only in the metasedimentary rocks (Ribeiro et al., 2015). In general, the disseminated ore is associated to fine-grained arsenopyrite developed parallel to the main foliation (Dias et al., 2022). The ore found in veins is associated to berthierite and stibnite, and also occurs as free gold in quartz in association with sulfides.

The metasedimentary sequences of the CdS Lineament deposits are characterized by hydrothermal wall-rock alterations characterized by chloritization, sericitization, carbonatization, silicification, and sulfidation. The hydrothermal assemblage in metamafic rocks comprises chlorite, epidote, calcite, quartz, muscovite and rare biotite. Magnetite, ilmenite, rutile, pyrrhotite, pyrite, chalcopyrite, galena and sphalerite comprise the accessory phases. One of the most significant features of wall rock alteration in transitional zones, recognized by Porto et al. (2006) and Roncato et al. (2015) as the stratigraphic break between metasedimentary and metamafic rocks, is the marked bleaching of the carbonaceous phyllites.

Roncato et al. (2015) proposed that the sulfide phases occur in different textures according to the respective hydrothermal alteration zone. In distal or non-mineralized zones, pyrite is disseminated in circular or rounded aggregates that may be partly disintegrated. Porous pyrite may be replaced by arsenopyrite and occurs associated with other sulfide phases. These porous crystals, as well as the porous pyrrhotite, are mainly described in ore zones hosted by metagraywackes. Late-stage euhedral pyrite with no pores is represented by isolated crystals, which are interpreted as generated from borders of the porous pyrite.

Arsenopyrite is found as euhedral crystals in proximal/ ore zone and as subhedral, from intermediate to mineralized zone. Is characterized by non-porous, very fine-grained prismatic or acicular crystals.

As a structurally controlled gold deposit, the CdS mineralization is also associated to hydrothermal alteration-related mineralogy characterized by chlorite, carbonate, sericite, sulfide-sulfosalt, and a large volume of silica, accordingly in the distal, intermediate and proximal ore zones (Figure 36). The three main deposits exhibit similarities in terms of mineralization styles, although with particularities for each one.

According to Lima (2012) and Roncato et al. (2015), the Cachorro Bravo deposit is distinguished by structurally controlled mineralization styles as disseminated, sulfide replacement and associated with quartz-carbonate-sulfide ± sulfosalts veins. Roncato et al. (2015) reported that the typical metaturbiditic sequence in the Cachorro Bravo deposit varies from a metapsammitic to metapelitic, from N to S, with compositional banding S_0 dipping to

SE with moderate to high angles. There is a pervasive S_{1-2} foliation, parallel or sub-parallel to these bedding planes, which are clearer in the carbonaceous phyllite and the hydrothermally altered metamafic rocks. The S_3 crenulation cleavage is characterized by an opposing dip in relation to $S_{1-2,}$ dipping to NW with moderate angles. The carbonaceous phyllite displays, in a more pronounced way, shear zones with S-C structures parallel or sub-parallel to S_{1-2}, and NW-SE striking faults.

The Laranjeiras gold deposit comprises a set of ore bodies which are elongated and subparallel according to the strike of the host rocks (N30-45ºE), with variable dip from 60º to 75º to southeast. Mineralized quartz-carbonate veins, containing sulfide and sulfosalts and free gold, and anastomosed lenses are commonly hosted in quartz-sericite carbonaceous schists or in metagraywackes (Lima, 2012),

Ribeiro et al (2013) classified the quartz-carbonate-sulfide ± sulfosalt vein systems for the Carvoaria deposit, based on their structure and mineralogy. The V1, V2 and V3 vein types are hosted in metasedimentary rocks, while the V4 type is hosted in metamafic dikes and sills. The V1 type comprises quartz-ankerite-pyrite-berthierite-gold veins, which are parallel to the main regional foliation S_n. The V2 type, classified as quartz-ankerite-pyrite veins, rarely minerailized in gold, is related to the crenulation cleavage (S_{n+1}). The third type V3 is commonly free of sulfides and sulfosalts, characterized by quartz-ankerite filling S_{n+3} fractures. The V4 quartz-calcite veins are strictly associated to the metamafic dikes and sills.

The main gold mineralization event in the Quadrilatero Ferrífero region is known to be related to the Neoarchean (Lobato et al., 2001a, b; Araújo et al., 2020; Baltazar and Lobato, 2020). However, there was an important Ediacaran-Cambrian fluid flow event, which might have influenced some of the main structures that control mineralization in the eastern Quadrilátero Ferrífero area, as shown by hydrothermal monazite (U-Pb SHRIMP) ages of ca 510 Ma and ca 540 Ma) in host rocks from the Córrego do Sítio lineament deposits (Dias et al. 2022).

5.3 Material and Methods

The petrographic characterization was based on samples of ore bodies hosted in metaturbidites of the three main deposits of the CdS Lineament: Carvoaria, Cachorro Bravo and Laranjeiras (Figure 33). Six polished thin sections were prepared for each sample, considering the variations in terms of lithotypes and hydrothermal alteration levels and features, and studied using optical and scanning electron microscopy techniques.

The polished and carbon-coated thin sections (Figure 33) were mapped using Scanning Electron Microscope (SEM) coupled to a Mineral Liberation Analyzer (MLA) software and to an Energy Dispersive Spectrometer (EDS) system, at the Centro de Microscopia, Universidade Federal de Minas Gerais, Brazil.

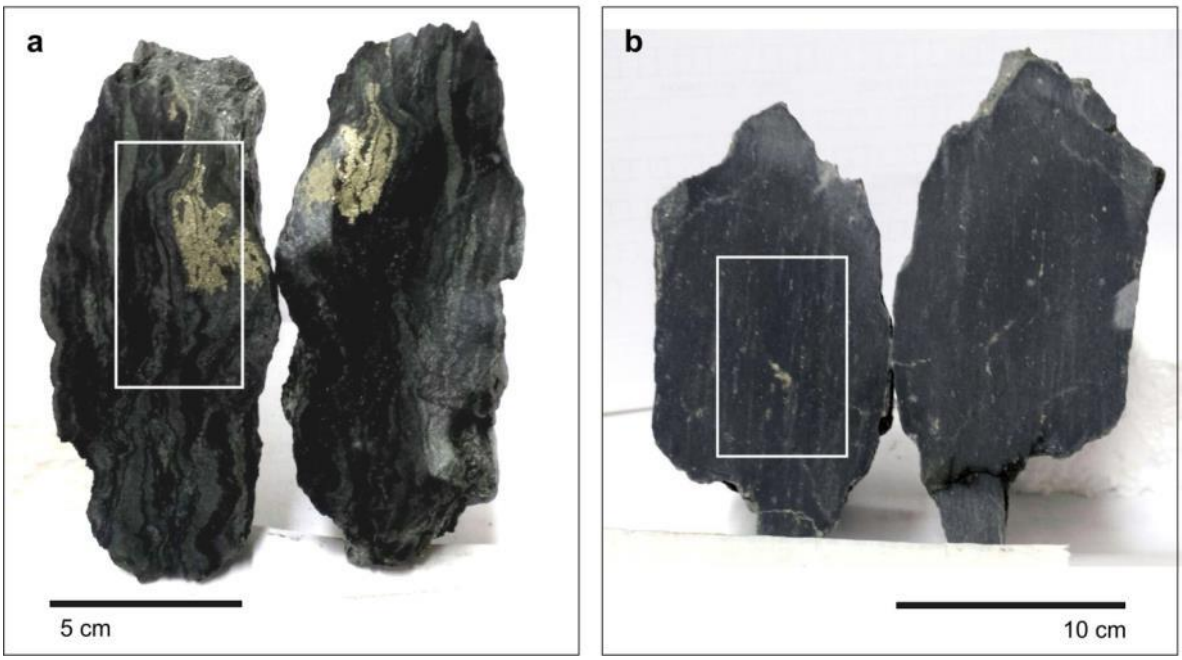

Figure 33: Representative samples selected for petrographic characterization. The white rectangles represent the polished and thin sections (a) Carbonaceous quartz-sericite metapelite with massive sulfide from Cachorro Bravo deposit; (b) Quartz-sericite metapelite with disseminated sulfide from Laranjeiras deposit.

Whole-rock geochemical analysis of seven metapelite samples was conducted at the SGS Geosol laboratories, Vespasiano, Minas Gerais, by ICP-MS (Inductively Coupled Plasma Mass Spectrometry), and by ICP-OES (Inductively Coupled Plasma Optical Emission Spectometry) for the major, trace and rare earth elements. Analytical errors are within 2% for major oxides and 5% for trace elements. Base and precious metal contents were determined by digestion in Aqua Regia followed by ICPMS analysis. The loss on ignition (LOI) was determined by weighing the difference after ignition at 450°C and/or 1,000°C.

The samples selected for Sm-Nd isotopic analyses are unweathered and with varied degrees of hydrothermal alteration of the mineralized turbiditic sequence of the CdS deposits. All samples were sent to the LAGIR-UERJ (Laboratório de Geocronologia e Isótopos Radiogênicos, Rio de Janeiro State University) laboratory for analysis of isotope dilution Sm-Nd isotopes and followed the methodology described in Valeriano et al. (2008). An aliquot of each sample of around 50 mg was mixed with proportional volume of ^{149}Sm-^{150}Nd double tracer

solution. The samples were then acid-digested in steel-jacketed high-pressure PTFE bombs and two in PTFE beakers on hot plate. Sample dissolution was done in two 5-day cycles using a mixture of HF (6mL) and HNO_3 6N (0.5 mL). Separation of Sm and Nd was performed using HCl in two ion exchange columns: the primary one separates the rare-earth elements from the sample solution with the AG 50 W-X8 (100-200 mesh) resin, and the secondary column uses the LN-spec (150 mesh) resin for separation of Sm and Nd. Samarium and neodymium were separately loaded on a previously degassed double Re filament mount, using HCl (1N) as the ionization activator. The isotopic ratios were obtained by a TRITON-Finnigan Thermal Ionization Mass Spectrometer (TIMS–- Thermal Ionization Mass Spectrometry). Sm-Nd isotopic results are listed in Table 2. Data acquisition was performed in multi-collector static mode using an array of 8 Faraday cups. The measured Nd isotope ratios are normalized to the constant $^{146}Nd/^{144}Nd$ ratio of 0.7219, and corrections were applied for tracer. Measured blanks are below 1 ng for Nd and 0.1 ng for Sm.

5.4 Results

5.4.1 Petrography

In the main active deposits hosted by the metaturbidite units of the Rio das Velhas Greenstone Belt, arsenopyrite is the most important gold-associated sulfide. In the CdS lineament, the mineralization styles depend on the proximity with the metamafic dikes along the CdS Lineament, which locally control the hydrothermal alteration marked by chlorite, carbonate, sericite, sulfide-sulfosalt, and large amounts of silica. Figure 36 illustrates the paragenetic sequence, considering the gold mineralization and related hydrothermal alteration halos.

In mineralized domains with lower incidence of metamafic dikes and sills, as the Carvoaria and Laranjeiras deposits, the vein mineralization type is more common and is represented by quartz-carbonate-sulfide ± sulfosalts veins with free gold in quartz. This ore type, classified as quartz-ankerite-pyrite-berthierite-gold veins, which is parallel to the main regional foliation $S_{n,}$, striking NE and dipping to SE, is related to the early stage of the hydrothermal alteration. The mineralization is hosted mainly by metasedimentary rocks, such as metagraywacke, schist and phyllite of the CdS Lineament (Ribeiro et al., 2013). On the other hand, toward southwest of the CdS Lineament, the gold mineralization of the Cachorro Bravo deposit is dominated by disseminated Au-arsenopyrite style, also parallel to the main foliation. Gold occurs as inclusions in euhedral and subhedral very fine-grained crystals of arsenopyrite,

with the typical prismatic or acicular habits (Figure 34 a), mainly associated with pelitic domains of the CdS metaturbiditic sequences (Figure 34 b).

Antimony sulfides and sulfosalts are very common both in the disseminated sulfide associated ore and in the vein mineralization domains. Berthierite and stibnite are closely related to gold mineralization and occur associated with arsenopyrite (Figure 34 c) and more expressively in mineralized veins. In disseminated ore bodies, these minerals are observed in association with galena (Figure 34 d). Other antimony minerals, such as ullmannite and jamesonite are also very common, mainly in some of the Laranjeiras deposit orebodies, as inclusions in arsenopyrite or as associated minerals (Figure 34 e and f).

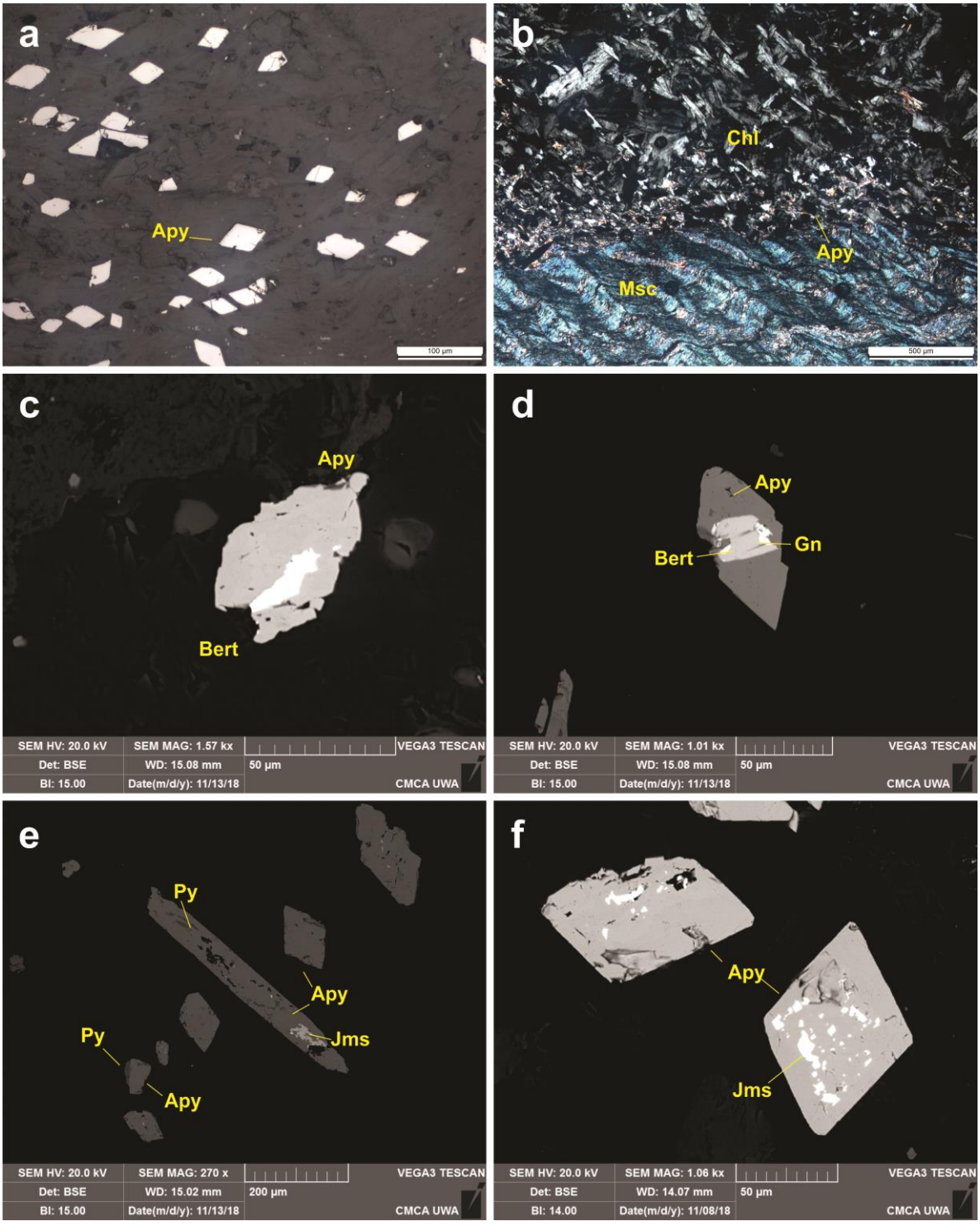

Figure 34: Typical mineralogical phases and features of metapelite from metaturbidite sequences found in CdS deposit (a) Photomicrograph (reflected light) of disseminated euhedral arsenopyrite (Apy); and of (b) metapelite, that shows crenulation cleavage ,composed mainly by muscovite (Msc), and chlorite (Chl), with disseminated pyrite (transmitted light), from Cachorro Bravo deposit; (c) Berthierite associated to arsenopyrite and also (d) to galena (Gn); Secondary phase of antimony phase, jamesonite (Jms), as inclusions in arsenopyrite (Apy), as well as pyrite (Py), from Laranjeiras deposit (e and f).

Fine-grained rutile is the main titanium mineral and occurs as elongated mineral aggregates oriented parallel to the foliation.

Rare earth-bearing phases are dominated by monazite, frequently associated with arsenopyrite (Figure 35 a) and pyrite (Figure 35 b). Minor to rare allanite, bastnaesite (Figure 35 c and d), xenotime and thorite are also present.

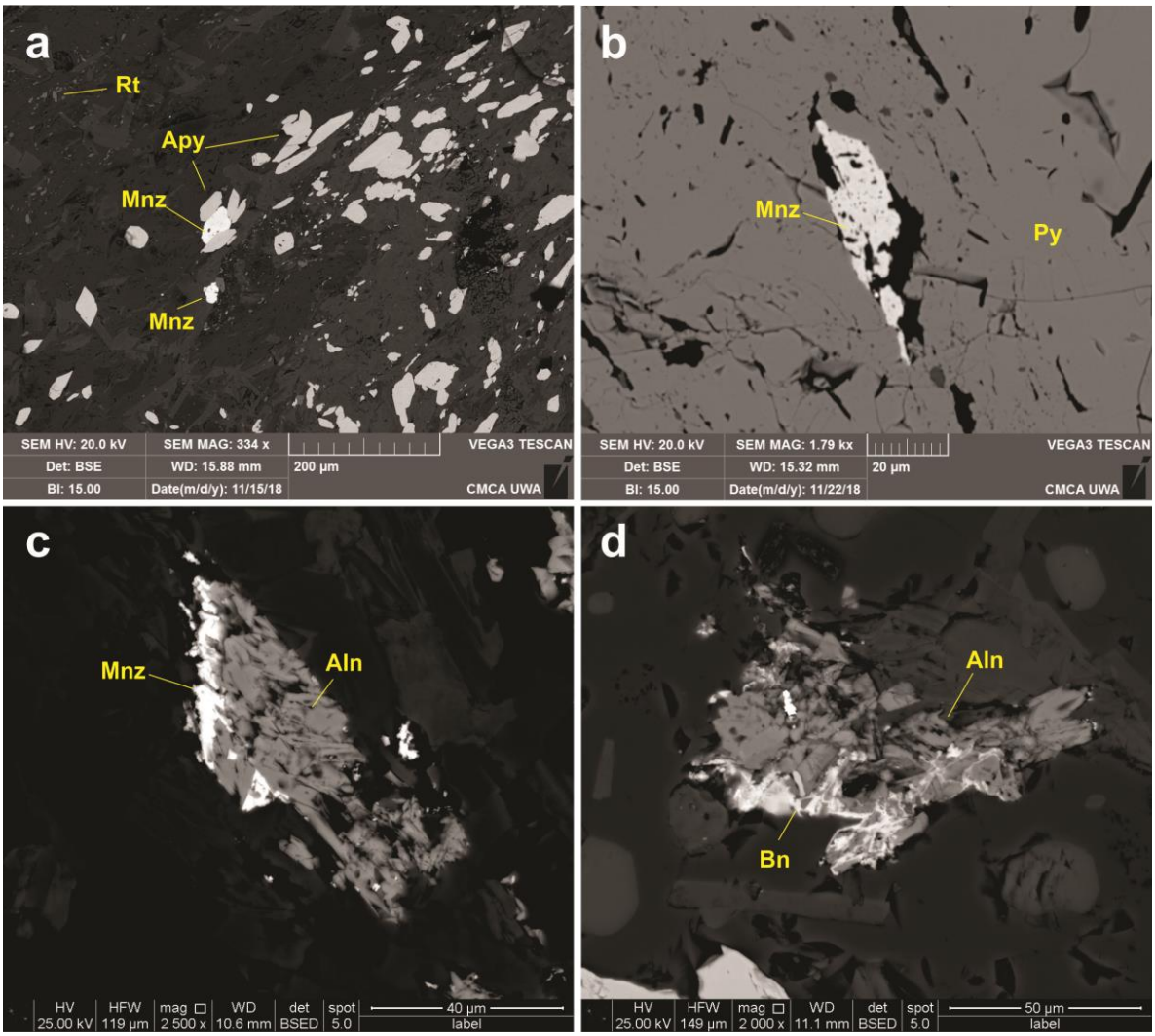

Figure 35: Back-scattered electron EDS images of rare earth-bearing phases found in metaturbidite lithotypes samples of CdS deposit. Monazite (Mnz) occurs frequently associated to (a) arsenopyrite (Apy) and pyrite (Py; b). Allanite (Aln; c) and bastnaesite (Bn; d) are also observed in metapelites.

The hydrothermal alteration phases typically found in the metaturbidite wall rocks are ankerite, calcite, chlorite, fine rutile and titanite, muscovite, quartz, albite, uncommon apatite, and ore minerals as arsenopyrite, pyrite, pyrrhotite, chalcopyrite, tetrahedrite, rare hematite, berthierite/ stibnite, galena and gold (Figure 36).

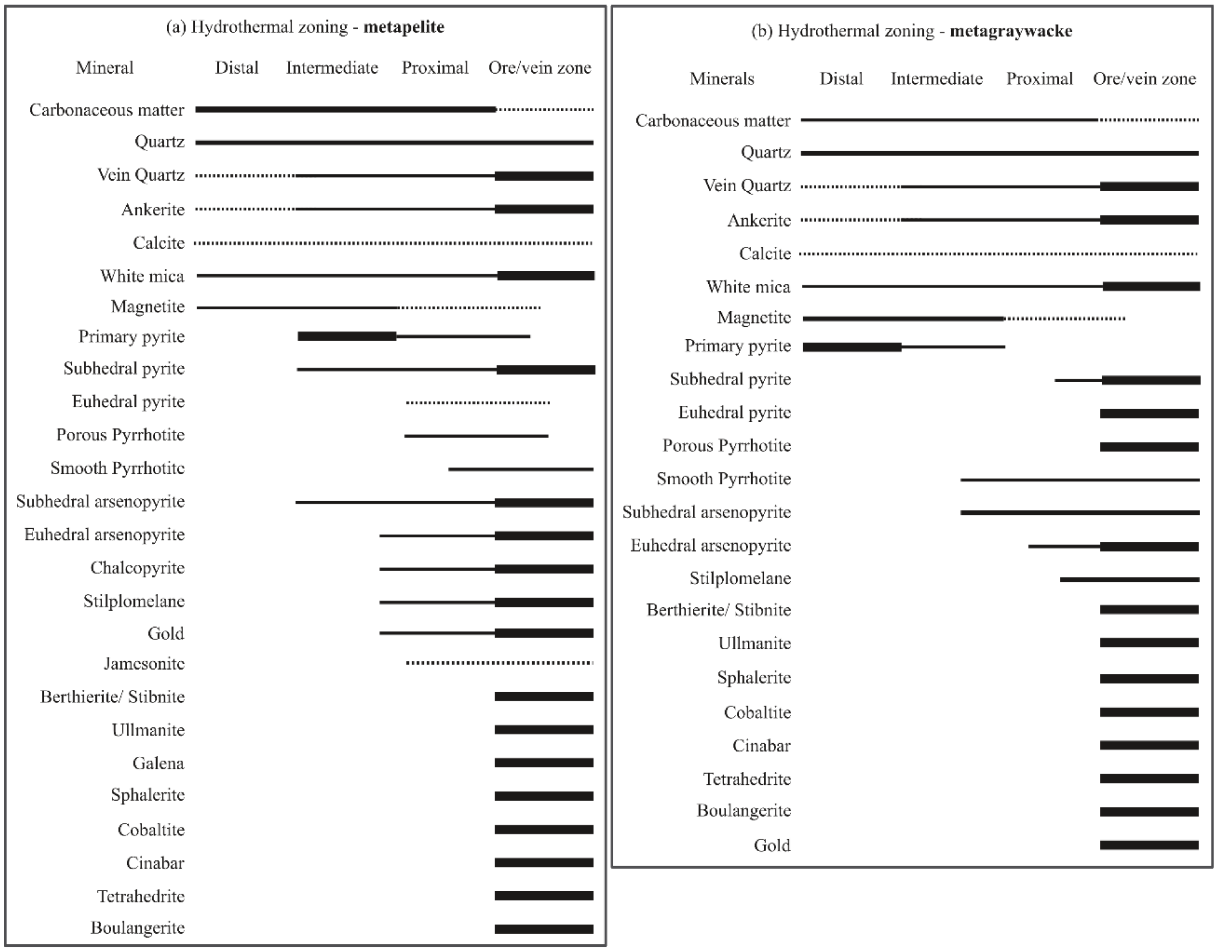

Figure 36: Paragenetic sequence of the hydrothermal alteration zones, from distal to proximal/ore, of (a) metapelite and (b) metagraywacke wall rocks of the Córrego do Sítio Lineament (modified after Porto 2008 and Roncato et al., 2015).

5.4.2 Lithochemistry

Lithochemical analyses of the seven samples are compared with data presented by Roncato (2015) totaling thirteen metapelite samples from different deposits of the Córrego do Sítio Lineament (Tabela 5).

Tabela 5: Litochemistry–- analyzed samples and origin deposits.

Sample		Deposit
LJ02 LJ04	Carbonate-quartz-sericite-schist	Laranjeiras
CB01	Carbonaceous sericite-schist, veined	Cachorro Bravo
CV01	Carbonate-quartz-sericite-schist	Carvoaria
FCSII–- 157	Carbonate-chlorite-quartz-sericite-schist	Anomalia 1
FCSII–- 187	Sericite schist, veined	Sangue de Boi
FCSII–- 279	Veined sericite-quartz-chlorite schist	Anomalia1

As the main objective of this work is to characterize the provenance and source areas of the CdS metaturbidites and then to assess the importance of TTG versus ultramafic sources in detrital gold provenance, care was taken to select homogeneous portions of samples (i.e., with no veins or other hydrothermal features). Nevertheless, the minute and pervasive nature of veinlets sometimes cannot be avoided. We will further discuss the geochemical features which suggest a primary nature (i.e., sedimentary) for the studied samples.

The metaturbidite samples (including data for metagreywacke samples of the CdS deposit from the PhD Thesis of Roncato, 2015 for comparison) show a range of 43.45 to 62.21% of SiO_2 and 9.78 to 16.74% of Al_2O_3 reflecting the different proportions of pelite levels in the protolith. Contents of TiO_2 varies from 0.58 to 2.85%; Fe_2O_3: 4.12 to 16.36%; MnO: 0.04 to 0.22%; CaO: 0.18 to 7.40 %; MgO: 1.77 to 5.36 wt.%; Na_2O: 0.23 to 7.19; K_2O: 0.06 to 3.98 wt.%, and P_2O_5: 0.03 to 0.49 wt.%.

The rare earth element contents of the CdS samples tend to be similar to sligthly depleted when compared to Archean shale, from Limpopo Province (Figure 37; Taylor et al., 1986). The only exception is sample FCSII157, a metapelite with strong hydrothermal alteration features and quartz veinlets with sulfide, which shows heavy rare earth element (HREE) enrichment. Chondrite-normalized rare earth elements (REE) patterns of metaturbidites litotypes (Figure 38) are moderately enriched in light rare earth elements (LREE) (La_N / Yb_N = 4.04 – 14.55).

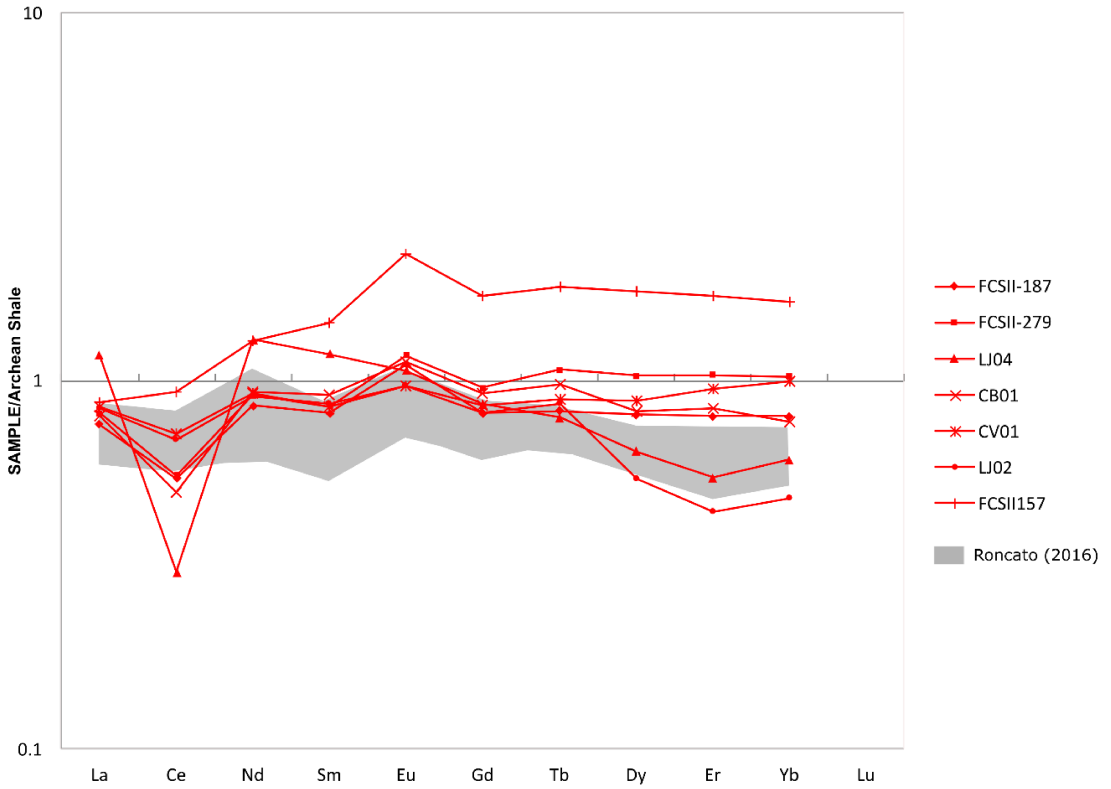

Figure 37: Archaen shale-normalized diagram (Taylor et al., 1986) of rare earth elements patterns for metapelite samples from the CdS deposit. The gray shaded field represents metagraywacke patterns from the same CdS deposit, published by Roncato (2016).

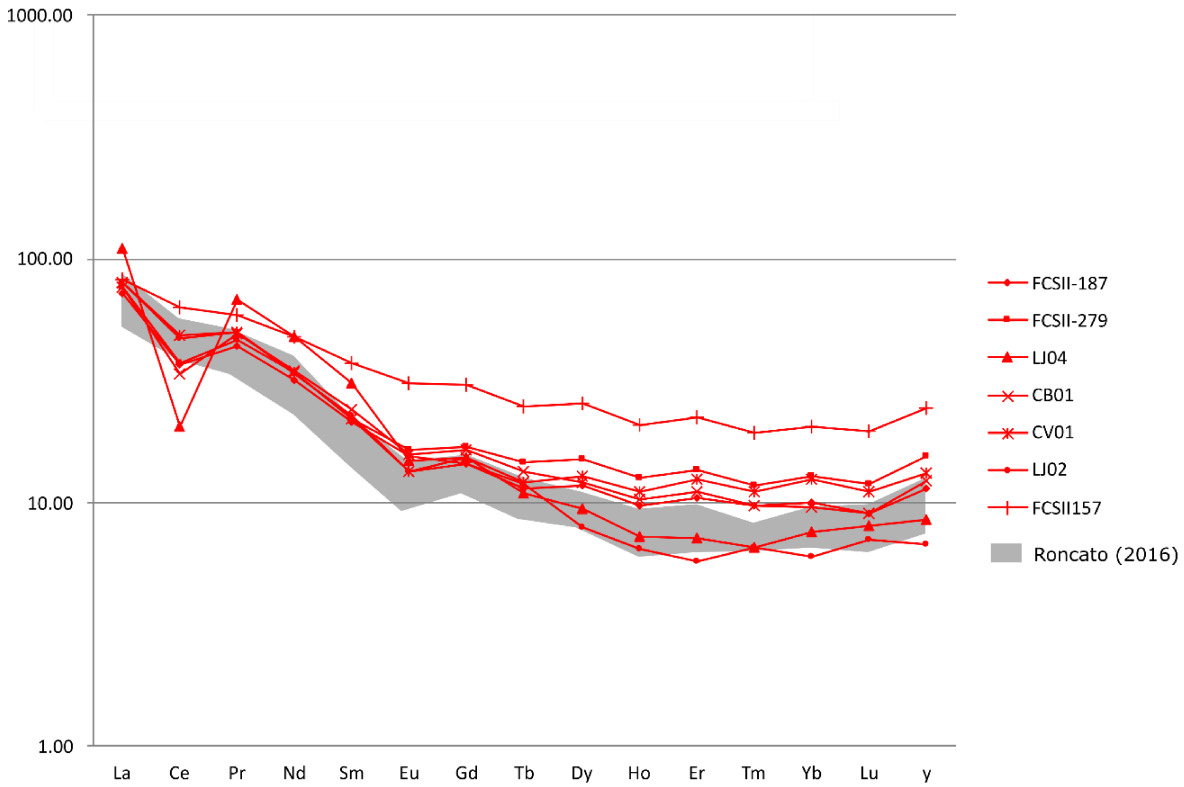

Figure 38: Chondrite-normalized diagram (Taylor & McLennan 1985), of rare earth elements patterns for metapelite samples from the CdS deposit. The gray shaded field represents metagraywacke patterns from the same CdS deposit, published by Roncato (2016).

5.4.3 Sm-Nd isotopes

The initial Nd isotope ratios were recalculated to ca. 2.7 Ga according to the ages obtained for the RVGB volcanics and gold mineralization (Lobato et al., 2007). The studied metaturbidite samples (Tabela 6) show Archean depleted mantle model ages (TDM) varying in a narrow range between 2.99 Ga and 3.19 Ga with corresponding initial εNd (2.7 Ga) from -1.3 to -3.6. The exception is sample FCSII-157 which shows a TDM of 2.84 Ga and initial εNd (2.7 Ga) of 1.0. This sample also shows higher contents of Nd (32.7 ppm) and of Sm (7.8 ppm) than the others, which have in general Nd below 25 ppm and Sm below 5 ppm, except for sample LJ04.

Tabela 6: Sm-Nd isotopic data for the CdS turbidite samples.

Sample	Sm (ppm)	Nd (ppm)	$^{143}Nd/^{144}Nd$	Std. Err. Abs (2σ)	$^{147}Sm/^{144}$ Nd
4493	2.9	13.4	0.511334	0.000008	0.1305
4496	3	14.6	0.51124	0.000007	0.1247
4497	3.2	15.6	0.511198	0.000008	0.1244
4500	4.7	24.5	0.511031	0.000006	0.1169
4501	4	19.4	0.511197	0.000005	0.1246
4503	4	19.5	0.511259	0.000014	0.1235
4504	4.1	20.8	0.511087	0.000007	0.1182
4505	3.8	19.2	0.511096	0.000004	0.12
4506	3.9	21.2	0.511033	0.000006	0.112
FCSII-187	4.3	21.2	0.511177	0.000005	0.1237
LJ04	6.5	33.3	0.51117	0.000002	0.118
CV-01	4.7	24.3	0.511101	0.000003	0.1163
LJ-02	4.7	23.9	0.51117	0.000006	0.1197
FCSII-157	7.8	32.7	0.511765	0.000005	0.1449
FCSII-279	5	24.2	0.511204	0.000012	0.1251

5.5 Discussion

5.5.1 Sedimentary x Hydrothermal nature of Rare Earth and isotope compositions of the metaturbidite samples

Vikent'eva et al. (2013) suggested that the REE can be mobilized during hydrothermal alteration of host rocks during the formation of large orogenic gold deposits. Mobility of REE in hydrothermal processes can be useful for the reconstruction of composition and source of the ore-bearing fluid.

The REE contents of metaturbidites from CdS show, however, that most of the samples present patterns that are very similar to the Archean shale and to other common shale

compositions in the chondrite-normalized diagram. This suggests that the trace element contents of the rocks do not differ significantly from the most common Archean shale composites (e.g. Taylor et al., 1986), indicating, overall, a preservation of the primary, sedimentary compositions of the groundmass rock. SiO_2, Al_2O_3 and other major oxides are also within the range of normal shale compositions. The exception is sample FCSII157, which, despite the REE having historically been regarded as insensitive to hydrothermal alteration, reveals an enrichment of HREE which might be caused by post-depositional fluids.

Nd isotope data, which will be discussed in detail in the next topic, also points to common provenance patterns from the surrounding TTG complexes, and a lack of disturbance of the Nd isotope system during hydrothermal alteration. The similarity of the metaturbidite groundmass with common shale composites might suggest that disseminated gold could have been enriched by sedimentary processes prior to hydrothermal concentration, a possibility that will be further addressed comparing the Nd isotope data and trace element contents in the next section.

5.5.2 Provenance of the gold-bearing metaturbidites and probable gold sources

The geochemical characteristics of most of the samples indicate a preservation of the original sedimentary composition, as shown by its signature similarity in relation to NASC. With this in mind, a discussion using Nd isotopes and incompatible elements, such as Cr and Ni, can be used to assess the importance of juvenile and ultramafic sources in the provenance of the metaturbidites and, most important, of gold concentrations.

In the Nd isotope evolution diagram (εNd x t) of Figure 39, all samples are plotted and represented as a dashed field. The grey field represents the Nd isotope evolution curves for samples of the TTG complexes adjacent to the Rio das Velhas greenstone belt (data from Carneiro et al., 1998). From this field, provenance of the metaturbidites could be assigned to the erosion of the Archean TTG complexes not involving significant juvenile mafic magmatism component. The older TDMs varying from 3.0 to 3.2 Ga reinforce the mostly recycled nature of the sediments composing the CdS area. This is in accordance with previous, unpublished Nd isotope data of metasedimentary rock samples from the CdS area (David, 2006) with similarly negatively fractionated εNd(t) around -6 and Archean TDM > 3 Ga.

Thus, although previous studies have suggested a possible influence of mafic-ultramafic sources in the provenance of the metasedimentary package of the RVGB (e.g. Zucchetti & Baltazar, 2000; Porto, 2008), mainly based on whole-rock elemental geochemistry data, our

new Nd isotope data presented here suggests that if that influence was present, it was only minor and that the main source areas correspond to the Archean TTG complexes of the QF. The next step is to address the influence of this possible minor mafic-ultramafic source in sedimentary processes that could led to gold concentration.

The lack of correlation between Au (ppb) contents and Nd isotope features (εNd, TDM), as shown in Figure 40, further supports that ultramafic rocks probably didn't play an important role in providing sources for gold hosted in the CdS metaturbidites. Similarly, Au (ppb) is not correlated to Cr (ppm), Ni (ppm) or MgO (%) contents. Thus, mafic-ultramafic sources are not considered as an important component neither for the sedimentary provenance of the studied samples nor for gold concentration prior to post-depositional, hydrothermal processes.

Altogether, the amassed petrographic, geochemical and isotopic data suggest that, although the metaturbidite groundmass preserves most of the sedimentary geochemical and isotopic compositions, sedimentary processes were probably not definitive in concentrating gold.

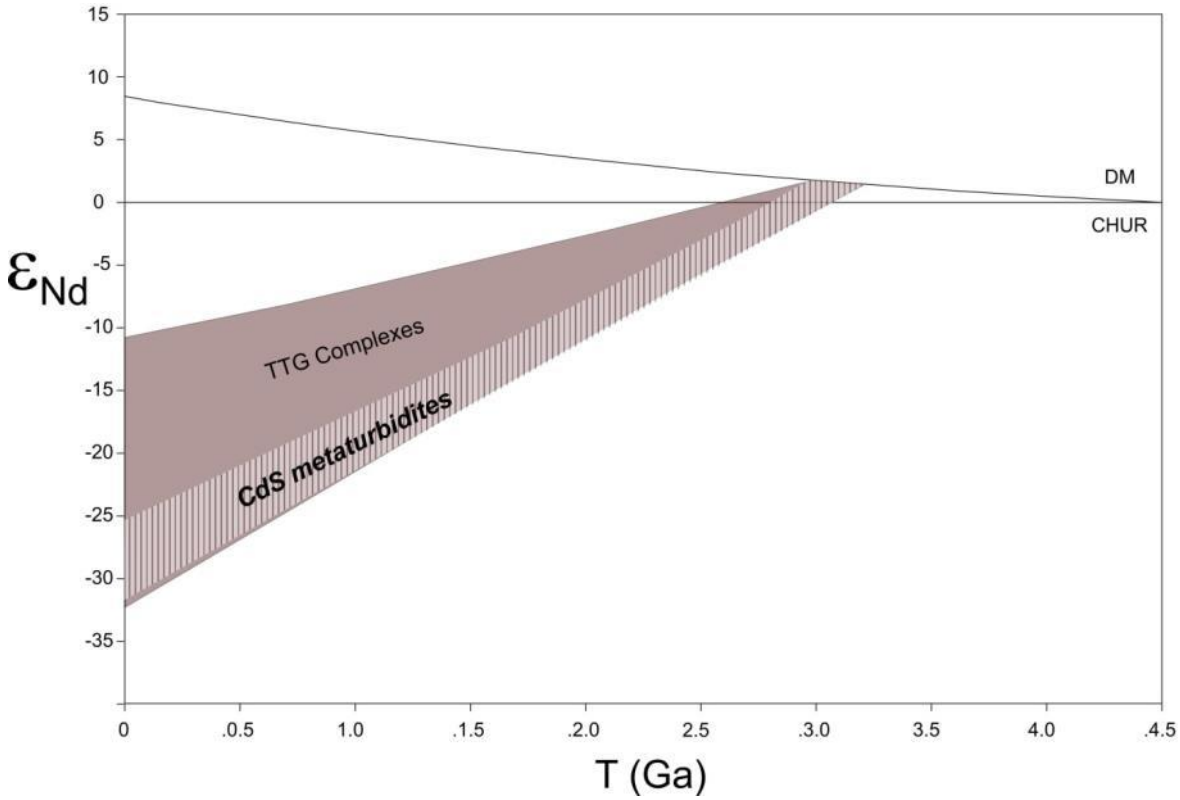

Figure 39: Nd isotopic evolution diagram for metaturbidite samples of the CdS deposit, as compared with data for TTG complexes in Carneiro et al. (1998).

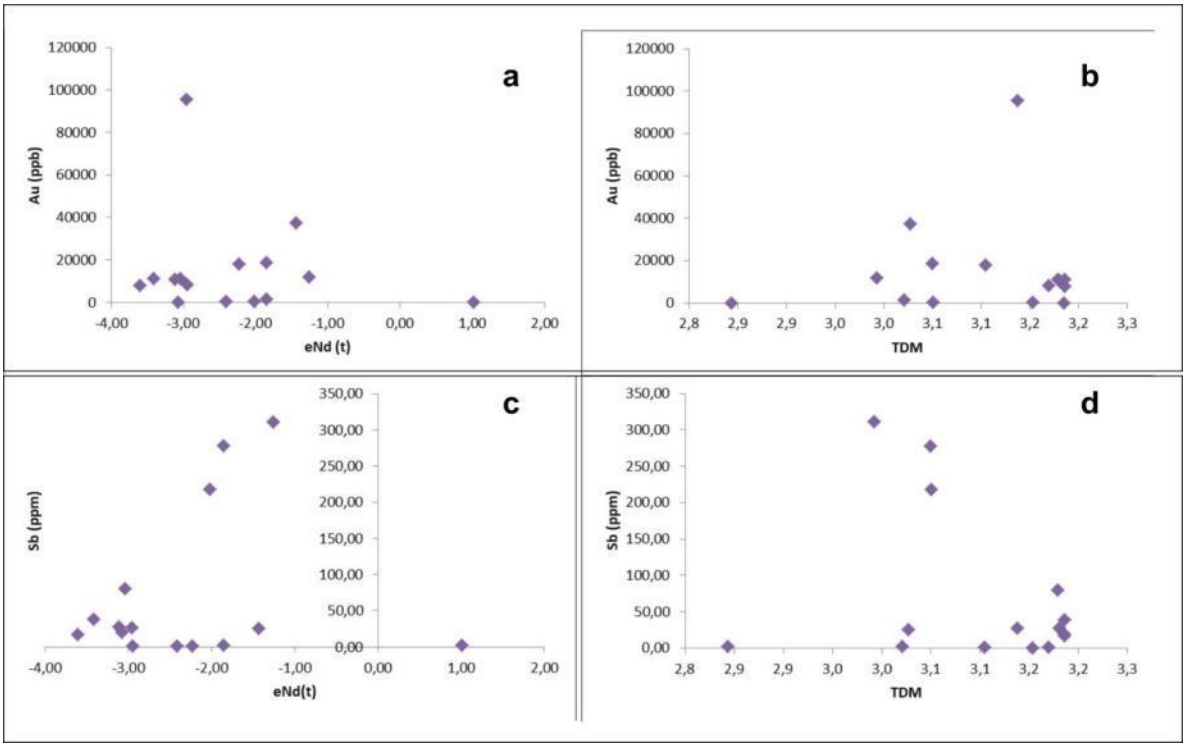

Figure 40: Plots of Nd isotopic data. ƐNd and TDM for (a and b) Au (ppb) and for (c and d) Sb (ppm) content.

5.6 Conclusions

- The gold deposits in the CdS Lineament and related ore areas in the surroudings are included in the most abundant metasedimentary unit of the Rio das Velhas greenstone belt in the Quadrilátero Ferrífero province (Baltazar & Zuchetti 2007). As indicated by petrographic analysis, the gold hosted by metaturbidites is associated with arsenopyrite and is mostly related to hydrothermal processes.

- Metaturbidites from the CdS area show NASC-like geochemical signatures indicating they are typical sedimentary rocks derived from the erosion of the upper crust.

- Archean TDM of 3.0-3.2 Ga and slightly evolved initial εNd (2.7 Ga) of -1 to -3 indicate that the TTG complexes of the Quadrilátero Ferrífero, especially the close by Santa Bárbara complex, were the main source areas for the metaturbidites. Both units overlap in the Nd isotope evolutionn diagram.

- Lack of correlation of Au contents and Nd isotope compositions suggest that erosion of ultramafic rocks (such as the Quebra Ossos komatiitic units) was not important as a source of detrital gold for the CdS area. This is also suggested by the lack of correlation between Au (ppb) contents and Cr, Ni (ppm) and MgO (%) contents.

- Nd isotope data presented for the first time here along with novel geochemical and petrographic data for the CdS rocks indicate the importance of the erosion of TTG complexes

for the provenance of RVGB metaturbidites. The RVGB is a typical sediment-dominated greenstone belt and thus erosion of ultramafic rocks doesn't seem to have been an important factor in gold enrichment in the sedimentary rock-hosted deposits.

ACKNOWLEDGMENTS

This study was funded in part by the Coordenação de Aperfeiçoamento de Pessoal de Nível Superior–- Brasil (CAPES)–- Finance Code 001 and the Fundação de Amparo à Pesquisa do Estado de Minas Gerais (Fapemig). The first author is fully financed by CAPES through scholarships granted during her thesis research and also PhD sandwich program. The authors thank AngloGold Ashanti Córrego do Sítio Mineração S/A-AGA for their logistic, technical support, and for allowing this publication. Our acknowledgements also to Postgraduate Program of Universidade Federal de Minas Gerais (UFMG), to Centro de Microscopia UFMG, to Centre for Exploration Targeting (CET) and Centre for Microscopy, Characterization and Analysis (CMCA) at University of Western Australia (UWA), to John de Laeter Research Centre at Curtin University and to Laboratory of Geochronology and Radiogenic Isotopes (LAGIR), of the Rio de Janeiro State University (UERJ). CMV holds CNPq (310585/2021-0) and FAPERJ (E-26/202.511/2019) research scholarships.

6 CONSIDERAÇÕES FINAIS

Os estudos desenvolvidos nesta tese apresentaram dados e contribuições de considerável relevância sobre o comportamento da associação ressedimentada do Greenstone Belt Rio das Velhas, frente às atividades hidrotermais, associadas aos diversos ciclos orogênicos sobre o Quadrilátero Ferrífero, responsáveis pela mineralização em ouro e geração de paragêneses minerais características.

Os primeiros resultados demonstraram a presença de cristais de monazita hidrotermal associados à mineralização dos metaturbiditos do Lineamento Córrego do Sítio e do xisto do depósito Pilar. As metodologias de análises geocronológicas *in situ* nesses minerais, associadas aos levantamentos isotópicos, petrográficos e litoquímicos, foram desenvolvidas de forma detalhada e sistemática, de forma pioneira para a região estudada (leste do Quadrilátero Ferrífero) e através de ferramentas não rotineiramente utilizadas no Brasil.

As principais contribuições deste trabalho são sintetizadas a seguir:

- Os depósitos de ouro hospedados em sequências turbidíticas do Lineamento Córrego do Sítio relacionam-se, principalmente, à arsenopirita e a outros minerais-minério, tais como pirita e pirrotita, além de sulfetos e sulfossais com Sb, Pb, Hg, Cu, Zn, além de Co e Ni;

- Dados litoquímicos demonstraram diferentes proporções em material pelítico para os protólitos dos metaturbiditos, reafirmando a variedade nas fontes sedimentares. As assinaturas de elementos terras raras (REE) obtidas, normalizadas ao NASC, indicam que as atividades hidrotermais exerceram pouca ou insignificante influência sobre a geoquímica dessas rochas;

- Dados geocronológicos de estudos anteriores recentes apresentados sugerem a impressão da Orogenia Brasiliana Ediacarana-Cambriana tardia em rochas hospedeiras dos depósitos de ouro no Quadrilátero Ferrífero, anteriormente interpretados como exclusivamente Arqueanos (ca. 2,7 Ga), bem como modificações estruturais e evidências de alterações hidrotermais relatadas, que antecedem a mineralização arqueana. As análises *in-situ* U-Pb SHRIMP, desenvolvidas neste trabalho, em cristais hidrotermais de monazita dos depósitos Carvoaria e Cachorro Bravo do lineamento Córrego do Sítio e do depósito de ouro Pilar trouxeram novas contribuições nesse sentido;

- As análises SHRIMP realizadas em monazita hidrotermal dos metapelitos mineralizados do depósito Carvoaria resultaram em uma Discordia U-Pb com interceptos em 2.514 ± 22 Ma e 555 ± 19 Ma. Três cristais mais jovens concordantes forneceram uma idade U-Pb Concordia de 539 ± 9 Ma;

- As idades obtidas em amostras mineralizadas do depósito Cachorro Bravo produziram idades SHRIMP U-Pb de 551 ± 10 Ma e 510 ± 11 Ma;

- Para o depósito Pilar, a leste do Lineamento Córrego do Sítio, foi obtida uma idade Pb-Th de 508,2 ± 6,4 Ma, em monazita de xisto sulfetado;

- Os dados geocronológicos obtidos, junto ao acervo de dados geocronológicos de trabalhos citados neste trabalho, reforçam a proposta de uma forte influência Ediacarana-Cambriana, relacionada à atividade hidrotermal produzida aos estágios finais do evento orogênico Brasiliano, sobre depósitos de ouro orogênico Arqueano em todo o Quadrilátero Ferrífero. Os resultados apontam para a importância do entendimento das estruturas brasilianas que controlam o arranjo espacial das jazidas auríferas, como o Lineamento Córrego do Sítio, que compreende importantes alvos de exploração. Esta zona de cisalhamento transcorrente, com *trend* NE-SW pode representar uma estrutura Arqueana reativada durante a Orogenia Brasiliana, que possivelmente condicionou o grande volume de fluidos hidrotermais relacionados ao colapso pós-colisional do Orógeno Araçuaí (Ediacarano-Cambriano) no setor leste do Quadrilátero Ferrífero. Especificamente, as idades cambrianas obtidas em alguns cristais de monazita hidrotermal sugerem que a fase de colapso do Orógeno Araçuaí, que envolveu enorme volume de atividade magmática na forma de intrusões pós-colisionais e circulação de fluidos em escala regional, podem ter influenciado sobremaneira no desenvolvimento final destas estruturas;

- Embora a impressão Cambriana seja persistente em todo QF nos depósitos Arqueanos e Paleoproterozoicos, a total remobilização e desenvolvimento de mineralizações importantes nesse período permanece como uma questão em aberto. Dessa forma, ferramentas de geocronologia de minérios e sulfetos diretamente relacionados com as mineralizações de ouro (por exemplo, os métodos Re-Os para datação de arsenopirita) são sugeridas de forma complementar a este estudo.

- As assinaturas geoquímicas dos metapelitos mineralizados, analisados neste trabalho, dos depósitos de CdS são compatíveis com rochas sedimentares típicas derivadas da erosão da crosta superior;

- Idades T_{DM} Arqueanas de 3,0 - 3,2 Ga e εNd levemente evoluído (2,7 Ga) de -1 a -3 indicam que os complexos TTG do Quadrilátero Ferrífero, especialmente o Complexo de Santa Bárbara, foram as principais áreas de origem dos metaturbiditos. Ambas as unidades se sobrepõem no diagrama de evolução do isótopo Nd. Dessa forma, considerando ainda o Greenstone Belt Rio das Velhas como dominado por rochas metassedimentares, as rochas

ultramáficas podem ser definidas como fontes de menor relevância para a deposição das rochas hospedeiras dos depósitos de ouro do Lineameanto Córrego do Sítio.

- Embora as assinaturas geoquímicas apontadas em trabalhos anteriores (e.g. Zucchetti e Baltazar, 2000) tenham refletido proveniências a partir de fontes distintas para as rochas metassedimentares (depletadas e não depletadas) do Grupo Nova Lima, a falta de correlação dos teores de Au (ppb) e características isotópicas de Nd (εNd (2,7 Ga) e TDM), além das baixas razões La/Yb, sugerem que a erosão de rochas ultramáficas (como as unidades komatiíticas Quebra Ossos) não foi importante como fonte de ouro detrítico, ao menos para os metapelitos que hospedam os principais depósitos que compõem o Lineamento Córrego do Sítio. Da mesma forma, não se observa correlação entre os teores de Au (ppb) e os teores de Cr, Ni (ppm) e MgO (%);

- Os dados de isótopos de Nd, juntamente com novos dados geoquímicos e petrográficos para as rochas CdS, indicam a importância da erosão de complexos TTG para a proveniência de metaturbiditos RVGB. O RVGB é um cinturão de *greenstones* dominado por sedimentos e, portanto, a erosão de rochas ultramáficas não parece ter sido um fator importante no enriquecimento de ouro nos depósitos de rochas sedimentares hospedadas;

- Estudos geoquímicos mais extensos e sistemáticos nos litotipos que hospedam ouro nestes depósitos são sugeridos de forma a apontar possíveis fontes menos fracionadas para as rochas hospedeiras.

7 REFERÊNCIAS

ALKMIM F. F. 2004. O que faz de um cráton um cráton? O Cráton do São Francisco e as revelações Almeidianas ao delimitá-lo. In: Mantesso-Neto V., Bartorelli A., Carneiro C. D. R., Brito-Neves B. B. (eds.). Geologia do Continente Sul-Americano: evolução da obra de Fernando Flávio Marques de Almeida. São Paulo, Beca, p. 17-35.

ALKMIM, F. F. 2018. História Geológica de Minas Gerais. In: Pedrosa-Soares, A.C., Voll, E., Cunha, E.C. Recursos Minerais de Minas Gerais. Companhia de Desenvolvimento de Minas Gerais (CODEMGE), 2018, v. 1, p. 1-35.

ALKMIM, F. F., MARSHAK, S. 1998. Transamazonian orogeny in the Southern Sao Francisco region, Minas Gerais, Brazil: evidence for Paleoproterozoic collision and collapse in the Quadrilátero Ferrıfero. Precambrian Research, v. 90, p. 29-58.

ALKMIM, F. F., MARSHAK, S., PEDROSA-SOARES, A. C., PERES, G. G., CRUZ, S. C. P., WHITTINGTON, A. 2006. Kinematic evolution of the Araçuaí - West Congo orogen in Brazil and Africa: Nutcracker tectonics during the Neoproterozoic assembly of Gondwana. Precambrian Research, v. 149, p. 43-64.

ALKMIM, FF, MARTINS-NETO, MA. 2012. Proterozoic first-order sedimentary sequences of the São Francisco craton, eastern Brazil. Marine and Petroleum Geology, 33 (1), 127-139.

ALKMIM, F. F., NOCE, C. M. (eds.). 2006. The Paleoproterozoic Record of the São Francisco Craton. IGCP 509 Field workshop, Bahia and Minas Gerais, Brazil. Field Guide & Abstracts, 114 p.

ALKMIM F. F. & TEIXEIRA W. 2017. The Paleoproterozoic Mineiro Belt and the Quadrilátero Ferrífero. In: Heilbron M., Cordani U. G., Alkmim F. F. (eds.). São Francisco craton, eastern Brazil. Tectonic Genealogy of a Miniature Continent. Regional Geology Reviews, Springer International Publishing Co., p. 71-94.

ALMEIDA F. F. M. 1967. Origem e evolução da plataforma brasileira. Boletim do Departamento Nacional de Produção Mineral. Divisão de Geologia e Mineralogia, Rio de Janeiro, n. 241, 36 p.

ALMEIDA, F.F.M. 1977. O Cráton do São Francisco. Rev. Bras. Geosci. 7, 349–364.

ARAÚJO, J., FERREIRA R., FREITAS, F., MAGALHÃES, J. 2020. The Archean Rio Das Velhas Greenstone Belt Revisited: New Insights into Stratigraphy. Journal of the Geological Survey of Brazil v. 3, p. 113-49.

BABINSKI, M., CHEMALE JR., F., VAN SCHMUS, W.R.1991. Pb/Pb geochronology of carbonate rocks of Minas Supergroup, Quadrilátero Ferrífero, Minas Gerais, Brazil. Eos Trans. Am. Geophys. Union 1991 Fall Meet. Suppl. 72, 531.

BABINSKI, M., CHEMALE JR., F., VAN SCHMUS, W. R. 1995. The Pb/Pb age of the Minas Supergroup carbonate rocks, Quadrilátero Ferrífero, Brazil. Precambrian Research. 72, 235-245.

BALTAZAR O. F., CORRÊA NETO A. V., SILVA S. L., ZUCCHETTI M., CARVALHO J. B., RAPOSO F. O. 1994. Uma tentativa preliminar de aplicação da estratigrafia de seqüências ao greenstone belt Rio das Velhas, Quadrilátero Ferrífero (MG). In: 38th Congresso Brasileiro de Geologia. SBG, Camboriú, 82–83.

BALTAZAR, O. F., PEDREIRA, A. J. 1996. Associações de litofácies. In: CPRM - Companhia de Pesquisa de Recursos Minerais. Projeto Rio das Velhas - Texto Explicativo do Mapa Geológico Integrado, escala 1:100.000. Departamento Nacional de Produção Mineral/CPRM–Serviço Geológico do Brasil, Belo Horizonte, p. 43–48.

BALTAZAR, O.F., PEDREIRA, A.J. 1998. In: Departamento Nacional de Produção Mineral. Associações litofaciológicas. (Belo Horizonte), DNPM.

BALTAZAR, O.F., SILVA, S. L. 1996. Projeto Rio das Velhas: Mapa Geológico Integrado do Supergrupo Rio das Velhas, escala 1:100.000. Departamento Nacional de Produção Mineral/CPRM–Serviço Geológico do Brasil, Belo Horizonte.

BALTAZAR O.F. & SILVA S.L. 1998. Projeto Rio das Velhas - texto explicativo do mapa geológico integrado, escala 1: 100.000. Belo Horizonte, Departamento Nacional de Produção Mineral. 126 p.

BALTAZAR, O. F., ZUCCHETTI, M. 2007. Lithofacies associations and structural evolution of the Archean Rio das Velhas greenstone belt, Quadrilátero Ferrífero, Brazil: a review of the setting of gold deposits. Ore Geology Reviews, v. 32, p. 471-499.

BALTAZAR, O. F., LOBATO, L. M. 2020. Structural Evolution of the Rio das Velhas Greenstone Belt, Quadrilátero Ferrífero, Brazil: Influence of Proterozoic Orogenies on Its Western Archean Gold Deposits. Minerals 10, 983.

BIERLEIN F.P., FULLER T., STUWEL K., ARNE D.C., KEAYS R.R. 1998. Wallrock alteration associated with turbidite-hosted gold deposits examples from Central Victoria. Ore Geology Reviews, 13(1-5):345-380.

BOUMA A.H. 1983. Intraslope basins in northwest Gulf of Mexico: a key to ancient submarine canyons and fans. American Association of Petroleum Geologists Special Publication, 32:567-581.

BRANDO SOARES M., CORRÊA NETO A.V., ZEH A., CABRAL A. R., PEREIRA L .F., PRADO M. G. B., ALMEIDA A. M., MANDUCA L. G., SILVA P. H. M., MABUB R. O. A., SCHLITA T. M. 2017. Geology of the Pitangui greenstone belt, Minas Gerai, Brazil: Stratigraphy, geochronology and BIF geochemistry. Precambrian Res., 291: 17-41.

BRUECKNER, H. K., CUNNINGHAM, D., ALKMIM, F. F., MARSHAK, S. 2000. Tectonic implications of Precambrian Sm-Nd dates from the southern São Francisco craton and adjacent Araçuai and Ribeira belts, Brazil. Precambrian Res. 99, 255-269.

CABRAL, A. R., BEAUDOIN, G., KWITKO, R., LEHMANN, B., POLÔNIA, J. C., AND CHOQUETTE, M. 2006. Platinum-palladium nuggets and mercury-rich palladiferous platinum from Serro, Minas Gerais, Brazil: Canadian Mineralogist, v.44, p. 385–397.

CABRAL, A. R., LEHMANN, B., TUPINAMBÁ, M., SCHLOSSER, S., KWITKO-RIBEIRO, R., ABREU, F. R. 2009. The platiniferous Au-Pd belt of Minas Gerais, Brazil, and genesis of its botryoidal Pt-Pd-Hg aggregates. Economic Geology and the Bulletin of the Society of Economic Geologists, v. 104, p. 1265–1276.

CABRAL, A. R., ZEH, A., KOGLIN, N., GOMES, A. A. S., VIANA, D. J., LEHMANN, B. 2012. Dating the Itabira iron formation, Quadrilátero Ferrífero of Minas Gerais, Brazil, at 2.65 Ga: depositional U-Pb age of zircon from a metavolcanic layer. Precambrian Res. 204, 40-45.

CABRAL A. R., EUGSTER, O., BRAUNS, M., LEHMANN, B., RÖSEL, D., ZACK, T., ABREU, F. R., PERNICKA, E., BARTH, M. 2013. Direct dating of gold by radiogenic helium: testing the method on gold from Diamantina, Minas Gerais, Brazil. Geology, v. 41, p. 163-166.

CABRAL, A.R., ZEH, A., GALBIATTI, H. F., LEHMANN, B. 2015. Late Cambrian Au–Pd mineralization and Fe enrichment in the Itabira district, Minas Gerais, Brazil, at 496 Ma: constraints from U–Pb monazite dating of a jacutinga lode. Economic Geology, v. 110, p. 263-272.

CABRAL, A. R, ZEH, A. 2015. Detrital zircon without detritus: a result of 496-Ma-old fluid–rock interaction during the gold-lode formation of Passagem, Minas Gerais, Brazil. Lithos p. 212-215, 415–427.

CANALE A.L. 1999. Geologia do depósito Córrego do Sítio, Quadrilátero Ferrífero (MG), e caracterização mineralógica do minério sulfetado.MS Dissertation, Universidade Federal do Rio Grande do Sul, Porto Alegre, 142 p.

CANUTO, J. R. 2010. Estratigrafia de sequências em bacias sedimentares de diferentes idades e estilos tectônicos. Rev. Bras. Geociências 40 (4), 537-549.

CARNEIRO, M.A., CARVALHO JR. I. M., TEIXEIRA, W.1998. Petrologia, geoquímica e geocronologia dos diques máficos do Complexo Metamórfico Bonfim Setentrional (Quadrilátero Ferrífero) e suas implicações na evolução crustal do Craton do São Francisco Meridional. Revista Brasileira de Geociências, 29 (1), 29–44.

CASTAÑEDA, C., PEDROSA-SOARES, A. C., BELÉM, J., GRADIM, D., DIAS, P. H. A., MEDEIROS, S. R., OLIVEIRA, L. 2006. Mapa Geológico e Nota Explicativa da Folha Ecoporanga, 1:100.000. In: Folha Ecoporanga. Programa Geologia do Brasil, ContratoCPRM-UFMG, CD-ROM.

CAXITO, F.A., HAGEMANN, S., GONÇALVES DIAS, T., BARROTE, V., DANTAS, E.L., CHAVES, A.O., CAMPELLO, M.S., CAMPOS, F.C. 2020. A magmatic barcode for the São Francisco Craton: Contextual in-situ SHRIMP UPb baddeleyite and zircon dating of the Lavras, Pará de Minas and Formiga dyke swarms and implications for Columbia and Rodinia reconstructions. Lithos.

CHEMALE JR., F., ROSIÉRE, C. A., ENDO, I. 1994. The tectonic evolution of the Quadrilátero Ferrífero, Minas Gerais, Brazil. Precambrian Res. 65, 25-54.

COX S.F., SUN S.S., ETHERIDGE M.A., WALL V.J., POTTER T.F. 1995. Structural and geochemical controls on the development of turbidite-hosted gold quartz vein deposits, Wattle Gully mine, central Victoria, Australia. Economic Geology, 90:1722-1746.

DAVID, M. E. V., 2006. Composição Isotópica de Pb – Sr e Nd da Mineralização de Ouro do Depósito Córrego do Sítio, Quadrilátero Ferrífero (M.G.): implicações na modelagem conceitual. IGc-USP. Dissertação de Mestrado. p. 76.

DE CAMPOS, C.P., DeMedeiros, S.R., Mendes, J.C., Pedrosa-Soares, A.C., Dussin, I., Ludka, I.P., Dantas, E.L. 2016. Cambro-Ordovician magmatism in the Araçuaí Belt (SE Brazil): snapshot from a post-collisional event. Journal of South American Earth Sciences 68, 248–268.

DE WIT, M. J. 1991. Archaean greenstone belt tectonism and basin development: some insights from the Barberton and Pietersburg greenstone belts, Kaapvaal Craton, South Africa. v.13(1), p-45-63.

DIAS, T. G., FIGUEIREDO E SILVA, R. C., LOBATO, L. M., DE ANDRADE CAXITO, F., HAGEMANN, S., SCHNEIDER SANTOS, J. O., & BARROTE, V. 2022. Ediacaran - Cambrian fluid flow in Archean orogenic gold deposits: Evidence from U–Pb SHRIMP hydrothermal monazite ages of the metaturbidite-hosted Córrego do Sítio and Pilar deposits, Quadrilátero Ferrífero, Brazil. Journal of South American Earth Sciences, 116, [103844].

DORR, J.V.N., GAIR, J. E., POMERENE, J. B., RYNEARSON, G. A. Revisão da estratigrafia pré-cambriana do Quadrilátero Ferrífero. Departamento Nacional de Produção Mineral. Divisão de Fomento à Produção Mineral, Avulso 81, 31 p. 1957.

DORR J.V.N II. 1965. Nature and origin of the high-grade hematite ores of Minas Gerais, Brazil. Economic Geology, 60: 1-46.

DORR, J.V.N. 1969. Physiographic, Stratigraphic and Structural Development of the Quadrilátero Ferrífero, Minas Gerais, Brazil. Regional Geology of the Quadrilátero Ferrífero, Minas Gerais, Brazil.

DUCLAUX, G., HOUGH, R., GAZLEY, M. F. 2012. Late tectonic evolution of plutonic gold mine and controls on gold mineralisation. Structural geology and Resources. Austr. Ins. Geosci. Bull. 56, 75–78.

ERIKSSON, K.A., KRAPEZ, B., FRALICK, P.W. 1994. Sedimentology of Archean greenstone belts: signatures of tectonic evolution. Earth Sci. Rev. 37, 1-88.

FARINA, F., ALBERT, C., LANA, C. 2015. The Neoarchean transition between mediumand high-K granitoids: clues from the Southern São Francisco Craton (Brazil). Precambrian Res. 266, 375 e 394.

FARINA, F., ALBERT, C., MARTÍNEZ DOPICO, C., AGUILAR GIL, C., MOREIRA, H., HIPPERTT, J., CUTTS, K., ALKMIM, F., LANA, C. 2016. THE ARCHEAN PALEOPROTEROZOIC EVOLUTION OF THE QUADRILÁTERO Ferrífero (Brasil): current models and open questions. J. South Am. Earth Sci.

GAZLEY, M. F. 2011. Metamorphism, Geochronology and Stratigraphy of an Amphibolite–Facies Greenstone–Hosted Gold Deposit: Plutonic Gold Mine, MarymiaInlier, Western Australia. PhD thesis. Victoria University of Wellington, New Zealand.

GAZLEY, M. F., VRY, J. K., MILLET, M. A., HANDLER PLESSIS, E. D., BAKER, J. A. 2016. New age constraints on metamorphism, metasomatism and gold mineralisation at plutonic gold mine, Marymia inlier, western Australia. Aust. J. Earth Sci. 63 (4), 413–426.

GRADIM, C., RONCATO, J., PEDROSA-SOARES, A.C., CORDANI, U., DUSSIN, I., ALKMIM, F.F., QUEIROGA, G., JACOBSOHN, T., SILVA, L.C., BABINSKI, M. 2014. The hot back-arc zone of the Araçuaí orogen, eastern Brazil: from sedimentation to granite generation. Brazilian Journal of Geology 44, 155–180.

GONÇALVES, G. O., LANA, C., SCHOLZ, R., BUICK, I. S., GERDES, A., KAMO, S. L., CORFU, F., MARINHO, M. M., CHAVES, A. O., VALERIANO, C., NALINI JR., H. A. 2016. An assessment of monazite from the Itambé pegmatite district for use as U–Pb isotope reference material for microanalysis and implications for the origin of the "Moacyr" monazite. Chemical Geology 424, 30–50.

GONÇALVES, G. O, LANA, C., BUICK, I. S., ALKMIM, F. F., SCHOLZ, R., QUEIROGA, G. 2019. Twenty million years of post-orogenic fluid production and hydrothermal mineralization across the external Araçuaí orogen and adjacent São Francisco craton, SE Brazil. Lithos (342–343) 557–572.

GRAND'HOMME, A. 2016. Hydrothermal monazite: the unavoidable accessory. Earth Sciences. Université Grenoble Alpes, English.

GROMET L.P., DYMEK R.F., HASKIN L.A., KOROTEV R.L. 1984. The "North American shale composite": Its compilation, major and trace element characteristics. Geochimica et Cosmochimica Acta, 48:2469-2482.

GROVES D. I., FOSTER R. P. 1991. Archaean lode gold deposits. In: K.P. FOSTER (Ed.) Gold Metallogeny and Exploration. Londres, p. 63-103

GROVES, D. I., GOLDFARB, R. J., GEBRE-MARIAM, M., HAGEMANN, S., ROBERT, F. 1998. Orogenic gold deposits: a proposed classification in the context of their crustal distribution and relationship to other gold deposit types. Ore Geology Reviews, v. 13, p. 7-27.

GROVES, D. I., GOLDFARB, R. J., ROBERT, F., HART, C. J. 2003. Gold deposits in metamorphic belts: overview of current understanding, outstanding problems, future research, and exploration significance. Economic Geology, v. 98, p. 1-29,

GROVES, D. I., RIDLEY, J. R., BLOEM, E. J. M., GEBRE-MARIAM, M., HRONSKY, J. M. A., KNIGHT, J. T., MCNAUGHTON, N. J., OJALA, V. J., VIELREICHER, R. M., HOLYLAND, P. W., MCCUAIG, T.C. 1995. Lode-gold deposits of the Yilgarn Block: products of late-Archaean crustal-scale overpressured hydrothermal systems. In: COWARD, M.P., RIES, A.C. (Eds.), Early Precambrian Processes, Journal of the Geological Society of London, Special Publication, vol. 95, pp. 155-172.

HARDER, E. C., CHAMBERLAIN, R. T. A. 1915. The geology of central Minas Gerais, Brazil. Journal of Geology, v. 23, n. 4, p. 341-378, n. 5, p. 385-424.

HARTMANN, L. A., ENDO, I., SUITA, M. T. F., SANTOS, J. O. S., FRANTZ, J. C., CARNEIRO, M. A., NAUGHTON, N. J., BARLEY, M. E. 2006. Provenance and age delimitation of Quadrilátero Ferrífero sandstones based on zircon U-Pb isotopes. J. S. Am. Earth Sci. 20, 273-285.

HEILBRON, M., MACHADO, N. 2003. Timing of terrane accretion in the Neoproterozoic-Eopaleozoic Ribeira orogen (SE Brazil). Precambrian Research, (125): 87-112.

JUNQUEIRA, P.A., LOBATO, L.M., LADEIRA, E.A., SIMÕES, E.J.M. 2007. Structural control and hydro-thermal alteration at the BIF-hosted Raposos lode-gold deposit, Quadrilátero Ferrífero, Brazil. Ore Geology Reviews, v. 32, p. 629-650.

KEMPE, U., LEHMANN, B., WOLF, D., RODIONOV, N., BOMBACH, K, SCHWENGFELDER, U., DIETRICH, A. 2008. U–Pb SHRIMP geochronology of Th-poor, hydrothermal monazite: An example from the Llallagua tin-porphyry deposit, Bolivia. Geochimica et Cosmochimica Acta (72) 4352–4366.

KOGLIN, N., ZEH, A., CABRAL, A. R., GOMES, A. A. S., NETO, A.V. C., BRUNETTO, W. J., GALBIATTI, H. 2014. Depositional age and sediment source of the auriferous Moeda Formation, Quadrilátero Ferrífero of Minas Gerais, Brazil: new constraints from U-Pb-Hf isotopes in zircon and xenotime. Precambrian Res. 255, 96-108.

KOVALEV, K. R., KALININ, Y. A., NAUMOV, E. A., MYAGKAYA, M. K. 2014. Relationship of antimony with gold mineralization in the ore districts of Eastern Kazakhstan. Russian Geology and Geophysics (55) 1170–1182.

KRAPEZ B. 1993. Sequence stratigraphy of the Archaean supracrustal belts of the Pilbara Block, Western Australia. Precambrian Research, 60:1-45.

LADEIRA, E. A. 1980. Metalogenesis of gold at the Morro Velho mine, and in the Nova Lima District, Quadrilátero Ferrífero, Minas Gerais, Brazil. Tese (Doutorado em Geologia) - Department of Geology, University of Western Ontario, London, Canada.

LADEIRA E.A. Genesis of gold in Quadrilátero Ferrífero: a remarkable case of permanency, recycling and inheritance – A tribute to Djalma Guimarães, Pierre Routhier and Hans Ramberg. In: E.A. Ladeira (ed.) 1991. Brazil Gold'91 The economics, geology, geochemistry and genesis of gold deposits. A.A. Balkema, Rotterdam, 11-30.

LANA, C., ALKMIM, F.F., ARMSTRONG, R., SCHOLZ, R., ROMANO, R., NALINI, H.A. 2013. The ancestry and magmatic evolution of Archaean TTG rocks of the Quadrilátero Ferrífero province, southeast Brazil. Precambrian Research, 230, 1–30.

LARIONOVA, Y. O., SAMSONOV, K. N., SHATAGIN, K. N., NOSOVA, A. A. 2013. Isotopic geochronological evidence for the paleoproterozoic age of gold mineralization in Archean greenstone belts of Karelia, the Baltic shield. Geol. Ore Deposits 55, 320–340.

LAURENT, O., MARTIN, H., MOYEN, J. F., DOUCELANCE, R. 2014. The diversity and evolution of late-Archean granitoids: evidence for the onset of “modern-style” plate tectonic between 3.0 and 2.5 Ga. Lithos 205, 208-235.

LIMA, L.C. 2012. Depósito LODE Au-As-Sb Laranjeiras, em metaturbitos do Grupo Nova Lima, Quadrilátero Ferrífero, Minas Gerais. Dissertação (Mestrado em Geologia) - Instituto de Geociências, Universidade Federal de Minas Gerais, Belo Horizonte.

LOBATO L.M. & PEDROSA-SOARES A.C. 1993. Síntese dos Recursos Minerais do Craton do São Francisco e Faixas Marginais em Minas Gerais. Geonomos, 1(1):51-64.

LOBATO, L. M., VIEIRA, F. W. R. 1998. Styles of hydrothermal alteration and gold mineralization associated with the Nova Lima Group of the Quadrilátero Ferrífero: Part II, the Archean mesothermal gold-bearing hydrothermal system. Revista Brasilera de Geociências, n. 1, v. 28, p. 355-366.

LOBATO, L.M., RIBEIRO-RODRIGUES, L.C., VIEIRA, F.W.R. 2001. Brazil's premier gold province. Part II: geology and genesis of gold deposits in the Archean Rio das Velhas greenstone belt, Quadrilátero Ferrífero. Mineralium Deposita, v. 36, p. 249-277.

LOBATO L.M., BALTAZAR O.F., REIS L.B., ACHTSCHIN A.B., BAARS F.J., TIMBÓ M.A., BERNI G.V., MENDONÇA B.R.V., FERREIRA D.V. 2005. Projeto Geologia do Quadrilátero Ferrífero - integração e correção cartográfica em SIG com nota explicativa. Belo Horizonte, CODEMIG. 1 CD-ROM.

LOBATO, L. M., RENGER, F. E., SILVA, R. C. F., ROSIERE, C. A., BAARS, F. J., ROLIN, V. K. 2014. Metalogênese do setor meridional do Cráton São Francisco. In: SILVA, M.G., NETO, M.B.R., JOST, H., KUYUMJIAN, R.M. (eds.). Metalogênese Das Províncias Tectônicas Brasileiras. Belo Horizonte, p. 119–140.

LOBATO, L., SANTOS, J., MCNAUGHTON, N., FLETCHER, I., NOCE, C. 2007. U–Pb SHRIMP monazite ages of the giant Morro Velho and Cuiabá gold deposits, Rio das Velhas greenstone belt, Quadrilátero Ferrífero, Minas Gerais, Brazil. Ore Geology Reviews, v.32, p. 674-680.

LOCZY, L., LADEIRA, E. A. 1976. Geologia Estrutural e Introdução à Geotectônica. São Paulo: Edgar Blücher, 528 p.

LUDWIG, K.R. 2003. Isoplot 3.00: A geochronological toolkit for Microsoft Excel. Berkeley Geochronology Center Special Publication, 4, p.70.

LUDWIG, K.R. 2009. SQUID 2: A User’s Manual, rev. 12 Apr, 2009. Berkeley Geochronology Center, Special Publication, 5, p.110.

MACHADO, N., NOCE, C.M., LADEIRA, E.A., DE OLIVEIRA, O.A.B. 1992. U-Pb geochronology of the Archean magmatism and Proterozoic metamorphism in the Quadrilátero Ferrífero, southern São Francisco Craton, Brazil. Geol. Soc. Am. Bull.104, 1221 e 1227.

MACHADO, N., SCHRANK, A., NOCE, C.M., GAUTHIER, G. 1996. Ages of detrital zircon from Archean-Paleoproterozoic sequences: implications for Greenstone Belt setting evolution

of a Transamazonian foreland basin in Quadrilátero Ferrífero, southeast Brazil. Earth Planet. Sci. Lett. 141, 259-276.

MACHADO, N., VALLADARES, C. S., HEILBRON, M., VALERIANO, C. M. 1996. U-Pb geochronology of Central Ribeira belt. Precambrian Research, (79): 347-361.

MARSHAK, S., ALKMIM, F. F., JORDT-EVANGELISTA, H. 1992. Proterozoic crustal extension and the generation of dome-and-keel structures in an Archaean granite-greenstone terrane. Nature 357, 491-493.

MARTINS, B. S., LOBATO, L. M., ROSIÈRE, C. A., HAGEMANN, S. G., SANTOS J. O. S., VILLANOVA, F. L. S. P., SILVA, R. C. F., LEMOS, L. H. A. 2016. The Archean BIF-hosted Lamego gold deposit, Rio das Velhas greenstone belt, Quadrilátero Ferrífero: Evidence for Cambrian structural modification of an Archean orogenic gold deposit. Ore Geology Reviews, v. 72, p. 963-988.

MARTINS PEREIRA, S.L., LOBATO, L.M., FERREIRA, J.E., JARDIM, E.C. 2007. Nature and origin of the BIF-hosted São Bento gold deposit, Quadrilátero Ferrífero, Brazil, with special emphasis on structural controls. Ore Geology Reviews, v. 32, p. 571–595.

MARTINS, R. 2016. Programa de Exploração Anglogold Ashanti Brasil. Simexmin. Disponível em:http://www.adimb.com.br/simexmin2012/wpcontent/themes/simexmin/palestras/02%20-%20Programas%20Empresariais/III_4_Martins.pdf. Acesso em 20/01/2020

MCMILLAN, N.M. 1996. Late–Archaean, Syn–Amphibolite Facies, Lode–Gold Deposits Overprinted by Palaeoproterozoic Deformation, Metasomatism and Hydrothermal Activity at Marymia, Western Australia. PhD Dissertation. The University of Western Australia, Perth WA (Perth, Western Australia).

MELO-SILVA, AMARAL, W. S., OLIVEIRA, E. P. 2020. Geochronological evolution of the Pitangui greenstone belt, southern São Francisco Craton, Brazil: Constraints from U-Pb zircon age, geochemistry and field relationships. Journal of South American Earth Sciences. v. 99, 102380.

MENDES, M. D. C. O., LOBATO, L. M., SUCKAU, V., LANA, C. 2014. Datação U-Pb in situ por LA-ICPMS em zircões detríticos da Formação Cercadinho, Supergrupo Minas. Geol. USP. Série Científica 14 (1), 55 - 68.

MENDES, J. C., MEDEIROS, S. R., MCREATH, I., DE CAMPOS, C. M. P. 2005. Cambro-Ordovician magmatism in SE Brazil: U-Pb and Rb-Sr Ages, combined with Sr and Nd isotopic data of charnockitic rocks from the Varzea Alegre Complex. Gondwana Research, 8 (3): 337-345.

MOLNÁR, F., O'BRIEN, H., LAHAYE, Y., KÄPYAHO, A., SORJONEN–WARD, P., HYODO, H., SAKELLARIS, G. 2016. Signatures of multiple mineralization processes in the Archean orogenic gold deposit of the Pampalo mine, Hattu schist belt, eastern Finland. Econ. Geol. 111, 1659–1703.

MORALES, M. J., SILVA, R. C. F., LOBATO, L. M., GOMES, S. D., GOMES, C. C. C. O, BANKS, D. A. 2016. Metal source and fluid–rock interaction in the Archean BIF-hosted Lamego gold mineralization: Microthermometric and LA-ICP-MS analyses of fluid inclusions in quartz veins, Rio das Velhas greenstone belt, Brazil. Ore Geology Reviews, v. 72, p. 510-531,

NOCE, C.M., MACHADO, N., TEIXEIRA, W. 1998. U-Pb geochronology of gneisses and granitoids in the Quadrilátero Ferrífero (Southern São Francisco Craton): age constraints for Archean and Paleoproterozoic magmatism and metamorphism. Rev. Bras. Geociências 28, 95 e 102.

NOCE, C. M., MACAMBIRA, M. J. B, PEDROSA-SOARES, A. C. 2000. Chronology of Neoproterozoic-Cambrian granitic magmatism in the Araçuaí Belt, Eastern Brazil, based on single zircon evaporation dating. Revista Brasileira de Geociências. 30(1): 025-029.

NOCE, C.M., ZUCCHETTI, M., BALTAZAR, O.F., ARMSTRONG, R., DANTAS, E.L., RENGER, F.E., LOBATO, L.M. 2005. Age of felsic volcanism and the role of ancient continental crust in the evolution of the Neoarchean Rio das Velhas greenstone belt (Quadrilátero Ferrífero, Brazil): U-Pb zircon dating of volcaniclastic graywackes. Precambrian Res. 141, 67 e 82.

NOCE, C. M., TASSINARI, C., LOBATO, L. M. 2007. Geochronological framework of the Quadrilátero Ferrífero, with emphasis on the age of gold mineralization hosted in Archean greenstone belts. Ore Geology Reviews, v. 32, p. 500-510.

PASSOS, R.V. 1999. Caracterização da geometria de zonas de alteração hidrotermal – Estudo de caso no Depósito Aurífero de Brumal, Quadrilátero Ferrífero/MG – São Paulo,95 p. (Dissertação de Mestrado, Inst. Geoc., UNICAMP).

PAQUETTE, J.-L., NÉDÉLEC, A., MOINE, B., RAKOTONDRAZAFY, M. 1994. U–Pb, single zircon Pb evaporation, and Sm–Nd isotopic study of a granulite domain in SE Madagascar. J. Geol. 102, 523–538.

PEDREIRA, A.J., SILVA, S.L. 1996. Sistemas deposicionais do greenstone belt Rio das Velhas, Quadrilátero Ferrífero, Minas Gerais. 39° Congresso Brasileiro de Geologia. Salvador, pp. 138–140.

PEDROSA-SOARES, A. C., WIEDEMANN-LEONARDOS, C. M. 2000. Evolution of the Araçuaí Belt and its connection to the Ribeira Belt, Eastern Brazil. In: U. CORDANI, E. MILANI, A. THOMAZ-FILHO & D. A. CAMPOS (eds), Tectonic Evolution of South America. São Paulo, Sociedade Brasileira de Geologia, p. 265-285.

PEDROSA-SOARES, A. C., CASTAÑEDA, C., QUEIROGA, G., GRADIM, C., BELÉM, J., RONCATO, J., NOVO, T., DIAS, P., GRADIM, D., MEDEIROS, S., JACOBSOHN, T., BABINSKI, M., VIEIRA, V. 2006. Magmatismo e Tectônica do Orógeno Araçuaí no extremo leste de Minas e norte do Espírito Santo (18°-19°S, 41°-40°30'W). Geonomos. 14(1, 2): 97 – 111.

PEDROSA-SOARES, A., DE CAMPOS, C.P., NOCE, C., SILVA, L.C., NOVO, T., RONCATO, J. 2011.Late Neoproterozoic-Cambrian granitic magmatism in the Araçuaí orogen

(Brazil), the Eastern Brazilian Pegmatite Province and related mineral resources. Geol. Soc. Lond. Spec. Publ. 350, 25–51.

PEIXOTO E., ALKMIM F. F., PEDROSA-SOARES A., LANA C., CHAVES A. O. 2018. Metamorphic record of collision and collapse in the Ediacaran-Cambrian Araçuaí orogen, SE-Brazil: Insights from P-T pseudosections and monazite dating. Journal of Metamorphic Geology, 36(2):147-172.

PEREIRA, S. M., LOBATO, L. M., FERREIRA, J. E., JARDIM, E. C. 2007. The BIF-hosted São Bento gold deposit, Quadrilátero Ferrífero, Brazil. Ore Geology Reviews, v. 32, p. 571-595.

PERRING, C. S., MCNAUGHTON, N. J. 1990. Geological note: Proterozoic remobilization of ore metals within Archaean gold deposits: lead isotope evidence from Norseman, Western Australia. Aust. J. Earth Sci. 37, 369–372.

PINTO C. P. AND SILVA M. A. 2014. Mapa Geológico do Estado de Minas Gerais, Escala 1:1.000.000. Companhia de Desenvolvimento Econômico de Minas Gerais, CODEMIG e Serviço Geológico do Brasil, CPRM.

PORTO C.G. 2008. A mineralização aurífera do depósito Córrego do Sítio e sua relação com o enxame de diques metamáficos no corpo Cachorro Bravo - Quadrilátero Ferrífero - Minas Gerais. MS Dissertação Universidade Federal de Minas Gerais, Belo Horizonte, 117 p.

PRESSACCO, R, SEPP, J. 2018. Jaguar Minig INC. Technical Report on the Roça Grande and Pilar Mines, Minas Gerais State, Brazil.NI 43-101 Report, Toronto, 217 p.

RAMSAY, W.R.H., BIERLEIN, F.P., ARNE, D.C., VANDENBERG, A.H.M.1998. Turbidite-hosted gold deposits of Central Victoria, Australia: their regional setting, mineralizing styles and some genetic constraints. Ore Geology Reviews 13, 131–151.

RAYNER, N.M. AND STERN, R.A. 2002. Improved sample preparation method for SHRIMP analysis of delicate mineral grains exposed in thin sections. Natural Resources Canada, Geological Survey of Canada.

RASMUSSEN, B. AND FLETCHER, I.R. 2010. Dating sedimentary rocks using in situ U-Pb geochronology of syneruptive zircon in ash-fall tuffs< 1 mm thick. Geology, 38(4), pp.299-302.

RENGER, F.E., NOCE, C.M., ROMANO, A.W., MACHADO, N. 1995. Evolução sedimentar do Supergrupo Minas: 500 Ma. de registro geológico no Quadrilátero Ferrífero, Minas Gerais, Brasil. Geonomos 2 (1), 1-11.

RIBEIRO-RODRIGUES, L. C., LOBATO, L. M. 1999. Classificação dos depósitos de ouro do Quadrilátero Ferrífero, Minas Gerais. Revista de Ciências, Caratinga, v. 1, n.2, p. 35-50.

RIBEIRO-RODRIGUES, L.C. GÜNTHER, F. LOBATO, M. L. DUNQUINI, JAIME, VIEIRA, F. W.R. 2000. Gold Mineralization in the Quadrilatero Ferrifero Minas Gerais. Zeitschrift Für Angewandte Geologie, p. 143-153.

RIBEIRO Y., SILVA R. C. F., LOBATO L. M., LIMA L. C., HAGEMANN S. G., CLIFF J. 2013. Estudo de inclusões fluidas em veios de quartzo e carbonato (± sulfetos e sulfossais) do depósito Carvoaria Velha, Lineamento Aurífero Córrego do Sítio, Santa Bárbara, Quadrilátero Ferrífero, MG. Geonomos, 21:7-28.

RIBEIRO, Y, SILVA, R. C. F., LOBATO, L, LIMA, L. C., RIOS, F. J., HAGEMANN, S. G., CLIFF, J. 2015. Fluid inclusion and sulfur and oxygen isotope studies on quartz-carbonate-sulfide veins of the Carvoaria Velha deposit, Córrego do Sítio gold lineament, Quadrilátero Ferrífero, Minas Gerais, Brazil. Ore Geology Reviews, n.1, v. 67, p. 11-33.

RIDLEY, J.R., DIAMOND, L.W. 2000. Fluid chemistry of orogenic lode gold deposits and implications for genetic models, in Hagemann, S.G., and Brown, P.E., eds., Gold in 2000: Society of Economic Geologists, Reviews in Economic Geology, v. 13, p. 141-162,

RIOS GUERRERO, L. J. 2016. Metalogênese do depósito aurífero Pilar, Santa Bárbara, MG. MSc Dissertation, Universidade Federal do Amazonas, Manaus,142 p. 100.

ROBERTS, R.G. 1988. Archean lode gold deposits. In: P.A. Sheahan, M.E. Cherry (eds.) Ore Deposit Models I. St. John's, Canada, Geol. Assoc. Canada, 1-199 (Geoscience Canada Reprint Series 3).

ROMANO A. 2007. Programa Geologia do Brasil. Folha Pará de Minas, SE- 23-Z-CI. Escala 1:100.000, relatório final: 72p. Belo Horizonte. UFMG – CPRM.

ROMANO, R., LANA, C., ALKMIM, F.F., STEVENS, G.S., ARMSTRONG, R. 2013. Stabilization of the southern portion of the São Francisco Craton, SE Brazil, through a longlived period of potassic magmatism. Precambrian Research 224, 143–159.

RONCATO, J. G, LOBATO, L. M, LIMA, L. C., PORTO, C. G., SILVA, R. C. F. 2015. Metaturbidite-hosted gold deposits, Córrego do Sítio lineament, Quadrilátero Ferrífero, Brazil. Brazilian Journal of Geology, n.1, v. 45, p. 5-22.

SEQUETTO-PEREIRA M.A., LOBATO L.M., ROSIÈRE C.A., SILVA R.C.F. 2013. Classificação dos veios quartzo-carbonáticos de depósitos auríferos no Lineamento Córrego do Sítio, QF, MG. Geonomos, 21:53-71.

SCHANDL, E. S.AND GORTON, M. P. 2004. A textural and geochemical guide to the identification of hydrothermal monazite: criteria for selection of samples for dating epigenetic hydrothermal ore deposits. Economic Geology. 99, pp. 1027–1035.

SCHORSCHER H.D., CARBONARI F.S., POLONIA J.C., MOREIRA J.M.P. 1982. Quadrilatero Ferrífero - Minas Gerais State: Rio das Velhas Greenstone Belt and Proterozoic Rocks. In: International Symposium on Archean and Early Proterozoic Crustal Evolution and Metallogenesis. Salvador, 46 p.

SCHORSCHER, H.D. 1978. Komatiítos na estrutura “Greenstone Belt” Série Rio das Velhas, Quadrilátero Ferrífero, Minas Gerais, Brasil. In: Congresso Brasileiro de Geologia, 30, Recife. Anais da Sociedade Brasileira de Geologia, p. 292-293.

SILVEIRA BRAGA, F.C., SANTOS, J.O.S., ROSIÈRE, C.A., ROLIM, V.K., ROBERTS, M.P., EVANS, N.J., HAGEMANN, S.G. 2020. Ediacaran-Cambrian far- field hydrothermal event in the southeast of the São Francisco Craton, Brazil : Evidence from zircon U-Pb SHRIMP, trace elements, Lu-Hf and oxygen isotopes. Lithos 56–357, 1–21.

SILVEIRA BRAGA, F.C., ROSIÈRE, C.A., SANTOS, J.O.S., ROLIM, HAGEMANN, S.G., DANYUSSHEVSKY, L., SALLES, P. V. 2021. Geochemical and tectonic constraints on the genesis of iron formation-hosted magnetite hematite deposits at the Guanhães Block (Brazil) by contact metasomatism with pegmatiteintrusions. Ore Geology Reviews. 129, 103931.

STERN R.A. AND SANBORN N. 1998. Monazite U-Pb and Th-Ph geochronology by high-resolution secondary ion mass spectrometry. Radiogenic age and isotopic studies, Report 11, Geological Survey of 890 Canada, Ottawa, ON, Canada, 1–18.

TAYLOR, S. R., MCLENNAN, S. M. 1985. The Continental. Crust: its Composition and Evolution. Blackwell Scientific Publications, Oxford. 312 p.

TAYLOR S. R., RUDNICK R. L., MCLENNAN S. M., AND ERIKSSON K. A. 1986. Rare earth element patterns in Archaean high-grade meta-sediments and their tectonic significance. Geochim. Cosmochim.Acta 50, 2267–2279.

TEIXEIRA, W., SABATE, P., BARBOSA, J., NOCE, C. M., CARNEIRO, M. A. 2000. Archean and Paleoproterzoic tectonic evolution of the Sao Francisco Craton, Brazil. In: Cordani, U. G., Milani, E. J., Thomaz Fo, A., Campos, D. A. (eds.). Tectonic Evolution of South America. Rio de Janeiro, p. 101–137.

TUPINAMBÁ, M., HEILBRON, M., TEIXEIRA, W. 2013. Evolução Tectônica e Magmática da Faixa Ribeira entre o Neoproterozoico e o Paleozoico Inferior na Região Serrana do Estado do Rio de Janeiro, Brasil. Anuário do Instituto de Geociências, v. 35, p.140-151.

UGARKAR, A. G., MALAPUR, M.A., KUMAR, B. C. 2015. Archean turbidite hosted orogenic gold mineralization in the Gadag greenstone belt, Western Dharwar Craton, Peninsular India. Ore Geology Reviews, v. 72 1224–1242.

VIKENT'EVA, O. V., GAMYANIN, G. N., BORTNIKOV, N. S. 2013. The REE DistributionPatterns inAlteredRocks: Implications for the Genesis of Orogenic Gold Deposits. Mineral deposit research for a high-tech world, 12th SGA Biennial Meeting Proceedings, Vol. 3.

VALERIANO, C. M., TUPINAMBÁ, M., SIMONETTI, A., HEILBRON, M., ALMEIDA, J. C. H., DO EIRADO, L. G. 2011. U-Pb LA-MC-ICPMS geochronology of Cambro-Ordovician post-collisional granites of the Ribeira belt, southeast Brazil: terminal Brasiliano magmatism in central Gondwana supercontinent. Journal of South American Earth Sciences 32, 416–428.

VALERIANO, C.M., MEDEIROS, S., VAZ, G.S., NETO, C.C.A. 2008. Sm-Nd isotope dilution TIMS analyses of BCR-1, AGV-1 and G-2 USGS rock reference materials: preliminary results from the LAGIR- UERJ laboratory, Rio de Janeiro. Proceedings of the VI South American Symposium on Isotope Geology. Bariloche, Argentina.

VALERIANO, C.M., MENDES, J. C, TUPINAMBÁ, M, BONGIOLO, E., HEILBRON, M., JUNHO, M. C. B. 2016. Cambro-Ordovician post-collisional granites of the Ribeira belt, SE-Brazil: A case of terminal magmatism of a hot orogen. Journal of South American Earth Sciences, v. 68, p. 269-281.

VERMA, S.K., OLIVEIRA, E.P., SILVA, P.M., MORENO, J.A., AMARAL, W.S. 2017. Geochemistry of komatiites and basalts from the Rio das Velhas and Pitangui greenstone belts, São Francisco Craton, Brazil: implications for the origin, evolution, and tectonic setting. Lithos 284–285, 560–577.

VIAL, D. S., DEWITT, E., LOBATO, L. M., THORMAN, C. 2007. The geology of the Morro Velho gold deposit in the Archean Rio das Velhas greenstone belt, Quadrilátero Ferrífero, Brazil. Ore Geology Reviews, v. 32, p. 511-542.

VIELREICHER, N. M., RIDLEY, J. R., GROVES, D. I. 2002. Marymia: an Archean–amphibolite facies–hosted, orogenic lode–gold deposit overprinted by Palaeoproterozoic orogenesis and base metal mineralisation, Western Australia. Miner. Deposita 37, 737–764.

ZUCCHETTI, M., BALTAZAR, O.F., RAPOSO, F.O., Estratigrafia. In: M. ZUCCHETTI, O.F. BALTAZAR (Eds.) 1998. Projeto Rio das Velhas–Texto explicativo do mapa geológico integrado, escala 1:100.000. 2nd ed. Departamento Nacional de Produção Mineral/CPRM–Serviço Geológico do Brasil, Belo Horizonte, p. 13–42.

ZUCCHETTI M. AND BALTAZAR O.F. 2000. Rio das Velhas Greenstone Belt lithofacies associations, Quadrilátero Ferrífero, Minas Gerais, Brazil. In: 31th International Geological Congress, Rio de Janeiro. CD-ROM.

ZHANG, J. Q., LI, S. R., SANTOSH, M., LU, J., WANG, C. L. 2018. Metallogenesis of Precambrian gold deposits in the Wutai greenstone belt: constrains on the tectonic evolution of the North China Craton. Geosci. Front. 9 (2), 317–333.